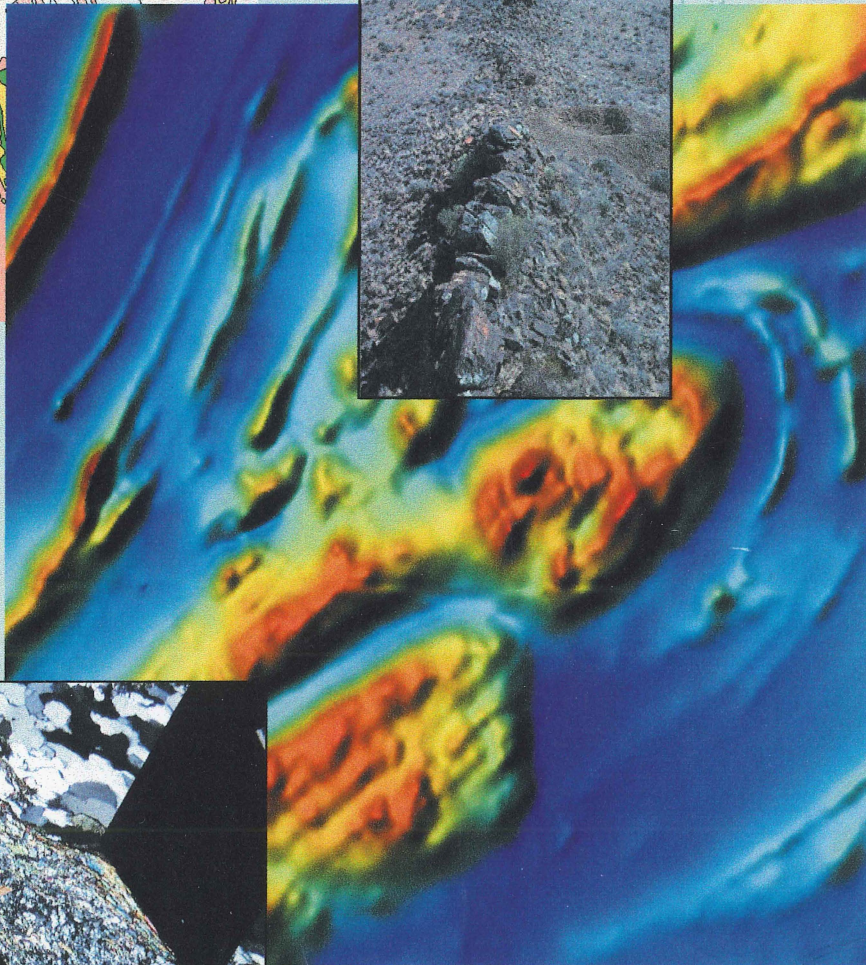
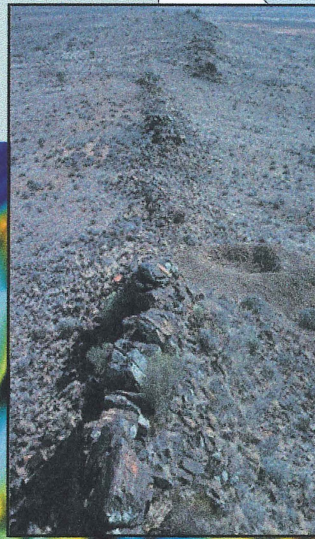
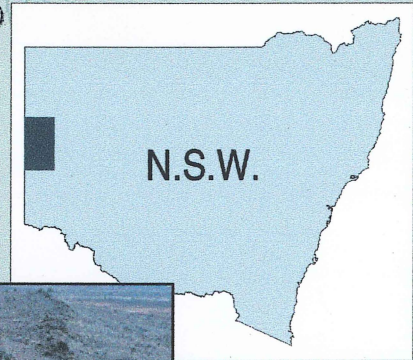
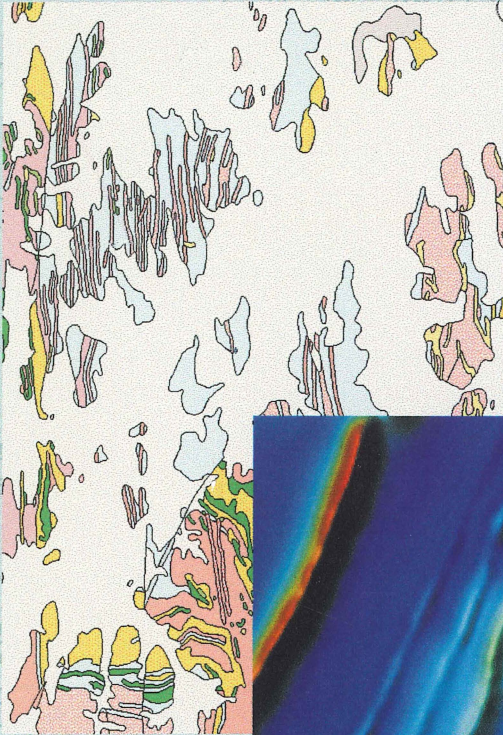


# SOURCES OF MAGNETIC ANOMALIES IN THE BROKEN HILL REGION, NSW

David W. Maidment & George M. Gibson

BMR PUBLICATIONS COMPACTUS  
(LENDING SECTION)



Record 1999/6



BMR COMP  
1999/06  
COPY 2

PRIMARY INDUSTRIES  
AND RESOURCES SA



# **Sources of magnetic anomalies in the Broken Hill region, NSW**

**D. W. MAIDMENT & G. M. GIBSON**

**RECORD 1999/6**

This record is a product of the Broken Hill Exploration Initiative, a collaborative National Geoscience Mapping Accord project between the Australian Geological Survey Organisation, the New South Wales Department of Mineral Resources and Primary Industries and Resources South Australia

## **Department of Industry, Science & Resources**

Minister for Industry, Science & Resources: Senator the Hon. Nick Minchin  
Parliamentary Secretary: The Hon. Warren Entsch, MP  
Secretary: Russell Higgins

## **Australian Geological Survey Organisation**

Executive Director: Neil Williams

© Commonwealth of Australia 1999

This work is copyright. Apart from any fair dealings for the purposes of study, research, criticism, or review, as permitted under the *Copyright Act 1968*, no part may be reproduced by any process without written permission. Copyright is the responsibility of the Executive Director, Australian Geological Survey Organisation. Requests and enquiries should be directed to the Executive Director, Australian Geological Survey Organisation, GPO Box 378, Canberra, ACT 2601.

ISSN 1039-0073  
ISBN 0 642 27382 0

Bibliographic reference: Maidment D.W. & Gibson G.M., 1999. Sources of aeromagnetic anomalies in the Broken Hill region, NSW. Australian Geological Survey Organisation, Record 1999/6.

AGSO has tried to make the information in this product as accurate as possible. However, it does not guarantee that the information is totally accurate or complete. Therefore, you should not rely solely on this information when making a commercial decision.

# Contents

Abstract	1
Introduction	2
Airborne geophysical data	2
Previous work	2
Regional geology and stratigraphy	3
Structural history	7
Regional aeromagnetic patterns	9
Sources of aeromagnetic anomalies	11
Stratigraphically controlled anomalies	11
Banded iron formation	11
Metamorphic magnetite in metasediments	13
Quartz-albite rocks	17
Redan Geophysical Zone	18
Structurally controlled anomalies	19
Early magnetite (D <sub>2</sub> ?)	19
Magnetite in S <sub>3</sub> fabrics	21
Magnetite at lithological contacts	26
Later-stage magnetite	30
Retrograde shear zones	32
Aeromagnetic signatures of igneous rocks	34
Mafic rocks	34
Amphibolite	34
Post peak metamorphic mafic/ultramafic rocks	40
Felsic rocks	44
Granite gneiss	44
Pegmatite	45
Granitic intrusives	45
Adelaide Supergroup	46
Other anomaly sources	48
Quartz-magnetite rocks	48
Maghemite	50
Pyrrhotite	51
Jacobsite	51
Remanent magnetisation	52
Oxidation of magnetite	52
Magnetic susceptibility patterns	53
Mineralisation and aeromagnetics	56
Discussion	57
Conclusions	60
Acknowledgments	61
References	62



## Abstract

Magnetic anomalies in the Palaeoproterozoic Willyama Supergroup have a number of different sources, including stratiform magnetite, structurally controlled magnetite and magnetite in igneous rocks.

Magnetic sedimentary units are relatively uncommon. Most metasedimentary rocks are geochemically reduced and host few stratiform anomalies. Exceptions to this rule include garnet-poor composite gneisses, migmatites and some units in the Paragon Group which are weakly anomalous. Banded iron formations are volumetrically minor stratiform rocks, but generate intense anomalies. Rocks of the Redan Geophysical Zone are generally oxidised and have a very different magnetic signature to the rest of the Willyama Supergroup, with a very high average magnetic susceptibility and complex anomalies. Quartz-magnetite rocks may have either a structural or stratigraphic origin. In contrast to the Willyama Supergroup, Adelaidean cover sequences have well-defined anomalies of stratigraphic origin.

Structurally-controlled anomalies are common across the region and are caused by magnetite in either: (1) high-temperature shear zones; (2) tectonic fabrics; or (3) in high-strain zones developed along the contact between rocks of contrasting competency. Magnetite formation occurred more than once during the deformational history, and formed during both high-grade and lower-grade metamorphism. Many of the observed anomalies coincide with the regional  $S_3$  fabric, which originated under amphibolite-facies conditions. Retrograde shear zones (mostly post- $D_3$  in age) are generally magnetite-destructive and form linear zones of low magnetic intensity.

Intrusive rocks in the region have a variable signature. Amphibolite is generally very weakly magnetic and not visible on aeromagnetic images, although certain units adjacent to shear zones are highly magnetic due to oxidation of iron by the introduction of fluid. Many post-peak-metamorphic gabbros and ultramafics are moderately to highly magnetic due to magnetite formation during alteration of primary olivine and orthopyroxene, while later metadolerite dykes have a very low magnetic susceptibility. Pegmatites are generally non-magnetic, although some that occur in linear magnetic zones contain coarse octahedral magnetite. Other felsic intrusive rocks, including granite orthogneisses and post-peak metamorphic granites are non-magnetic, but may be delineated on aeromagnetic images where they occur in regions of higher background magnetic intensity.

The abundance of structurally-controlled anomalies and the relative paucity of stratigraphic anomalies means that extrapolation of many lithological units beneath cover is difficult, if not impossible. A 'magnetic stratigraphy' is difficult to construct for the Willyama Supergroup. Rather, aeromagnetic data are useful in the location of high-strain zones, where oxidising fluids brought about the crystallisation of magnetite and retrograde shear zones where fluids have resulted in the destruction of magnetite.

## Introduction

The Broken Hill Exploration Initiative (BHEI) is a joint project between the Australian Geological Survey Organisation (AGSO), the New South Wales Department of Mineral Resources (NSWDMR) and Primary Industries and Energy South Australia (PIRSA) aimed at stimulating and improving exploration in the region through the provision of a new generation of geoscientific data. This has involved the acquisition of high-resolution airborne geophysics (aeromagnetics, gamma-ray spectrometrics and digital elevation model data). Extensive ground-truthing of aeromagnetic data has been an integral part of the interpretation process, with the aim of using aeromagnetics to extend known geology beneath cover. This ground truthing has shown that the aeromagnetic anomalies are multigenic and do not in many instances reflect original stratigraphic units. This record documents the sources of many of these anomalies and examines the implications this has for interpreting geology beneath cover and mineral exploration.

## Airborne geophysical data

AGSO acquired airborne geophysical data over the Broken Hill Block in 1995 and 1996 at 100 m line spacing and 60 m flying height. The intensity of anomalies quoted in this paper refers to these aeromagnetic data, reduced to pole and at 60 m flying height. All references to grid coordinates are from the Australian Map Grid using the WGS84 datum.

## Previous work

A considerable amount of work has been done on the interpretation of aeromagnetics in the Broken Hill region. Much of this work had a regional focus, with the area subdivided into broad zones or magnetic 'domains' (e.g. McIntyre & Wyatt 1978, Tucker 1983 and Isles 1983). Detailed correlation of aeromagnetics with geology has been more limited. McIntyre (1979, 1980a) field checked anomalies in selected areas and made the observation that magnetite was present in a range of lithologies and that there are numerous stratigraphic magnetite-bearing horizons that could be used to resolve structural and stratigraphic problems.

Clark (1981, 1988) investigated magnetic properties, magnetic fabric and magnetic stratigraphy in selected areas across the region. He concluded that magnetic anisotropy reflected metamorphic fabrics and could be used in structural analysis. More recently, Stevens (1997, 1998) studied some selected anomalies in detail and concluded that there is a strong stratigraphic control on magnetite in metasediments and discounted earlier suggestions by Gibson *et al.* (1996) that some magnetic anomalies in the region have a structural control.

Most of this earlier research has worked on the premise that most aeromagnetic anomalies are caused by original sedimentary units and that a 'magnetic stratigraphy'

could be erected that could be used to map out stratigraphic units and lithologies beneath cover (e.g. Tucker 1983). In this study, we aim to show that there are a variety of sources for the magnetic anomalies and that a significant proportion of these are structurally-controlled, thereby precluding their use as stratigraphic markers.

## Regional geology and Stratigraphy

The Broken Hill and Euriovie blocks are located in the far west of New South Wales (Fig. 1) and comprise deformed and metamorphosed rocks of the Palaeoproterozoic Willyama Supergroup which includes several suites of felsic and mafic lithologies. Willis *et al.* (1983) and Stevens *et al.* (1983) erected a stratigraphic sequence for the Willyama Supergroup (Figs. 2 & 3). In this scheme, gneissic units in the Redan area (Redan Gneiss, Ednas Gneiss & Mulculca Formation) and two migmatitic units (Clevedale Migmatite & Thorndale Composite Gneiss) are at the base of the sequence. These are overlain by the Thackaringa Group which is characterised by quartz-albite rocks, quartzofeldspathic (granite) gneiss and migmatised metasediments. The overlying Broken Hill Group is dominated by metasediments, 'Potosi'-type quartz-feldspar-biotite-garnet gneiss and minor quartz-gahnite rock, garnet-quartz rock, quartz-tourmaline rock and banded iron formation. The Broken Hill Group hosts the giant Broken Hill orebody (~280 Mt pre-erosion, Burton 1990). The Sundown Group overlies the Broken Hill Group and is characterised by pelitic to psammopelitic metasediments and locally abundant calc-silicate ellipsoids. The Paragon Group, the uppermost stratigraphic unit in the Willyama Supergroup comprises low-grade, graphitic and feldspathic metasediments.

Amphibolite is common through all the sequence below the Sundown Group and has previously been used to define stratigraphic units. For example, the base of the Parnell Formation is defined by Stevens *et al.* (1983) as 'the sole of the lowermost significant and continuous basic gneiss', while the top is defined as 'the top of the uppermost basic or felsic gneiss underlying Freyers Metasediments'. Recent work has shown that many, if not most, of the amphibolites are intrusive and not volcanic as previously interpreted (Gibson *et al.*, in prep.) with an emplacement age of around 1690 Ma.

Granite gneiss has also been used (Stevens *et al.*, 1983) to define parts of the stratigraphic sequence, although many workers now consider these quartzofeldspathic rocks to be orthogneisses (e.g. Vernon *et al.* 1988, Vernon 1996, Nutman & Ehlers 1998) emplaced around 1690 Ma (*cf.* ashflow tuffs with minor airfall tuffs and submarine lavas as previously interpreted by Brown *et al.*, 1983).

No detailed re-evaluation of the stratigraphy in light of this recent work has yet been attempted and the NSW Department of Mineral Resources interpretation remains the current working model.

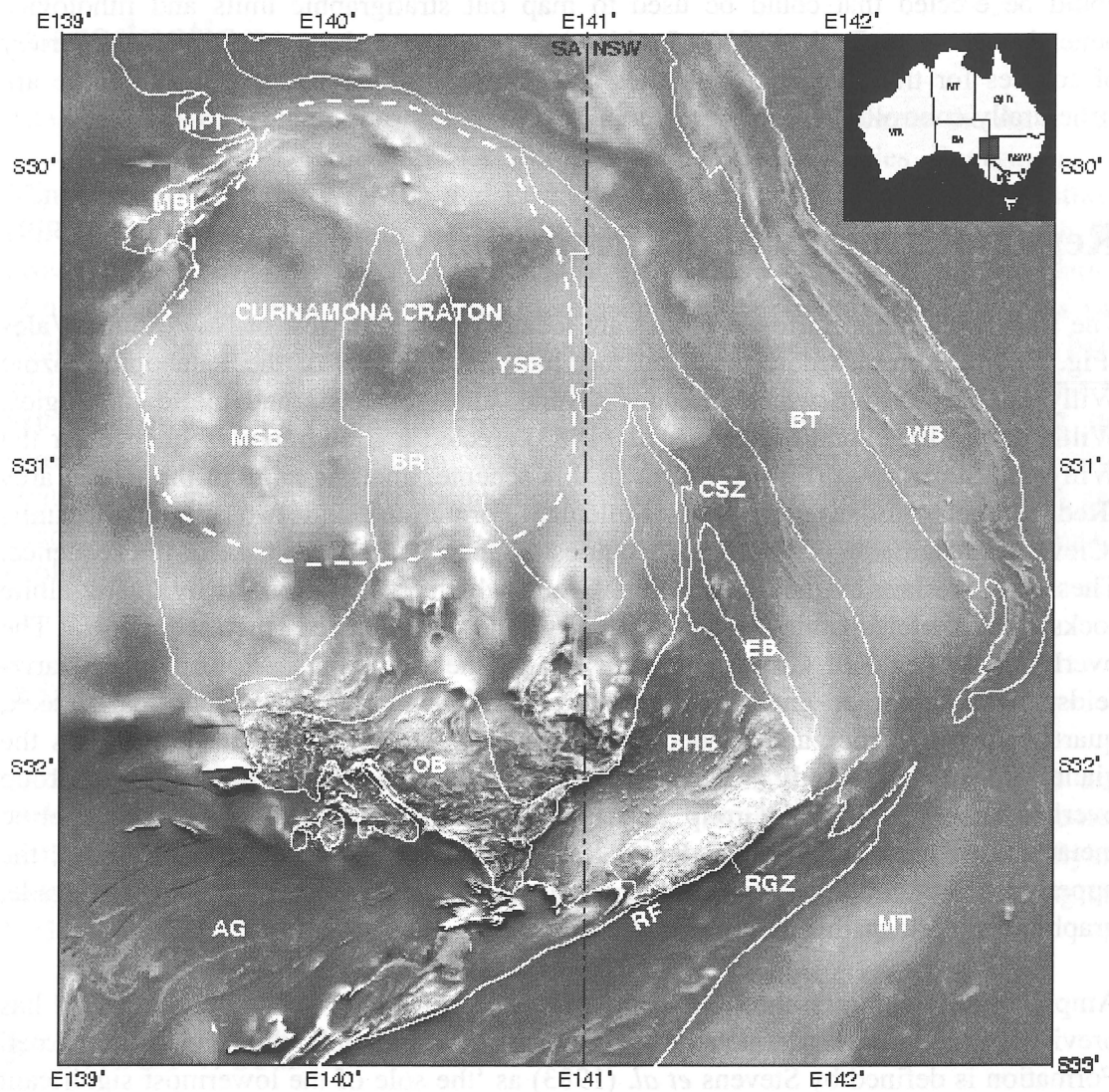
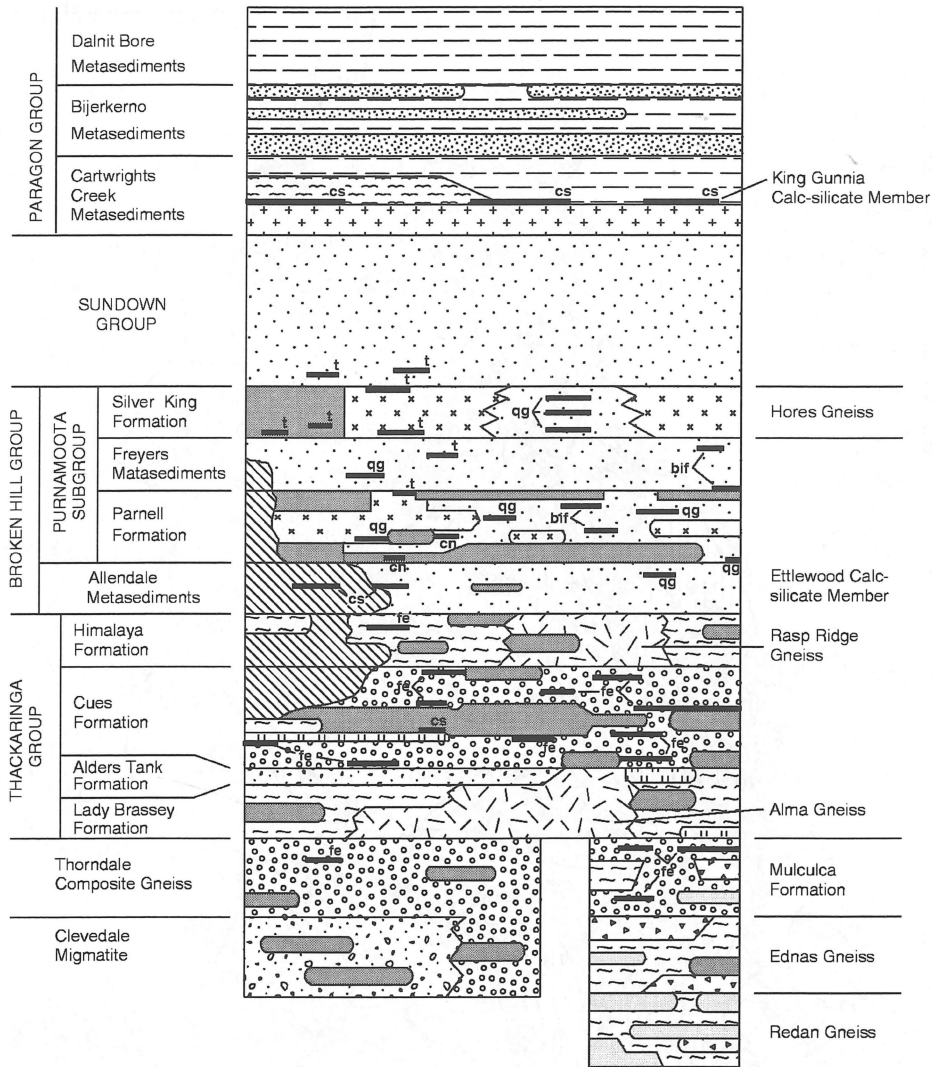
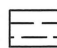


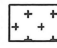
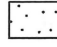

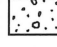
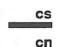
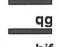
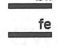

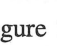
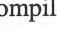


Figure 1. Total magnetic intensity (TMI) of the Curnamona Province. BHB: Broken Hill Block, EB: Euriowie Block, RGZ: Redan Geophysical Zone, RF: Redan Fault, OB: Olary Block, BR: Benagerie Ridge, MSB: Moorowie Sub-basin, YSB: Yalkalpo Sub-basin, MBI: Mount Babbage Inlier, MPI: Mount Painter Inlier, CSZ: Caloola Synclinorial Zone, BT: Bancannia Trough, WB: Wonominta Block, MT: Menindee Trough, AG: Adelaide Geosyncline.

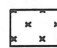



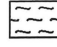







**METASEDIMENTARY ROCKS**

-  Graphitic pelitic to psammopelitic rocks
-  Fine-grained feldspar-rich psammite
-  Fine-grained graphitic psammite
-  Chistolite-bearing pelitic rocks
-  Non-graphitic pelitic to psammitic metasediments, calc-silicate nodules common
-  Metasedimentary composite gneiss and migmatite
-  Quartzo-feldspathic composite gneiss and migmatite
-  **cs** Bedded calc-silicate rock
-  **cn** Variably layered to non-layered calc-silicate rock
-  **qg** Quartz - gahnite rock, Mn garnet-rich rocks, Pb-Zn sulphide ore
-  **bif** Fine-grained Mn garnet - magnetite - quartz - apatite rock
-  **fe** Quartz - magnetite, quartz - Fe sulphide ± Fe garnet rocks
-  **t** Tourmaline-rich rocks

**OTHER ROCK TYPES**

-  Quartz - feldspar - biotite - garnet ("Potosi" type) gneiss
-  Quartz - feldspar - biotite ("granitic") gneiss
-  Leucocratic quartz - feldspar - rich rock and intermixed pegmatite
-  Leucocratic gneiss
-  Finely layered sodic plagioclase - quartz rock
-  Sodic plagioclase - quartz - magnetite gneiss
-  Amphibolite and basic granulite
-  Sodic plagioclase - quartz - amphibole rocks

16/154/19

Figure 2. Generalised stratigraphic sequence for the Willyama Supergroup in the Broken Hill Block. Compiled by B. Stevens (NSWDMR), 1989.

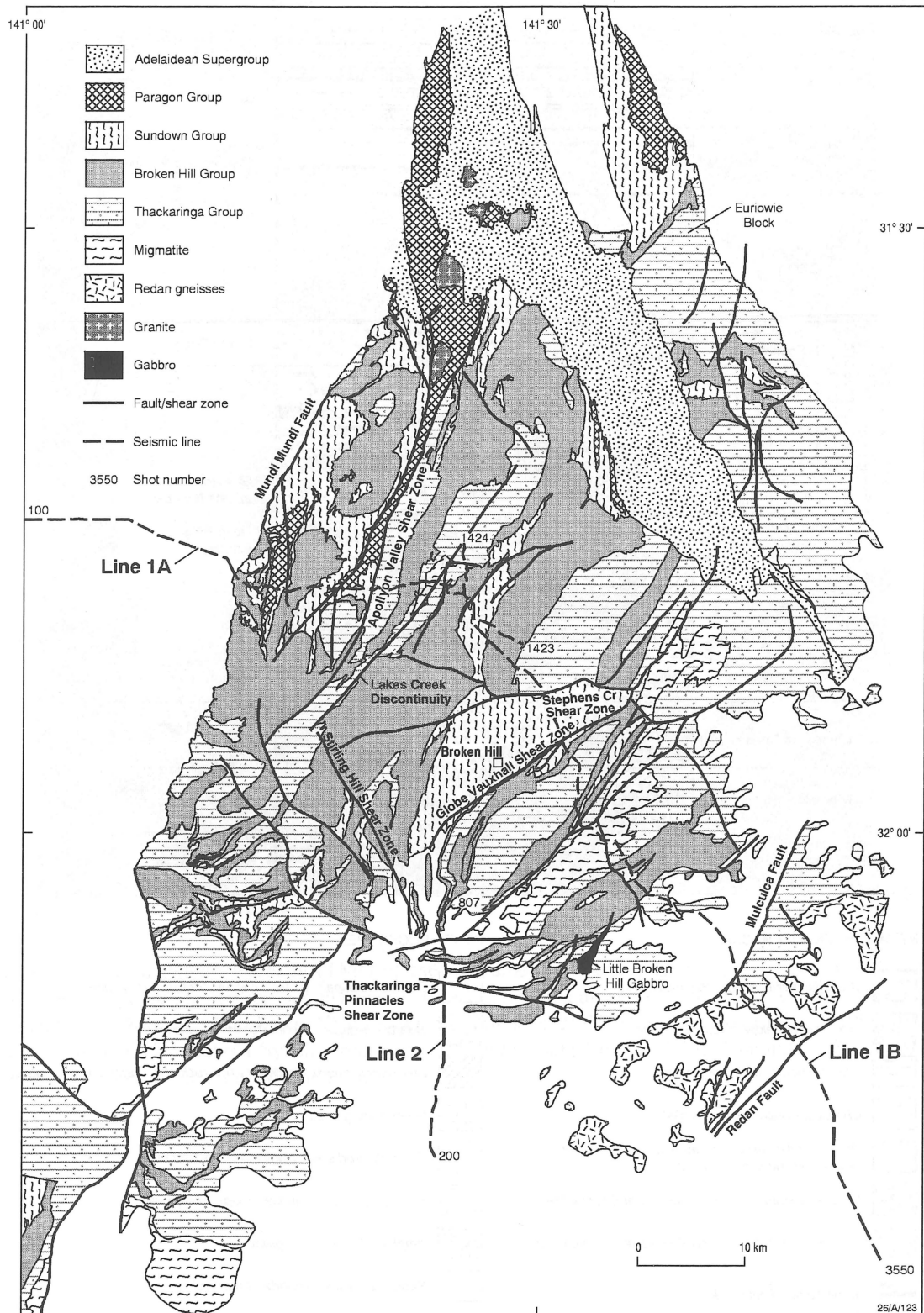


Figure 3. Interpreted regional stratigraphy of the Broken Hill and Euriowie Blocks (after NSWDMR 1:100 000 stratigraphic map, Willis 1989). The AGSO deep reflection seismic traverses are superimposed.

## Structural history

The most widely accepted structural interpretations in recent times have been those by Laing *et al.* (1978) and Marjoribanks *et al.* (1980). These workers proposed large, northerly-trending  $F_1$  nappes refolded coaxially about more upright  $F_2$  folds. Smaller, more open  $F_3$  folds with near-vertical axial planes overprint the earlier generations of folding.  $D_1$  and  $D_2$  coincided with high-grade metamorphism (Olarian Orogeny) while  $D_3$  occurred under retrograde conditions. Retrograde shear zones were thought to have developed during  $D_3$  and have undergone reactivation during the Delamerian Orogeny around 520 Ma ago.

More recently, White *et al.* (1995, 1996) proposed a fold and thrust belt model for the Broken Hill Block. In this model, the region was divided into a series of thrust packages, each with its own characteristic deformation style, separated by high-temperature shear zones (thrusts). The thrusts were considered to have originated during the Olarian Orogeny and resulted in tectonic transport towards the southeast. White *et al.* (1995) considered that many of the retrograde shear zones are high-temperature shear zones that were reactivated during later deformation.

Gibson *et al.* (1996, 1997, 1998a, b) re-evaluated the structural history of the region in light of the work done by White *et al.* (1995). They confirmed that three periods of major folding could be recognised ( $D_1$ - $D_3$ ), the first two of which were accompanied by amphibolite-granulite facies metamorphism. The  $D_3$  deformation occurred under lower grade amphibolite facies conditions.  $D_1$  is evident as an early high-grade schistosity.  $D_2$  formed asymmetric folds with a shallow- to moderately-dipping axial plane fabric.  $D_3$  was thrust-related and resulted in the development of major southeast-dipping thrust faults and regionally extensive upright folds with vertical to steeply-dipping northeast-trending axial plane fabrics. Subsequent deformations ( $D_4$ - $D_6$ ) took place under retrograde conditions and were mainly shear-related. Several retrograde shear zones developed by reactivation of  $D_3$  structures during  $D_4$  deformation as part of late Neoproterozoic continental rifting and the breakup of Rodinia. Both northeast and northwest-trending structures developed during  $D_4$ . Northeast-trending shear zones (e.g. the Redan Fault) developed as strike-slip faults with a sinistral sense of movement. Northwest-trending faults (e.g. the Stirling Hill shear zone) most likely developed as normal faults associated with crustal thinning. During  $D_5$  (attributed to the Delamerian Orogeny) many of the shear zones were reactivated as northwest-directed thrust faults with minor dextral displacement. A conjugate set of east-west and north-south-trending faults with dextral and sinistral offsets respectively overprint all earlier structures and are assigned to  $D_6$  (?mid-Palaeozoic Alice Springs Orogeny).

Seismic reflection data collected by AGSO in 1996 showed that the major structures in the region dip towards the southeast and that tectonic transport was directed towards the northwest (Gibson *et al.* 1998) and not the southeast as had been previously proposed (White *et al.* 1995, 1996). Large scale nappes could not be verified, although regionally significant shear zones extending to middle and lower parts of the crust were striking features of the dataset. Gibson *et al.* (1998a) considered these shear zones had likely experienced large volumes of fluid movement and noted that the some of the highest base metal values from geochemical sampling along the transect occurred in or

near major shear zones. More recent work (Gibson *et al.* 1998b) indicates that many of these shear zones originated during the D<sub>3</sub> deformation (cf. Laing *et al.* 1978, Marjoribanks *et al.* 1980).

References to fold generations and schistosity in this record use the structural framework of Gibson *et al.* (1996, 1997, 1998) as outlined in Table 1.

Phase	Gibson <i>et al.</i> , 1996, 1997, 1998	Laing <i>et al.</i> , 1978; Marjoribanks <i>et al.</i> , 1980	White <i>et al.</i> , 1995, 1996
D <sub>1</sub>	D <sub>1</sub> folds inferred but not observed; sillimanite grade schistosity (S <sub>1</sub> ) sub-parallel to bedding (S <sub>0</sub> ). Overturning of regional stratigraphy.	SE-verging nappes; high-grade S <sub>1</sub> fabric sub-parallel to S <sub>0</sub> . Overturning of regional stratigraphy.	D <sub>1</sub> -D <sub>3</sub> formed as part of single progressive deformational event related to southeast-directed thrusting. S <sub>1</sub> -S <sub>3</sub> fabrics formed at moderate to high metamorphic grade.
D <sub>2</sub>	Regional scale, E or SE-plunging gently reclined to recumbent asymmetric folds with moderately to shallow-dipping high-grade axial plane fabric (S <sub>2</sub> ). Mylonite development.	Upright, NE and SW-plunging tight folds with high-grade steeply-dipping axial plane fabric (S <sub>2</sub> ). Minor high-temperature shearing.	
D <sub>3</sub>	Upright, tight to isoclinal folds with sub-vertical or steeply-dipping amphibolite grade axial plane fabric (S <sub>3</sub> ). NW-directed thrusting and development of D <sub>3</sub> shear zones.	Upright, open folds with sub-vertical, generally retrograde axial plane fabric (S <sub>3</sub> ). Initiation of retrograde shear zones.	
D <sub>4</sub>	Development of extensional shear zones, dyke intrusion, reactivation of D <sub>3</sub> shear zones.	Various periods of localised deformation in retrograde schist zones.	Retrograde reactivation of high-temperature shears at various times
D <sub>5</sub>	Thrusting, reactivation of earlier shear zones; retrograde metamorphism.		
D <sub>6</sub>	Reactivation of earlier shear zones; transpression.		

Table 1. Structural history and fabric development in the Willyama Supergroup

## Regional Aeromagnetic Patterns

The Broken Hill Block is located southeast of the Curnamona Craton (Figs. 1, 4) and can be divided into two magnetic domains (Domains 2 and 3 of Tucker 1983). The bulk of the Willyama Supergroup is characterised by low background magnetic susceptibility and numerous linear anomalies (Domain 2 of Tucker 1983). These anomalies have a northeast trend in the northern part of the block and extend up to 20 km in length. South of the Thackaringa-Pinnacles shear zone, the anomalies are less continuous and apparently more tightly folded (Fig. 4), implying that there is a change in structural style between the two areas, or that the southern area has been tectonically reworked to a greater degree. In either event, the Thackaringa-Pinnacles shear zone appears to be a major structure separating different structural domains.

The Redan Geophysical Zone southeast of Broken Hill (Domain 3 of Tucker 1983) is characterised by high background susceptibility and complex anomaly forms (Fig. 4). Unfortunately, the region is poorly exposed so that interpretation of the anomalies is difficult.

The boundary between the Broken Hill and Olary Blocks is taken as a northeast-trending geophysical boundary separating the relatively magnetic rocks of the Olary Block from the less magnetic rocks of the Broken Hill Block (Stevens 1986).

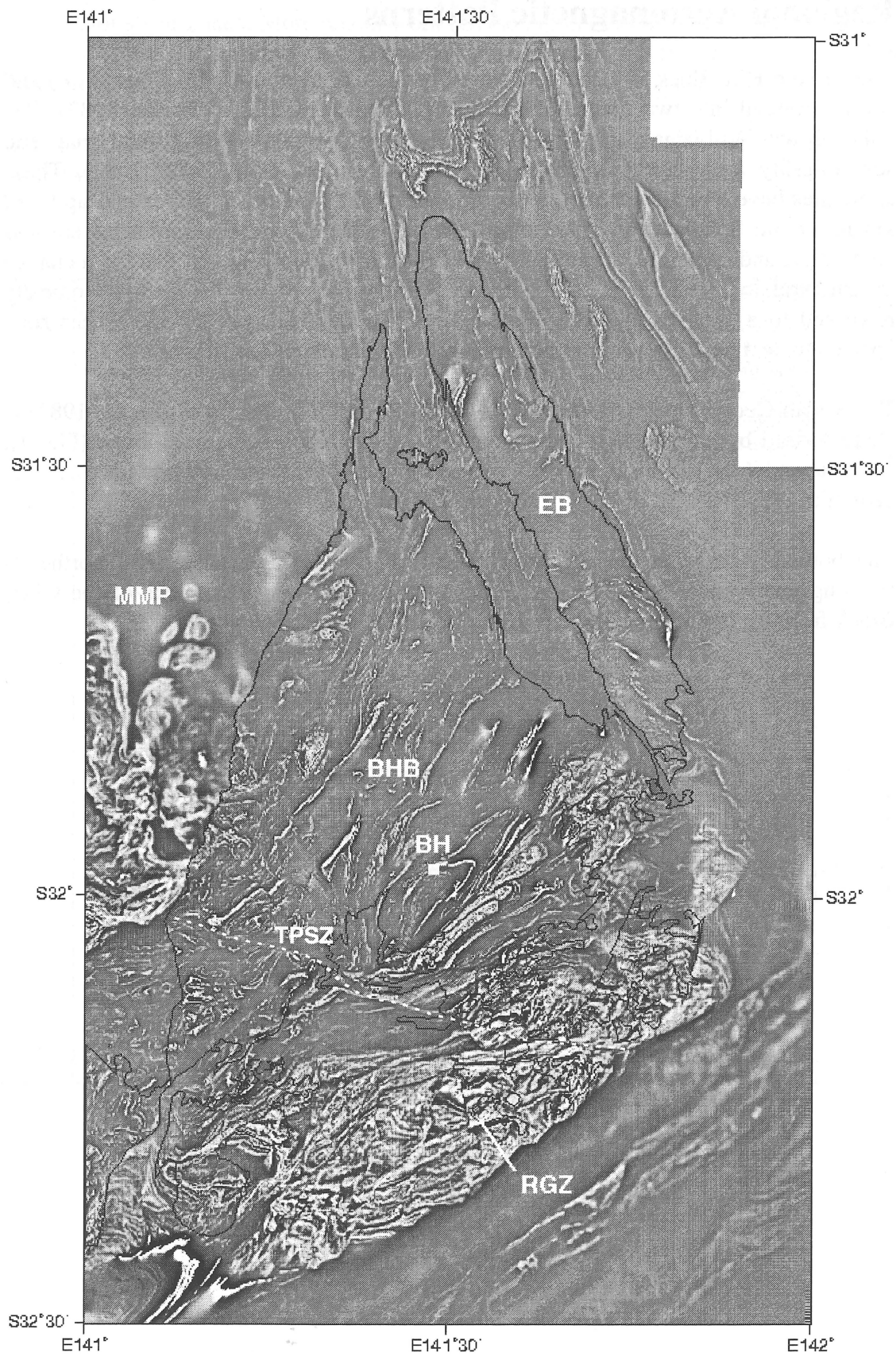


Figure 4. 1<sup>st</sup> vertical derivative of total magnetic intensity (TMI) for the Broken Hill and Euriowie Blocks. BH: Broken Hill, BHB: Broken Hill Block, EB: Euriowie Block, RGZ: Redan Geophysical Zone, MMP: Mundi Mundi Plain, TPSZ: Thackaringa-Pinnacles shear zone.

## Sources of aeromagnetic anomalies

A number of different sources of magnetic anomalies in the region have been identified. These include:

### Stratigraphically controlled anomalies

- Banded iron formation
- Metamorphic magnetite in metasediments
- Rocks of the Redan Geophysical Zone
- Adelaidean rocks

### Structurally controlled anomalies

- Early magnetite (D<sub>2</sub>?)
- Magnetite in S<sub>3</sub> fabrics
- Magnetite at lithological contacts
- Later-stage magnetite
- Remobilised magnetite
- Retrograde shear zones

### Igneous rocks

- Pegmatite
- Amphibolite
- Post-peak metamorphic mafic intrusives

### Others

- Quartz-magnetite rocks
- Maghemite
- Pyrrhotite

## Stratigraphically controlled anomalies

### Banded iron formation

Banded iron formation (BIF) in the Broken Hill region gives rise to striking linear aeromagnetic anomalies up to 1 000 nT in magnitude, but only occurs in minor amounts regionally, as bodies generally less than 1 m wide. BIF occurs in four areas of the outcropping Broken Hill Block: the Broken Hill synform; Little Broken Hill; the Clevedale-Rupee area and in minor amounts in the Stephens Creek area (Fig. 5). BIF is also present beneath the Mundi Mundi plain as thin horizons in association with magnetite-rich quartz-albite rock (R. Skirrow pers. comm.).

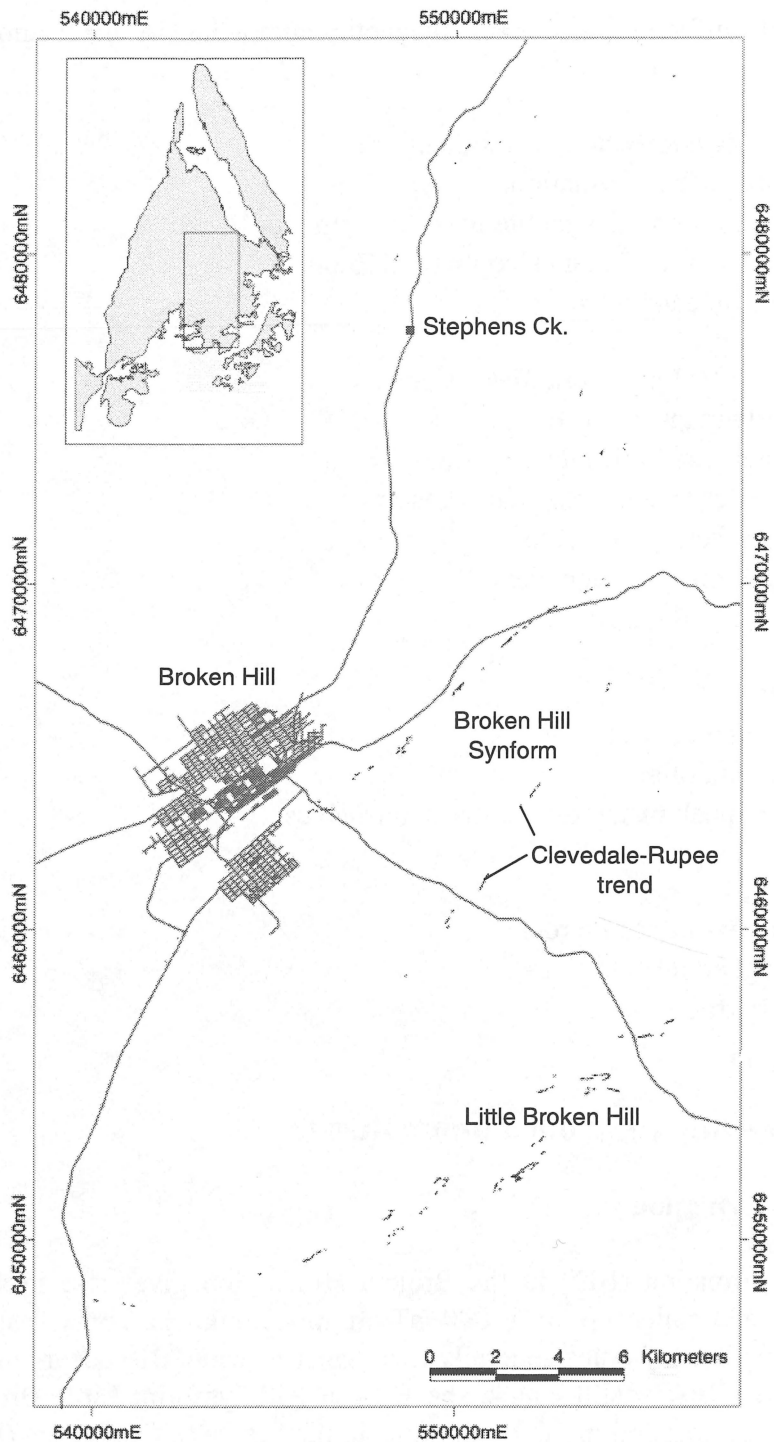


Figure 5. Distribution of outcropping banded iron formation (BIF) in the Broken Hill Block. BIF is restricted to four areas: the Broken Hill Synform; the Clevedale-Rupee area; Little Broken Hill and the Stephens Creek area.



The BIFs consist of compositionally layered, fine-grained magnetite-garnet-quartz-apatite rocks which are considered to be metamorphosed iron-rich chemical sediments (Richards 1966a, b; Stanton 1976a, b, c, d). Magnetite and garnet have an antipathetic relationship (Richards 1966a), with garnet-rich layers being poor in magnetite and vice versa. This is considered to reflect original chemical composition and oxidation state in sedimentary layers (Richards 1966a) and is evident in garnet-rich BIF from the western Little Broken Hill area which has no obvious aeromagnetic anomaly. The BIF in this area seems to be intermediate in composition between magnetite-rich BIF and garnet-quartz rocks mapped throughout the region.

## **Metamorphic magnetite in metasediments**

### *Stratiform magnetite in metasediments*

Few aeromagnetic anomalies which can be unequivocally ascribed to original bedding have been recognised in metasediments of the Willyama Supergroup. Minor variations in magnetite concentration on the outcrop scale may be observed. However, most of these are too small to generate anomalies in aeromagnetic images. Many major anomalies do occur in metasediments, although we ascribe these concentrations of magnetite to other processes (see below) rather than metamorphism of suitable original sedimentary beds.

Stratigraphic anomalies occur in the Paragon Group in the northern part of the Broken Hill Block (Fig. 6). The anomalies are weak but fairly continuous and are only apparent when a high-frequency filter, such as a vertical derivative, is applied to the data. The anomalies occur within interbedded graphitic pelites and psammopelites, although their precise location is difficult to determine in the field due to their low intensity. The generally weak nature of the anomalies may be due to the reducing action of carbon, which lowers the oxidation ratio and inhibits magnetite formation (McIntyre 1980b).

The lack of significant stratigraphic anomalies in the metasediments is not surprising given the oxidation state of the rocks making up the bulk of the Willyama Supergroup. The original oxidation state of sediments will tend to be retained through metamorphism due to the low mobility of oxygen in metamorphic environments (McIntyre 1980b). If the oxidation ratio ( $\text{Fe}^{3+}/(\text{Fe}^{2+}+\text{Fe}^{3+})$ ) is low, most of the iron will enter silicates. If the ratio is high, the iron will form hematite/ilmenite. An intermediate ratio will favour the formation of magnetite (Fig. 7; Chinner 1960; McIntyre 1980b; Grant 1985). The metasediments at Broken Hill generally have a low oxidation ratio (Fig. 8) and hence have little available  $\text{Fe}^{3+}$  to form magnetite, despite that fact that some sediments have a relatively high total iron content.

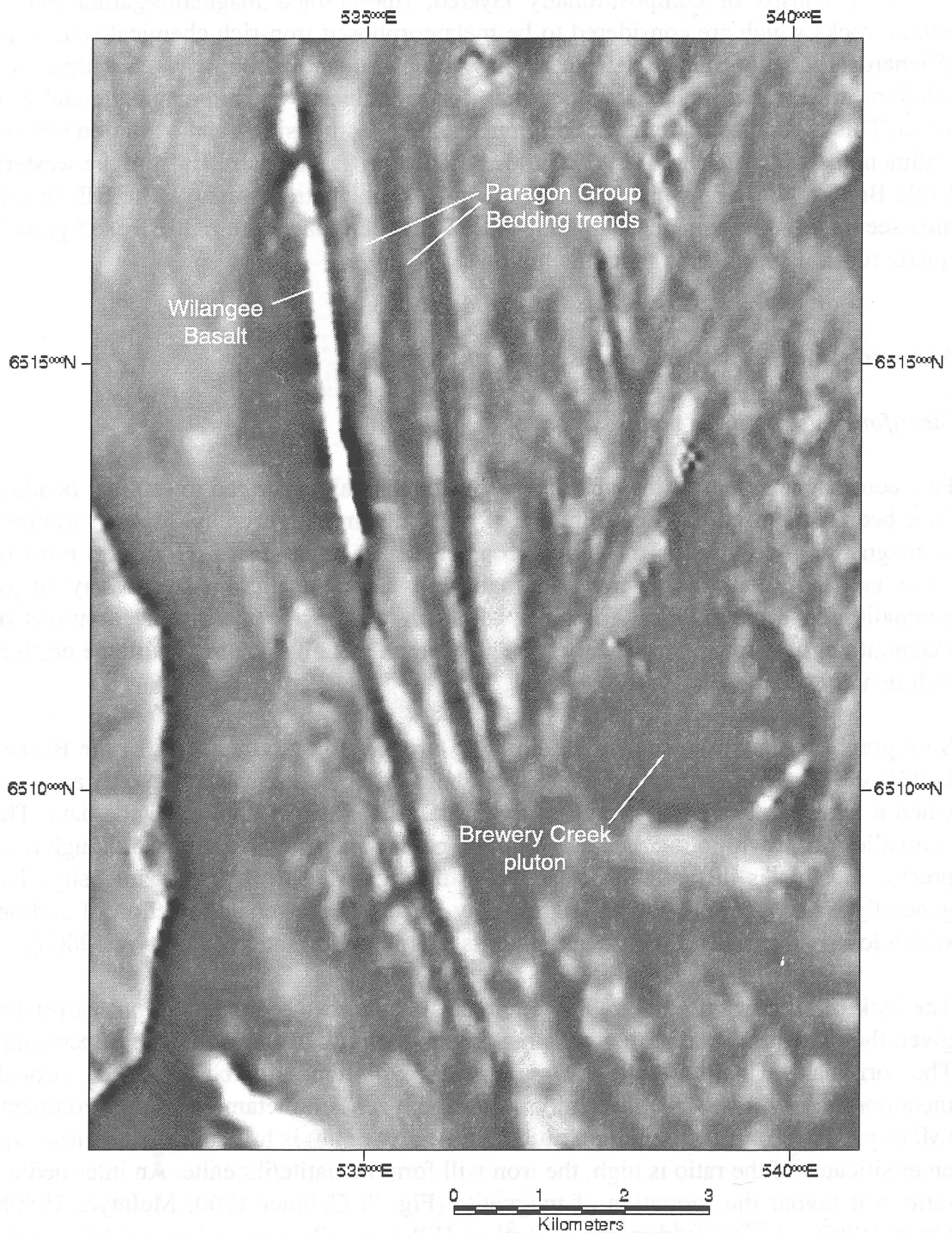


Figure 6. 1<sup>st</sup> vertical derivative of TMI (total magnetic intensity) of the Brewery Well area. Stratigraphic anomalies in Paragon Group metasediments are prominent. The strong linear anomaly is caused by a unit of Wilangee Basalt, part of the unconformably overlying Adelaidean sequence. The Brewery Creek pluton is evident as a 'teardrop'-shaped area with a magnetically 'quiet' signature.

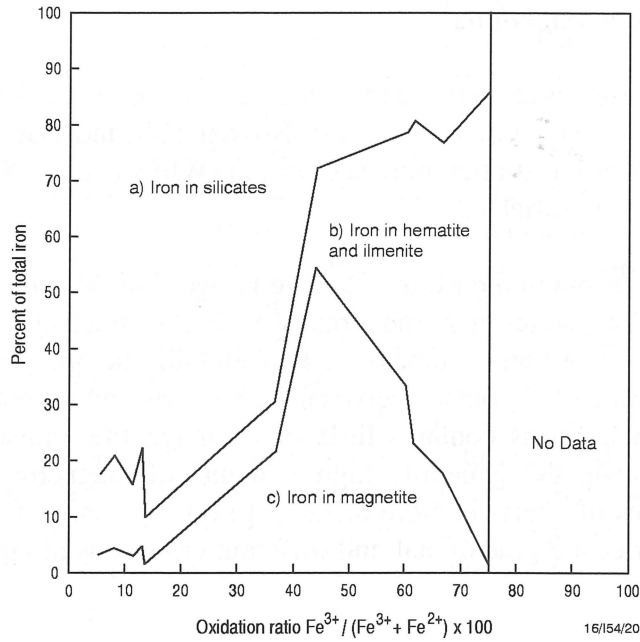


Figure 7. Oxidation ratio vs % of magnetite (after McIntyre 1980b; data from Chinner 1960).

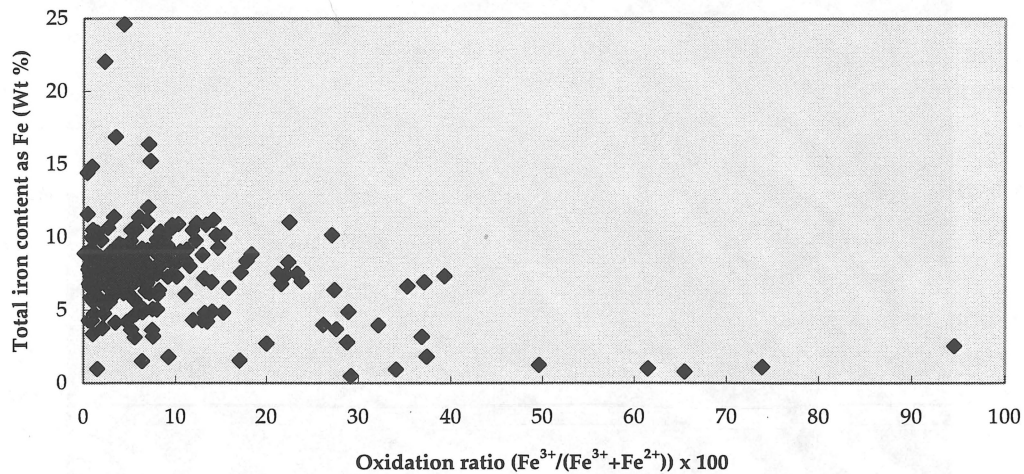


Figure 8. Oxidation ratio of 227 metasediments from across the Broken Hill Block (data from NSWDMR geochemical database). 95% of analyses have an oxidation ratio less than 30 and ~98% less than 40. Compare this to Fig. 7 and it can be seen that most of the iron is likely to be contained in silicates rather than magnetite. Four out of the five analyses with an oxidation ratio greater than 40 are Paragon Group sediments, which do show weak stratigraphic magnetic trends in places.

### *Composite gneisses and migmatite*

Composite gneisses (metasediments and leucocratic rocks with 10-50% melt) and migmatite (>50% melt) are found across the Broken Hill and Euriowie Blocks and occupy the lower part of the stratigraphic succession (Willis *et al.* 1983). The magnetic signature of these units is variable.

Composite gneiss crops out in the Mount Darling Range (Fig. 9) and can be subdivided on the basis of aeromagnetics into moderately to highly magnetic gneiss and non-magnetic gneiss. To the east and southeast of Broken Hill, the boundary between these two types corresponds to the contact between garnet-rich and garnet-poor composite gneiss. The garnet-rich gneiss contains little or no magnetite whilst the garnet-poor gneiss contains variable, but generally high amounts of magnetite. The distinction between the two types of gneiss is more difficult to distinguish in the Stephens Creek area, as unit boundaries are gradational and different criteria were employed to define map units.

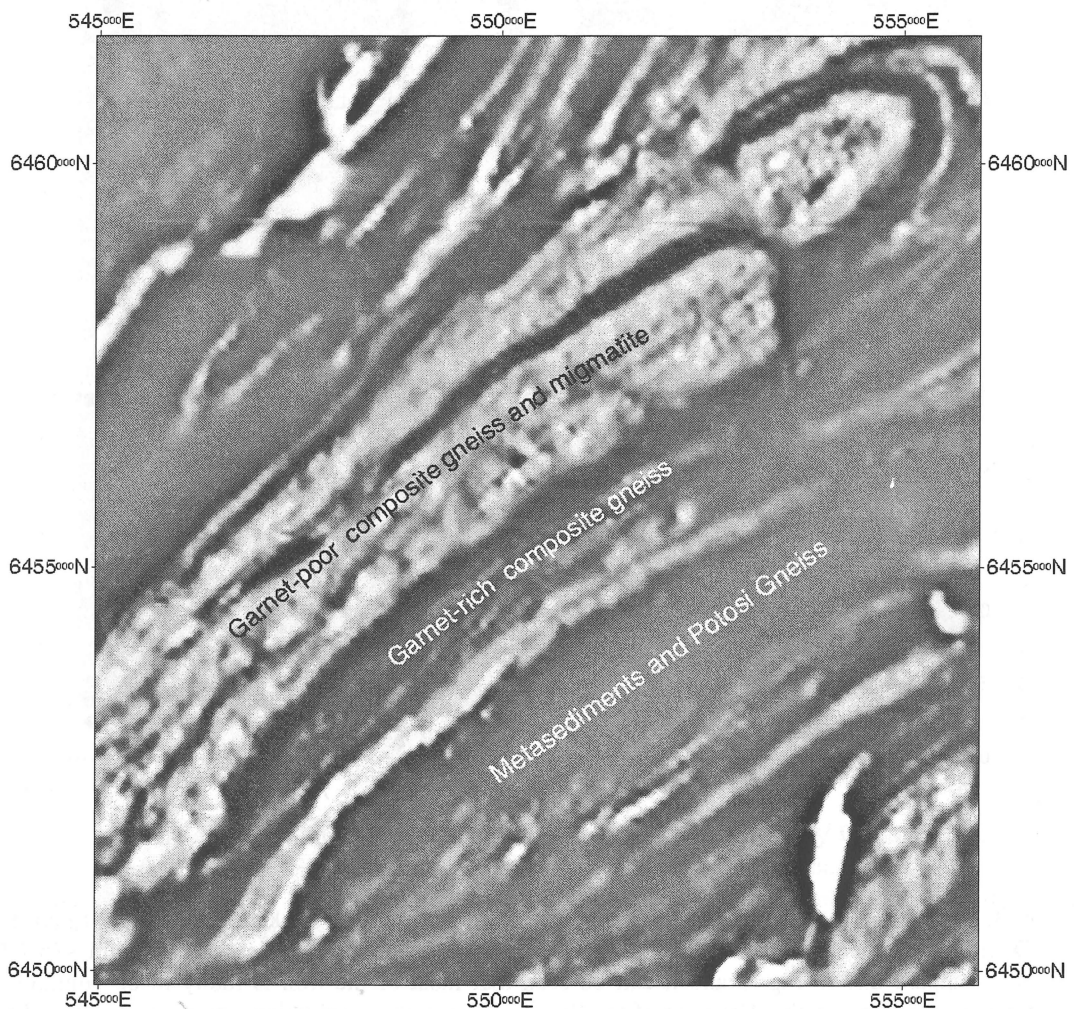


Figure 9. 1<sup>st</sup> vertical derivative of TMI of the Mount Darling Range, southeast of Broken Hill. Garnet-poor composite gneiss and migmatite are strongly magnetic and form a well-defined package of rocks in the aeromagnetics. Garnet-rich composite gneiss is uniformly non-magnetic and contrasts strongly with the garnet-poor gneiss. Metasediments and Potosi Gneiss of the Little Broken Hill area are also essentially non-magnetic.

Migmatite (assigned to the Clevedale Migmatite stratigraphic formation by NSWDMR) has a variable but generally high susceptibility. Variations in its aeromagnetic character can be ascribed to the variability of migmatisation in the unit.

Laurén (1969) describes magnetite-bearing pegmatites from southwest Finland. He considers these pegmatites to be essentially *in situ* partial melts and that the iron in the magnetite was derived from the breakdown of biotite and to a lesser extent, hornblende in the country rock. A similar process may explain the formation of magnetite in the composite gneisses and migmatites in the Broken Hill region. Willis *et al.* (1983) note that 'anatexis of the metasedimentary rocks in the Broken Hill Block probably proceeded in two stages by the breakdown of muscovite and biotite'. The iron released during anatexis became incorporated into the melt fraction and if the prevailing oxidation state was appropriate, formed magnetite. In more reduced composite gneiss, the iron seems instead to have been incorporated into garnet as Fe<sup>2+</sup>. The generally sharp and conformable contact between magnetic and non-magnetic composite gneisses suggests that the original oxidation state of the rocks influenced their subsequent magnetic signature.

Willis *et al.* (1983) consider that the composite gneisses and migmatites are not simply higher metamorphic grade equivalents of other metasediments in the same region. They argue that nearby metasediments are the same metamorphic grade and that it is the higher feldspar content of these rocks that gives rise to partial melting. They therefore consider the migmatitic rocks to be stratigraphically controlled, and confined to the lower parts of the sequence (Thackaringa Group and lower). If so, this would permit the extrapolation of mapped units below cover, albeit in a general manner, as these rocks do not occupy a unique stratigraphic position. One example is a large mass of garnet-poor composite gneiss interpreted beneath cover in the eastern part of the Mount Gipps 1:25 000 sheet (see Maidment *et al.* 1997). Aeromagnetic images delineate the approximate boundary of the unit and give some indication of structure, although detailed interpretation is problematic due to a lack of control from outcropping lithologies or drillhole data.

### **Quartz-albite rocks**

Quartz-albite rocks in the region are typically non-magnetic, often conspicuously so within a package of highly magnetic lithologies. There are, however, two areas where quartz-albite rocks contain appreciable magnetite: the Redan Geophysical Zone and an area to the northwest of Mount Gipps homestead in the northern part of the Block.

Northwest of Mount Gipps homestead, magnetite-bearing quartz-albite rocks occur in close association with quartz-magnetite rocks. Layering is continuous, with sharp contacts defined by variations in magnetite concentration and grain size (Fig. 42a). At one location (548860mE 6503760mN), quartz-magnetite rock is interlayered with quartz-albite rock, with quartz-magnetite layers ranging from 1 mm to several tens of centimetres thick. The quartz-magnetite layers show evidence of high strain, but it is unclear whether this strain is superimposed on original magnetite-rich sedimentary beds or whether the high-strain zone acted as a focus for magnetite formation.

At 548730mE 6502960mN, quartz-albite rock shows truncated layers, lenses and 'flame'-like structures defined by magnetite (Fig. 42b). These structures appear to be primary sedimentary features, but could conceivably be, in part, a result of high strain in these rocks.

The origin of the magnetite in the quartz-albite rocks is not clear. The magnetite may have replaced pelitic beds as a result of metasomatism adjacent to shear zones or be a metamorphic product. Alternatively, the magnetite may have formed along a pervasive tectonic fabric.

### **Redan Geophysical Zone**

The Redan Geophysical Zone (RGZ) is a poorly-exposed region to the southeast of Broken Hill with characteristically high and variable magnetic susceptibility (Fig. 4). The RGZ is comprised of the Thackaringa Group, the Mulculca Formation and the Ednas and Redan Gneisses in the New South Wales Department of Mineral Resources stratigraphic scheme.

The RGZ contains a variety of magnetite-rich rock types. Albite-quartz-hornblende-magnetite rocks (afm) are unique to the RGZ in the Broken Hill region and crop out as somewhat irregular masses up to 2 km long and 0.5 km wide. The afm rocks are typically well-layered and range in magnetite content from 3-10% (Corbett 1981). These rocks are considered by Stevens & Corbett (1993) to be detritus from an intermediate volcanic suite that had been variably altered and oxidised in shallow alkaline evaporitic lakes.

Quartzofeldspathic rocks in the RGZ are similar to those found throughout the rest of the region, but differ in that they have a variable, but generally high (up to 10%) magnetite content. These include quartz-albite rocks and leucocratic quartz-feldspar±biotite gneisses which have been interpreted as reworked acid volcanics or possibly syndeformational plutonic rocks (Stevens & Corbett 1993).

Although the aeromagnetic patterns over the RGZ are complex, there are areas where anomalies are more linear (Fig. 10). It is uncertain whether these anomalies correspond to particular lithologies due to the scarcity of outcrop.

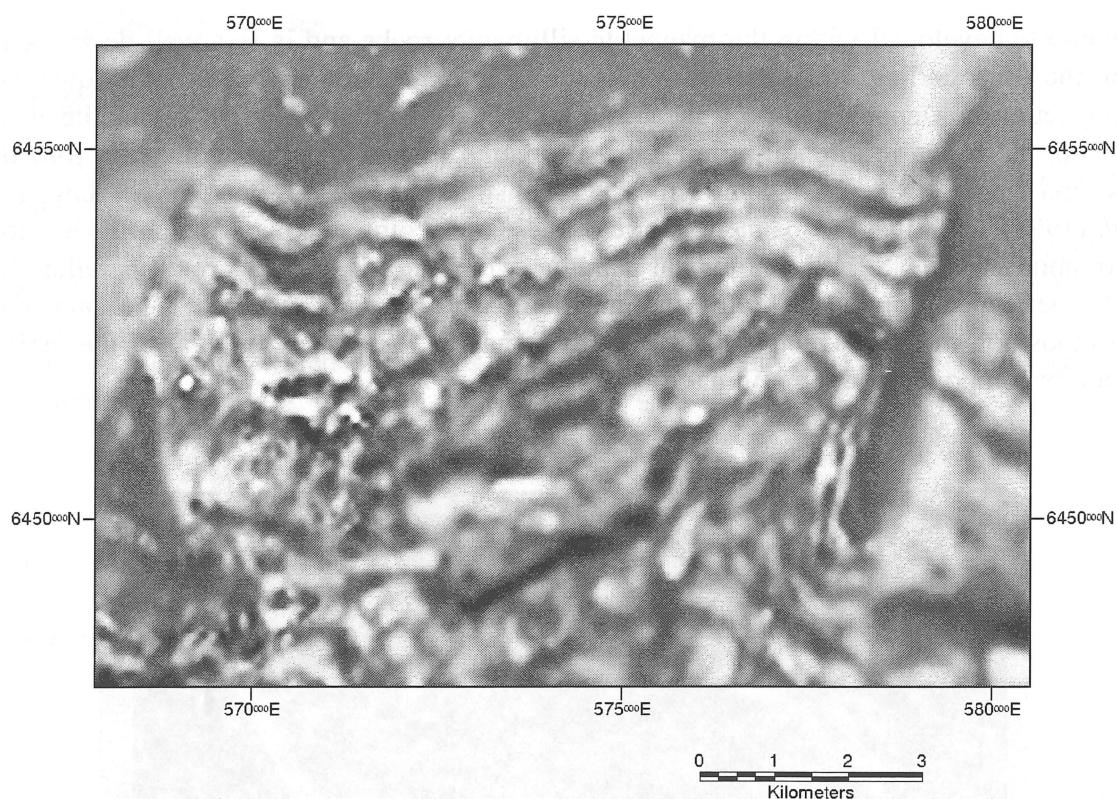


Figure 10. 1<sup>st</sup> vertical derivative of TMI over the northeastern part of the Redan Geophysical Zone. Numerous folded linear anomalies of uncertain (stratigraphic?) origin are present.

## Structurally controlled anomalies

Structurally controlled anomalies are widespread in the Willyama Supergroup and have not been previously recognised by earlier workers, who have considered the anomalies to be stratiform. Magnetite formed at various times, ranging from early ( $D_2?$ ) through  $D_3$  and in minor amounts at later times.

### Early magnetite ( $D_2?$ )

High-temperature shearing has long been recognised in the Broken Hill region (Andrews 1922, Gustafson *et al.* 1950, Archibald 1978), but received little detailed study until recently when White *et al.* (1995, 1996) published details of their structural analysis, suggesting that the Willyama Supergroup formed part of a fold and thrust belt. Both high-temperature and reactivated retrograde thrusts were recognised. Gibson *et al.* (1996, 1998) found that the tectonic transport direction of many of the thrusts was towards the northwest and not the southeast as had been previously thought and that thrusting had taken place later than implied by White *et al.* (1996). A  $D_3$  age for northwest-directed thrusting was inferred by Gibson (1998).

Magnetite-sillimanite rock in the Broken Hill Synform forms an intense, narrow anomaly (Fig. 11). The magnetite-sillimanite rock has a well-developed, steeply-dipping sillimanite lineation interpreted as a stretching lineation. Foliation is most

intensely developed within the magnetite-sillimanite rocks and is less well developed in the surrounding metasediments. A short, intense anomaly caused by quartz-magnetite rock appears to be truncated by the interpreted shear zone. Magnetite lies within the foliation in equilibrium with sillimanite (Fig. 42c). The anomaly is folded around the D<sub>3</sub> Broken Hill Synform, which constrains it as pre-D<sub>3</sub> in age. Giddings *et al.* (1998) noted that the magnetic fabric of these rocks dips steeply to the northwest, in common with S<sub>2</sub>, S<sub>3</sub> and lithological banding, which in this locality are all parallel. A D<sub>2</sub> (peak-metamorphic) age for the magnetite formation is inferred. The unusual composition of the magnetite-sillimanite rock may be due to the removal of the more mobile components of the original rock.

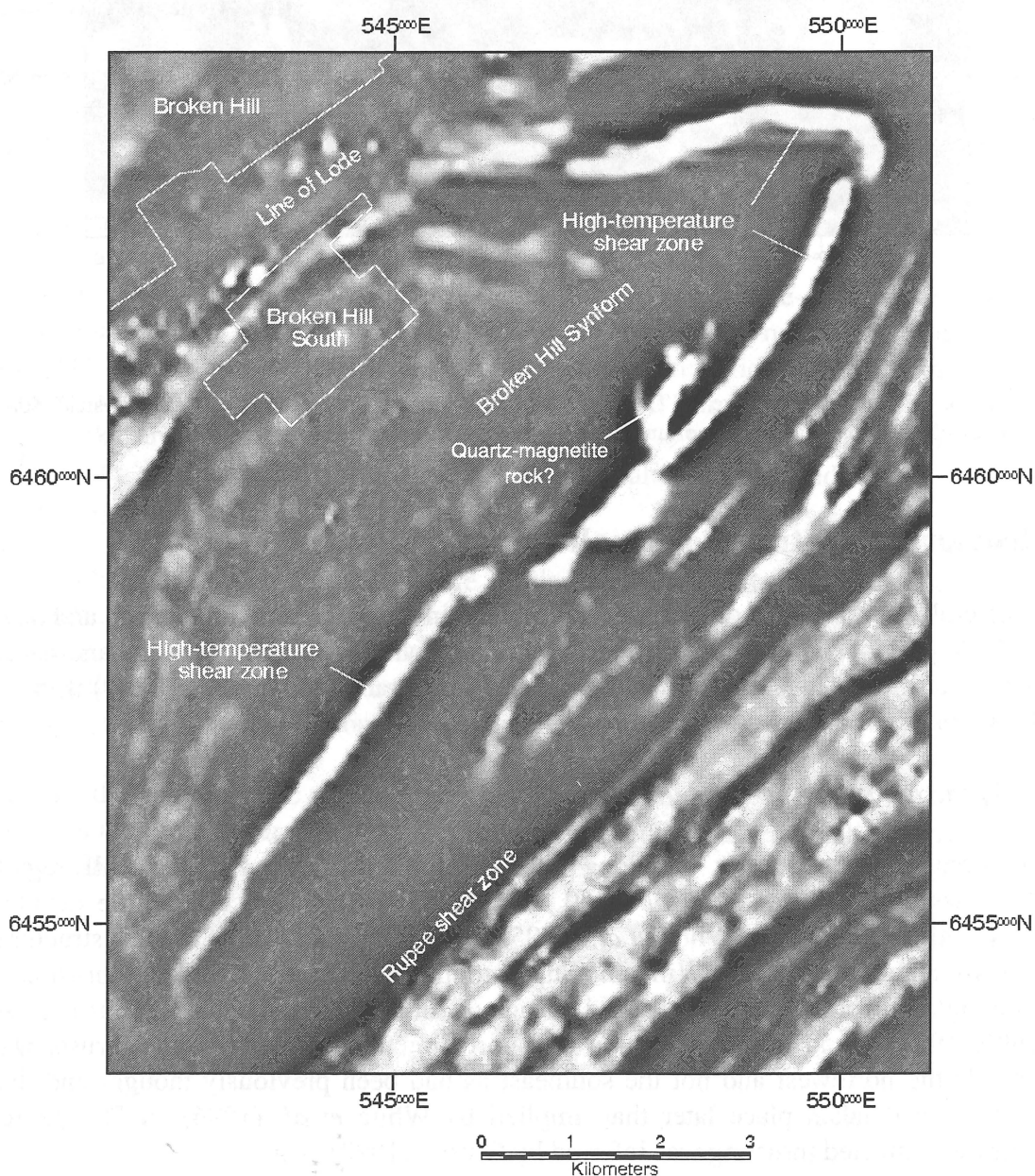


Figure 11. 1<sup>st</sup> vertical derivative of TMI of an area southeast of Broken Hill. The source of the intense, folded linear anomaly is mostly buried beneath cover, but does crop out in a few places as magnetite-sillimanite rock, interpreted as a high-temperature shear zone of probable D<sub>2</sub> age folded about the D<sub>3</sub> Broken Hill Synform. An intense anomaly, most likely caused by quartz-magnetite rock, is truncated against the shear zone.



## Magnetite in $S_3$ fabrics

### *Sculptures area*

An area close to the Sculptures, around 7 km NNW of Broken Hill was studied in detail as part of BHEI structural mapping. Aeromagnetic images indicate that a significant northeast-trending anomaly, or pair of anomalies, run through the area in apparent conformity with bedding trends marked on the NSWDMR 1:25 000 geological map (Fig. 12). The area comprises pelitic and psammitic schists of the Sundown Group, which in places are well-bedded and show preserved primary sedimentary structures.

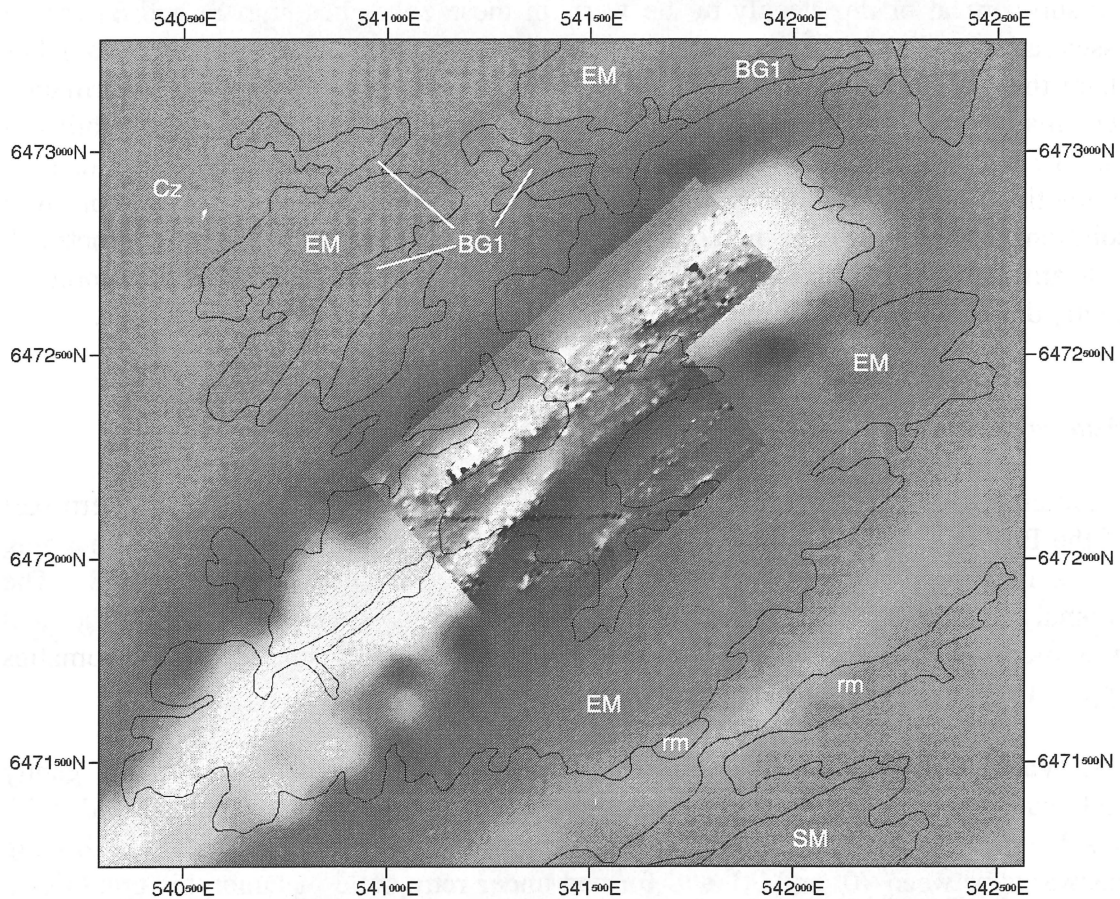


Figure 12. Detailed TMI data collected by NSWDMR superimposed on the 1<sup>st</sup> vertical derivative of TMI for an area close to the Sculptures, NNW of Broken Hill. The main anomalies trend northeast, with minor displacement across late E-W-trending shears. These anomalies coincide with intense development of the  $D_3$  schistosity, which locally draws bedding into parallelism, but cross-cut the general  $S_0$  enveloping surface to  $D_3$  folds, which strikes broadly northwest. EM: Pelite and psammopelite, BG1: Potosi gneiss, SM: psammite and psammopelite, rm: retrograde shear zone, Cz: Cainozoic alluvium.

Three high-grade fabrics are present in the Sundown Group (Gibson *et al.* 1996), the last of which ( $S_3$ ) is steeply-dipping and trends northeast. This fabric is recognised in the Sculptures area and was superimposed on an earlier, shallower-dipping  $S_2$  surface, producing a conspicuous crenulation cleavage in most lithologies. Development of the  $S_3$  fabric was accompanied by tight to isoclinal folding, widespread transposition and the formation of high-temperature shear zones which locally disrupt the  $D_3$  folds and local stratigraphy. A fourth phase of deformation produced crenulations and open folds. Unlike the earlier phases of deformation,  $D_4$  folds lack an obvious axial plane fabric.

A significant degree of strain partitioning accompanied the  $D_3$  deformation. This is best illustrated in the southern part of the area where packets of more shallow-dipping bedding are separated by high strain zones in which bedding and the earlier  $S_2$  fabrics are sub-vertical or dip steeply to the west. In these zones bedding,  $S_2$  and  $S_3$  are all essentially parallel and trend northeast. Significantly, the major magnetic anomalies share the same northeast trend, suggesting that the last phase of intense deformation ( $D_3$ ) may have exercised some degree of control on their formation. One possibility is that the  $D_3$  deformation led to a dynamically induced increase in permeability, thereby promoting fluid flow and the formation of magnetite by oxidation or precipitation from solution. It should also be noted that the magnetic anomalies are near-symmetrical, indicating that their source is steeply-dipping. Bedding, on the other hand, is commonly gently dipping outside the high-strain zones where there are no major anomalies.

#### ***Waukeroo Bore area***

An intense linear magnetic anomaly just north of Waukeroo Bore in the northern part of the Broken Hill Block was selected for detailed study. Detailed structural mapping and a rock property study were carried out (see also Giddings *et al.* 1998). The anomaly trends approximately north-northeast and is situated within pelitic and psammopelitic schists mapped as Sundown Group (Fig. 13). Smaller linear anomalies appear to truncate against the main anomaly.

The Waukeroo Bore area encompasses metre to kilometre-scale, recumbent to gently reclined  $D_2$  folds which are variably overprinted by upright, tight to isoclinal folds with a subvertical to steeply-dipping axial plane fabric ( $S_3$ ).  $S_3$  trends NNE, dipping eastwards between  $70^\circ$  and  $80^\circ$  and formed under retrograde metamorphic conditions, cutting obliquely across  $D_2$  fold axes. Magnetite lies within the  $S_3$  fabric as finely disseminated grains and crystals up to 1-2 cm in size.  $D_3$  folds plunge north or south and were superimposed upon a shallower-dipping, sillimanite-grade  $S_2$  surface which is axial planar to asymmetric, generally northwest-verging  $D_2$  folds. The enveloping surface to  $S_0$  is shallow-dipping notwithstanding steep dips in  $S_0$  for individual outcrops.

Giddings *et al.* (1998) conducted two detailed ground magnetometer traverses and collected oriented cores at regular intervals for magnetic property measurements. Modelling of the anomaly indicated a tabular body approximately 125m wide, of great depth extent, dipping steeply to the east at around  $80^\circ$ . Giddings *et al.* (1998) also examined the anisotropy of magnetic susceptibility and found a well-defined magnetic fabric dipping  $82^\circ$  to the ESE ( $109^\circ$ ). Both the source of the anomaly and the magnetic

fabric coincide with the orientation of the  $S_3$  fabric. The enveloping surface to  $S_0$ , in contrast, is shallow-dipping on a regional scale. It is thus apparent that the source of the magnetic anomaly is structurally controlled by the  $S_3$  fabric and does not reflect sedimentary bedding.

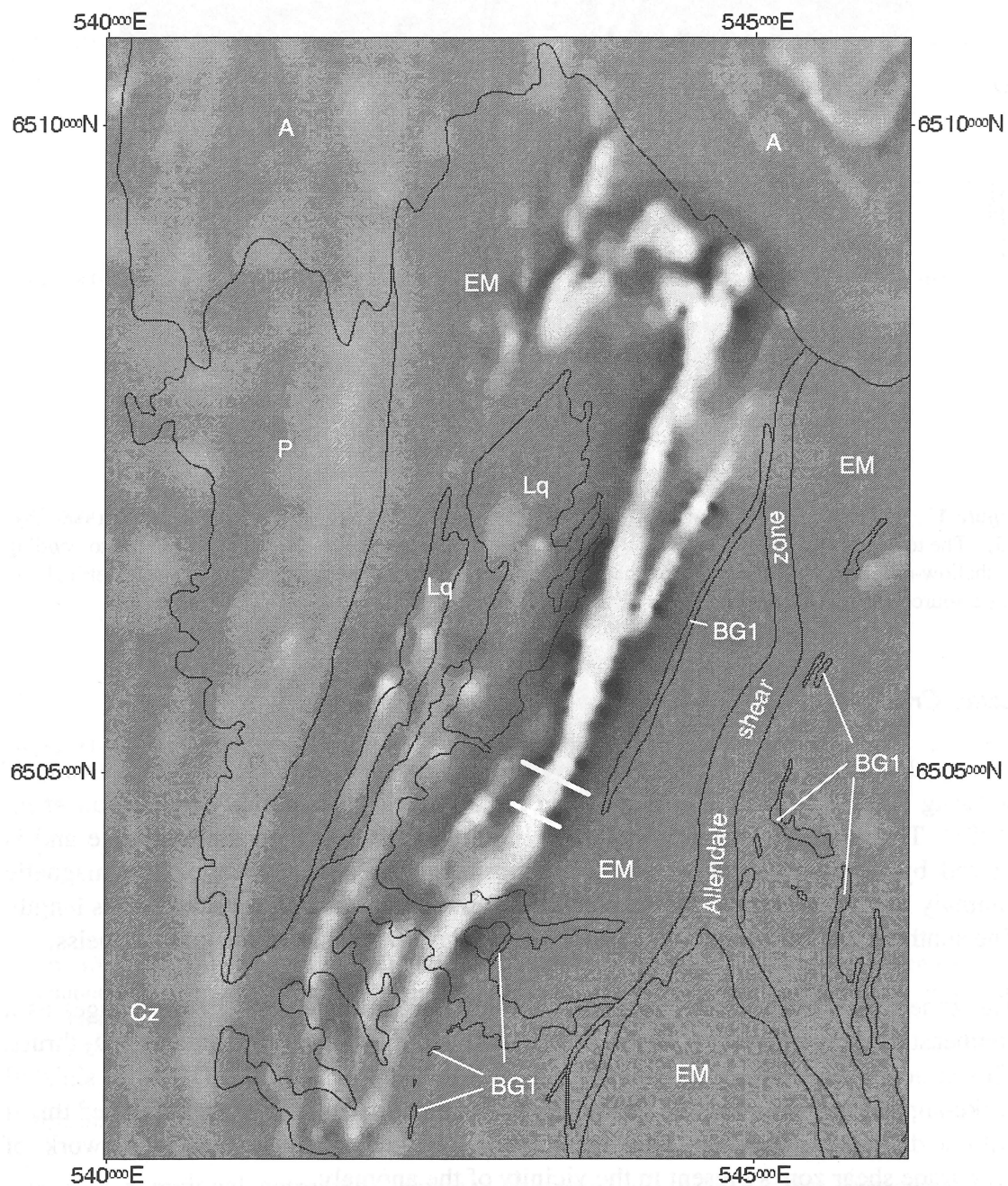


Figure 13. 1<sup>st</sup> vertical derivative of TMI of the Waukeroo Bore area in the north of the Broken Hill Block. The positions of two detailed magnetometer/structural traverses are shown as bold white lines. EM: Pelite and psammopelites, Lq: pegmatite, BG1: Potosi gneiss, P: Paragon Group, A: Adelaidean.

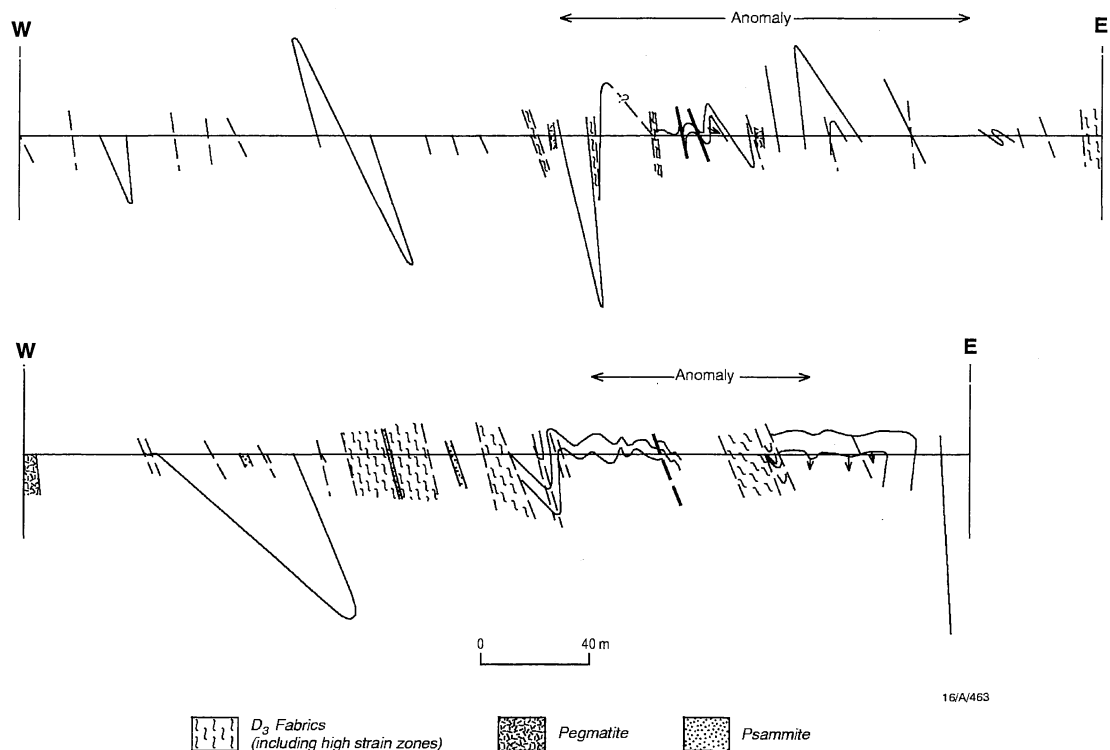


Figure 14. East-west cross sections across the main magnetic anomaly in the Waukeroo area (see Fig. 13). The top section lies ~500 m north of the lower section. Note that the enveloping surface to bedding is shallow-dipping on a regional as opposed to outcrop scale. The magnetic anomaly is symmetrical and has a source that dips steeply to the east, sub-parallel to  $S_3$ . Arrows indicate inverted bedding.

### **Lakes Creek area**

In the Lakes Creek region there is a northeast-trending linear anomaly within a zone of shearing (Fig. 15) informally named the Lakes Creek Discontinuity by Gibson *et al.* (1998). The anomaly is transgressive to lithological layering on a broad scale and is caused by magnetic metasediments, composite gneiss and pegmatite. The magnetic anomaly lies to the west of a thin, continuous granite gneiss unit for much of its length. The southern end of the anomaly, however, lies just to the east of the granite gneiss.

The zone of shearing which hosts the anomaly is represented on seismic images as a southeast-dipping reflector (Gibson *et al.* 1998) and may have originated as a  $D_3$  thrust. This structure was later reactivated during the breakup of Rodinia ( $D_4$ ) as a sinistral strike-slip shear and during the Delamerian Orogeny ( $D_5$ ) as a northwest-directed thrust with a dextral component. This reactivation resulted in the extensive network of retrograde shear zones present in the vicinity of the anomaly.

Giddings *et al.* (1998) examined the southern part of the anomaly in the Acacia Vale area and found that the anomaly source, anisotropy of magnetic susceptibility,  $S_0$  and the  $S_3$  schistosity all have similar steep dips. From these data they were unable to determine whether the anomaly is hosted by a magnetic stratiform unit or whether magnetite has formed during  $D_3$ . However, the close spatial association between the

anomaly and a D<sub>3</sub> shear zone and the fact that the anomaly is regionally transgressive to lithological layering favours a structural control of probable D<sub>3</sub> age.

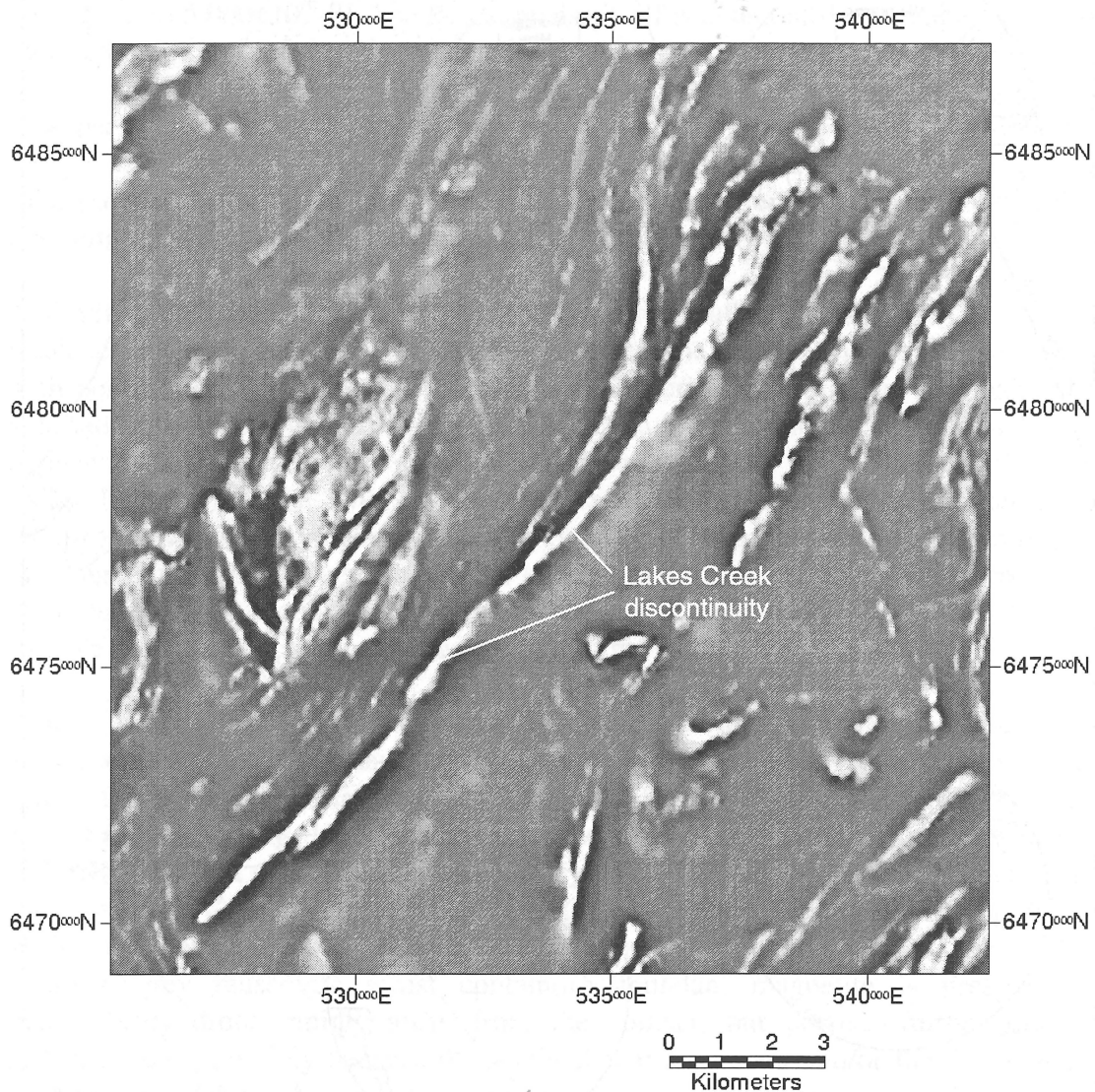


Figure 15. 1<sup>st</sup> vertical derivative of TMI of the Lakes Creek discontinuity, northwest of Broken Hill. The discontinuity is interpreted as having originated as a D<sub>3</sub> thrust reactivated during the breakup of Rodinia (D<sub>4</sub>) and the Delamerian Orogeny (D<sub>5</sub>).

### ***Regional S<sub>3</sub> control on magnetite***

There is a regional correlation between the trend of many of the linear magnetic anomalies and the orientation of S<sub>3</sub> (compare Figures 4 and 16). In the northern part of the Broken Hill Block, S<sub>3</sub> strikes approximately NNE. Further to the south, S<sub>3</sub> has a more northeasterly trend. This correlation suggests that S<sub>3</sub> had a significant regional control on magnetite formation and that a large proportion of the anomalies are of D<sub>3</sub> age.

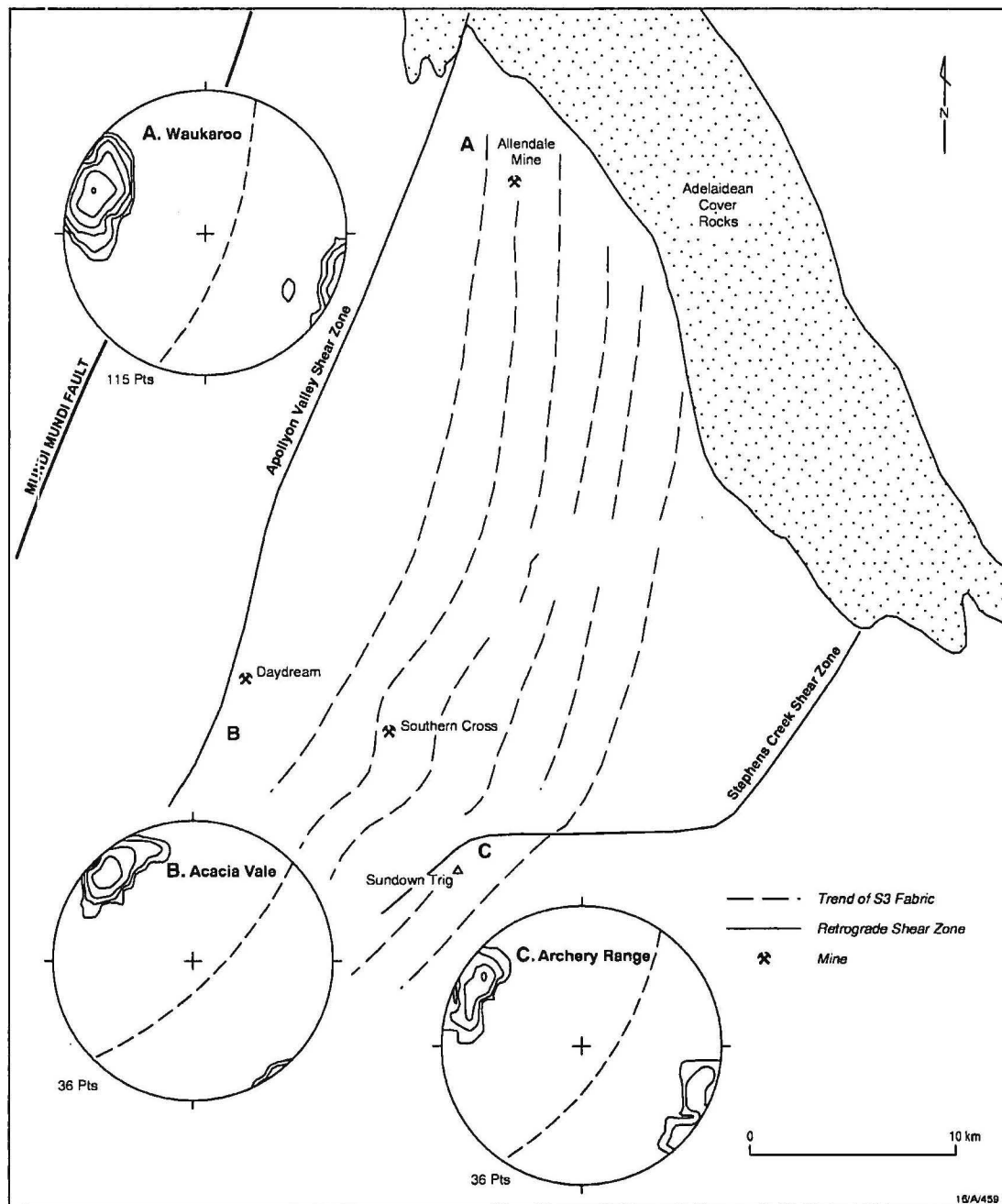


Figure 16. Trend of  $S_3$  across the central and northern part of the Broken Hill Block. The  $S_3$  fabric parallels many magnetic anomalies (cf Fig. 4) and appears to be a significant factor in concentrating magnetite in the region.

### Magnetite at lithological contacts

The superposition of aeromagnetic data upon 1:25 000 scale geological maps reveals a close spatial association between some Potosi gneiss units and magnetic anomalies. Detailed ground truthing reveals that it is not the main mass of the Potosi gneiss itself which is magnetic, but the contact zone between Potosi gneiss and surrounding metasediments.

An example occurs about 1.2 km southeast of the Centennial Mine where a unit of Potosi gneiss lies within pelitic schist. At this locality, the highest magnetic susceptibilities occur in metasediments adjacent to the Potosi unit. Magnetic susceptibilities at the eastern contact range up to  $18\,000 \times 10^{-6}$  SI and on the western contact up to  $5\,000 \times 10^{-6}$  SI. The Potosi gneiss itself is essentially non-magnetic and the metasediments away from the contact also have a low susceptibility.

It appears that strain has been partitioned into the zone between the relatively competent Potosi units and less competent metasediments. Fluid flow has been focussed along this zone which has resulted in the formation of magnetite, either from precipitation from the fluid, or by oxidation of iron by the fluid.

A similar situation occurs about 700 m NNE of the Southern Cross Mine. A relatively weak aeromagnetic anomaly ( $\sim 150$  nT) occurs over the eastern contact of Potosi gneiss with pelitic metasediments. The contact is characterised by abundant tourmaline and sillimanite, commonly occurring as very coarse-grained interlocking crystals. The highest magnetic susceptibilities occur in lenses and pods of tourmaline-sillimanite rocks along the contact. Thin sections of these rocks show euhedral zoned tourmaline intergrown with sillimanite and magnetite in an equilibrium assemblage indicating that the magnetite formed under high-grade conditions (Fig. 42d). The western contact of the Potosi is with pegmatite and hosts no magnetite, presumably due to the lack of a suitable competency contrast to localise fluid flow.

Granite gneisses have a similar competency contrast with surrounding metasediments and in some locations also have anomalies at their margin. A granite gneiss body in the Mount Darling Range near Clevedale homestead has a fairly intense, narrow anomaly around its margin (Fig. 17). The granite gneiss is situated in a zone of intense shearing and mylonitisation which hosts a number of strong anomalies. The granite gneiss itself is conspicuously non-magnetic set against this background. The highest susceptibilities are located along the contact between the gneiss and surrounding metasediments where a silvery-grey muscovite schist containing abundant magnetite is present. The susceptibility drops rapidly away from the contact, but persists further into the metasediments, possibly because of their higher iron content and/or the fact that their schistose fabric was more permeable than the granite gneiss.

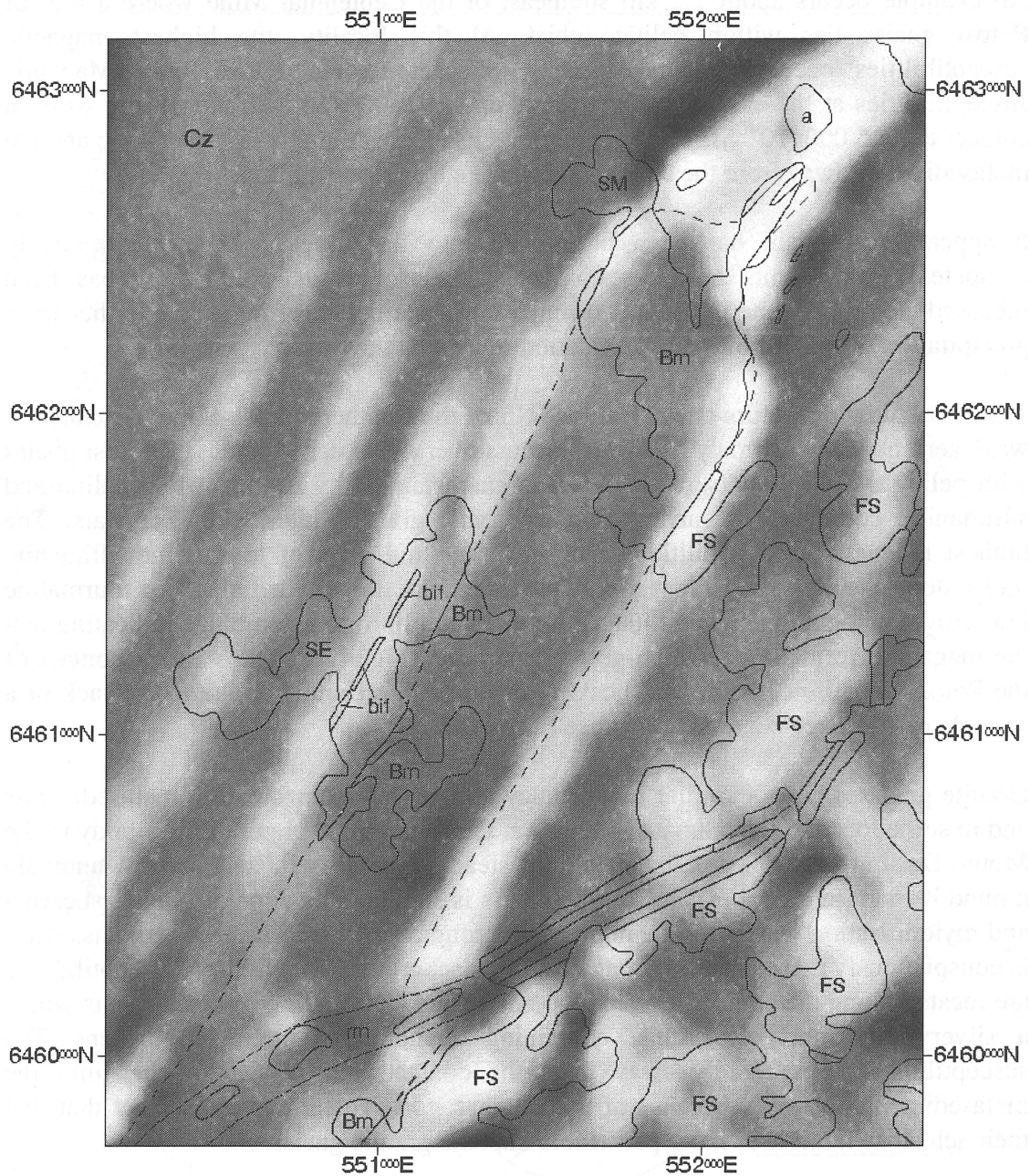


Figure 17. 1<sup>st</sup> vertical derivative of TMI for an area near Clevedale Homestead, east of Broken Hill. Magnetite has formed around the margin of a granite gneiss body where strain has been partitioned between the relatively competent quartzofeldspathic gneiss and less competent metasediments and composite gneiss. Bm: granite orthogneiss, FS: psammitic composite gneiss, SE: psammite and pelite, bif: banded iron formation, rm: retrograde shear zone, Cz: Cainozoic alluvium.

A granite gneiss body in the northwest part of the Lakes Creek 1:25 000 sheet also is ringed by an aeromagnetic anomaly (Fig. 18). The highest susceptibilities are again found along the contact between the granite gneiss and metasediments where deformation has been focussed.



The precise timing of magnetite formation around the margins of competent units is uncertain, but typically occurred during high-temperature conditions, as evidenced by the association of sillimanite with magnetite. Reactivation of the contact zones under retrograde conditions tends to obscure higher temperature assemblages and fabrics and it possible that the anomalies may have formed at different times during the tectonothermal history of the region.

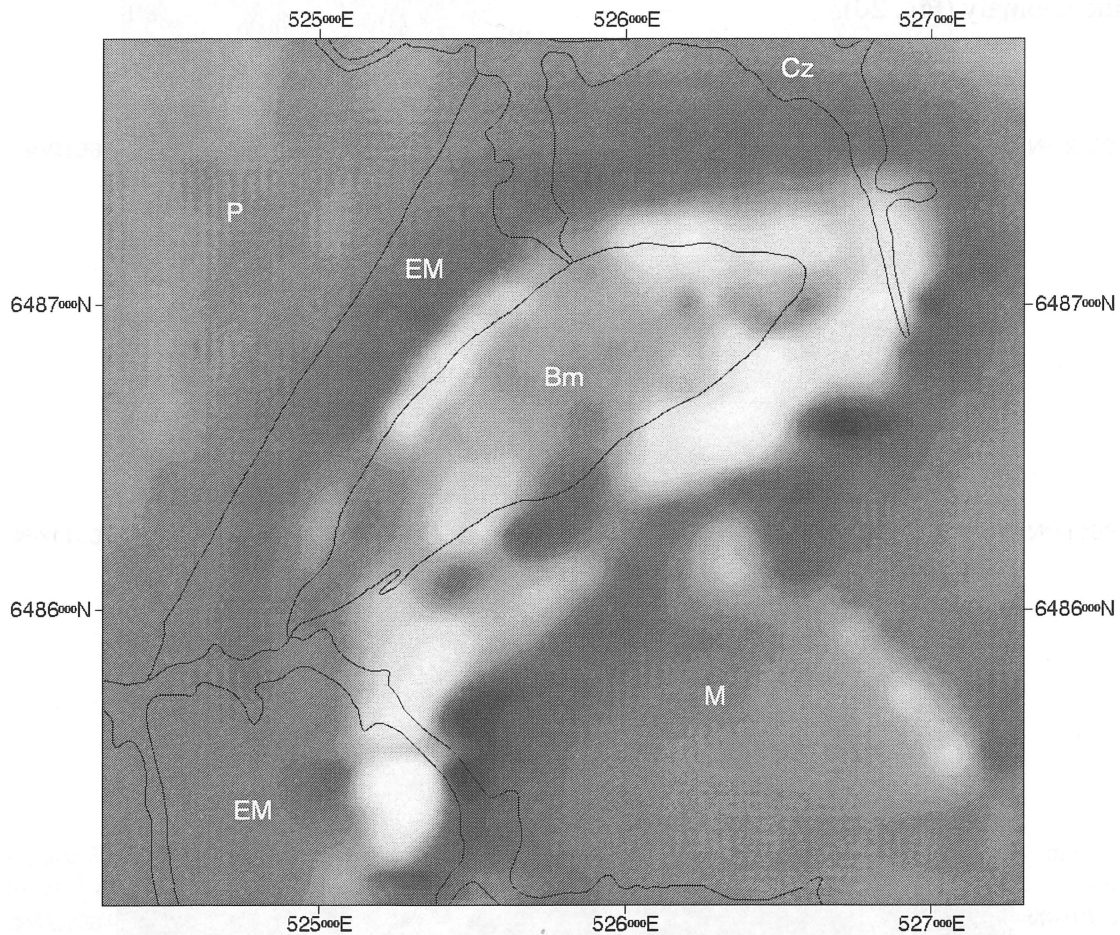


Figure 18. 1<sup>st</sup> vertical derivative of TMI for an area in the northwest of the Lakes Creek region, northwest of Broken Hill. An elliptical granite gneiss body is ringed by a magnetic anomaly possibly caused by focussing of fluid flow around the granite gneiss margin. Bm: granite gneiss, M: psammopelitic metasediments and composite gneiss with amphibolite. EM: pelite and psammopelite, Cz: Cainozoic alluvium.

## Later-stage magnetite

### *Gairdners Tank area*

An isolated linear magnetic anomaly occurs around 2 km NNE of Gairdners Tank near the eastern margin of the Euriowie Block (Fig. 19). It coincides with the northern section of a fault mapped on the Gairdners Tank 1:25 000 geological sheet (Brown 1985). Adjacent lithologies are non-magnetic and have a strike oblique to the trend of the anomaly (Fig. 20).

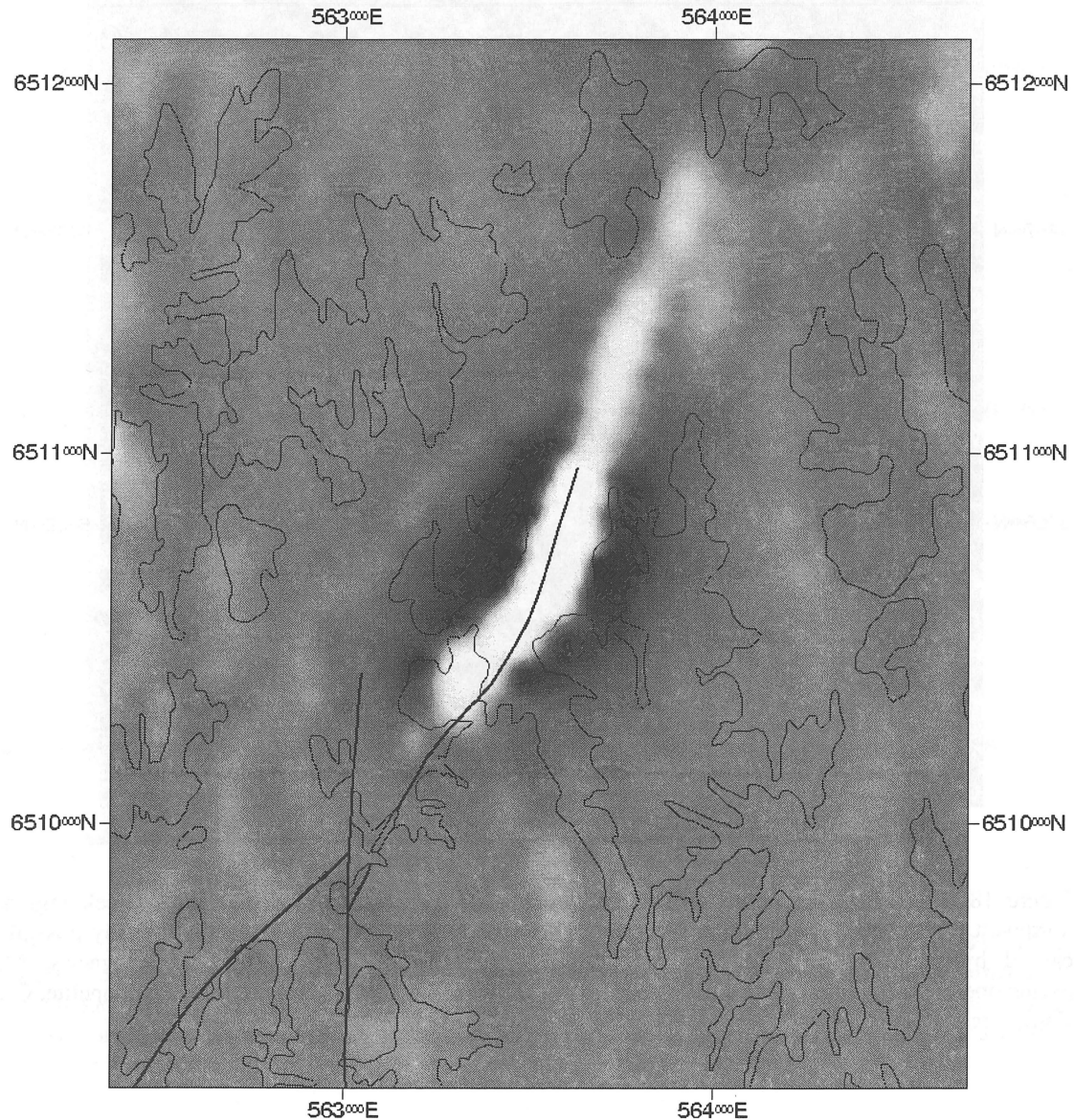


Figure 19. 1<sup>st</sup> vertical derivative of TMI of an area on the eastern margin of the Euriowie Block, NNE of Gairdners Tank. The magnetic anomaly is structurally controlled and follows the trace of a mapped shear zone. The anomaly formed post-peak metamorphism and is caused by coarse, euhedral magnetite in chloritic schist and pegmatite.

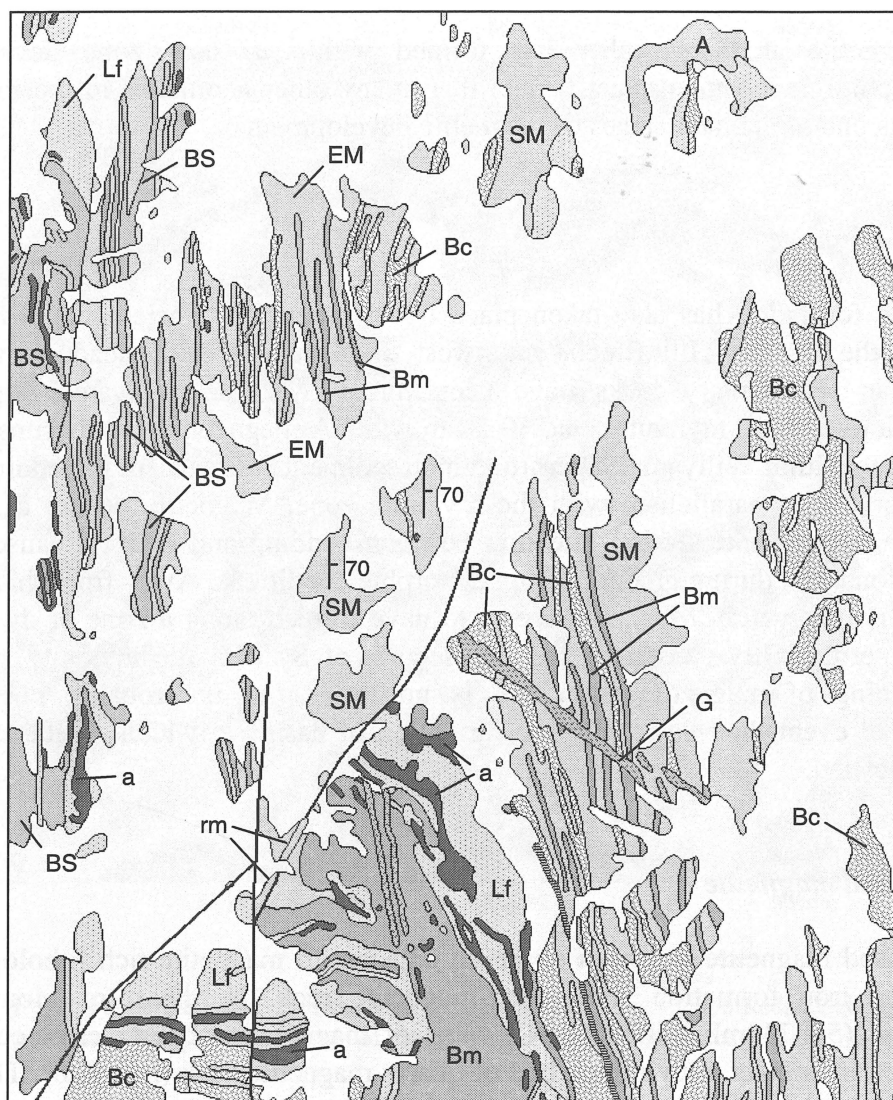


Figure 20. Geological map of the same area as Figure 19 (from Gairdners Tank 1:25 000 geological map). Lithological trends are oblique to the orientation of the main magnetic anomaly, which is sub-parallel to the mapped fault. SM: psammite and psammopelite, EM: pelite and psammopelite, Bm: medium-grained granite gneiss, Bc: augen-rich granite gneiss, BS: sillimanite-rich granite gneiss, a: amphibolite, Lf: leucocratic gneiss, rm: retrograde schist, A: Adelaidean.

The source of the anomaly is coarse- to very coarse-grained euhedral magnetite in schistose psammitic metasediments and pegmatite. The magnetite lies within a steeply-dipping, chlorite-rich schistosity which wraps around some crystals and abuts against others suggesting that the magnetite and the schistosity are penecontemporaneous (Fig. 42e). Chlorite is also found within pressure shadows surrounding magnetite crystals. Iron oxide pseudomorphs after pyrite ('devils dice') are found in the magnetite-bearing rocks, some slightly strained by later deformation. The pseudomorphs commonly have a selvage of quartz and overprint the magnetite. Minor tourmaline is also associated with the magnetite.

The magnetite at this locality has formed within a shear zone during lower metamorphic grade (greenschist facies) than many other anomalies in the region and represents one of the later stages of magnetite development.

### ***Wendelapa area***

Magnetite formation has also taken place under greenschist facies conditions in the north of the Broken Hill Block, southwest of Wendelapa homestead. In this area, Adelaidean sedimentary rocks have been thrust over the Willyama Supergroup, forming a retrograde mylonite zone 30-50 m wide. A magnetic anomaly runs adjacent to this zone within Willyama Supergroup metasediments, discordant to bedding and  $S_3$  which curve into parallelism with the mylonite zone. Magnetite occurs as euhedral crystals along the intersection lineation between bedding and a fabric caused by the reactivation of  $S_3$  during greenschist metamorphic conditions. Away from this zone,  $S_3$  contains no magnetite. Magnetite seems to have formed along a zone of dynamically induced permeability caused by the intersection of  $S_3$  with the mylonite zone. The exact timing of magnetite formation is uncertain, but is probably post- $D_4$ , the extensional event that resulted in the formation of basins in which Adelaidean rocks were deposited.

### ***Remobilised magnetite***

Remobilised magnetite has been observed adjacent to magnetite-rich lithologies such as banded iron formation and quartz-magnetite rock. Northeast of Mount Gipps homestead (548730mE 6502960mN), veins of magnetite + quartz cross-cut quartz-albite rock in contact with a thick bed of quartz-magnetite rock (Fig. 42b). The timing of these veins is uncertain; they cross-cut tight folds in the quartz-albite rock and are folded themselves by a later deformation.

Remobilised magnetite is also present adjacent to banded iron formation on the western limb of the Broken Hill Synform and in the Little Broken Hill area. In these areas, thin veins of magnetite cross-cut enclosing rocks within one metre of the contact with banded iron formation. In the Little Broken Hill area, magnetite veins are developed along the axial plane of north-south-trending, upright folds in BIF.

### **Retrograde shear zones**

Retrograde shearing in the Broken Hill and Euriowie Blocks is widespread and is generally magnetite-destructive, forming linear zones of low susceptibility on aeromagnetic images. Identification of these shear zones is relatively easy where the background susceptibility is high (e.g. the Redan Geophysical Zone - Fig. 21) but is more difficult in the bulk of Willyama Supergroup rocks, where susceptibilities are generally low. In these areas, retrograde shear zones can be delineated where they offset magnetic anomalies (Fig. 22).

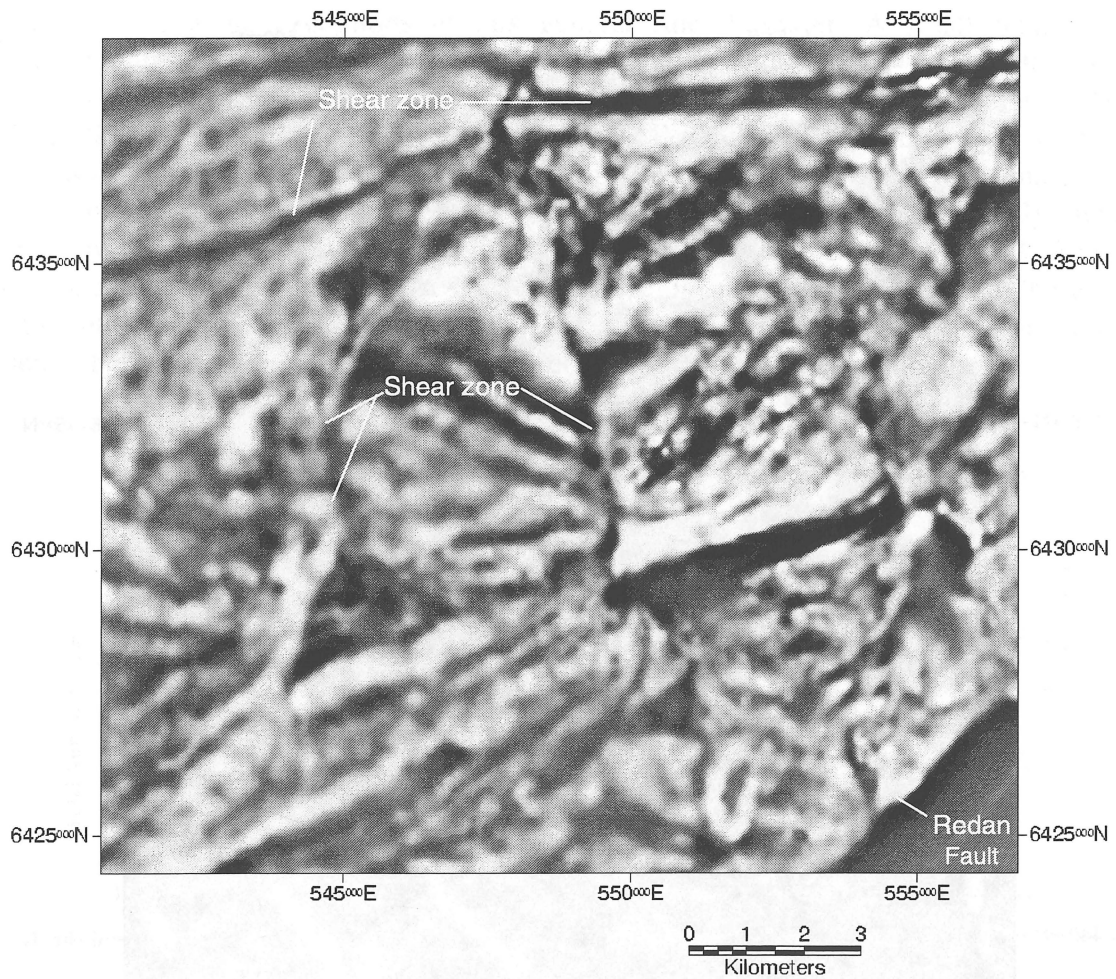


Figure 21. 1<sup>st</sup> vertical derivative of TMI showing retrograde shear zones in the Redan Geophysical Zone. The shear zones are evident as linear zones of low magnetic intensity that truncate other magnetic trends.

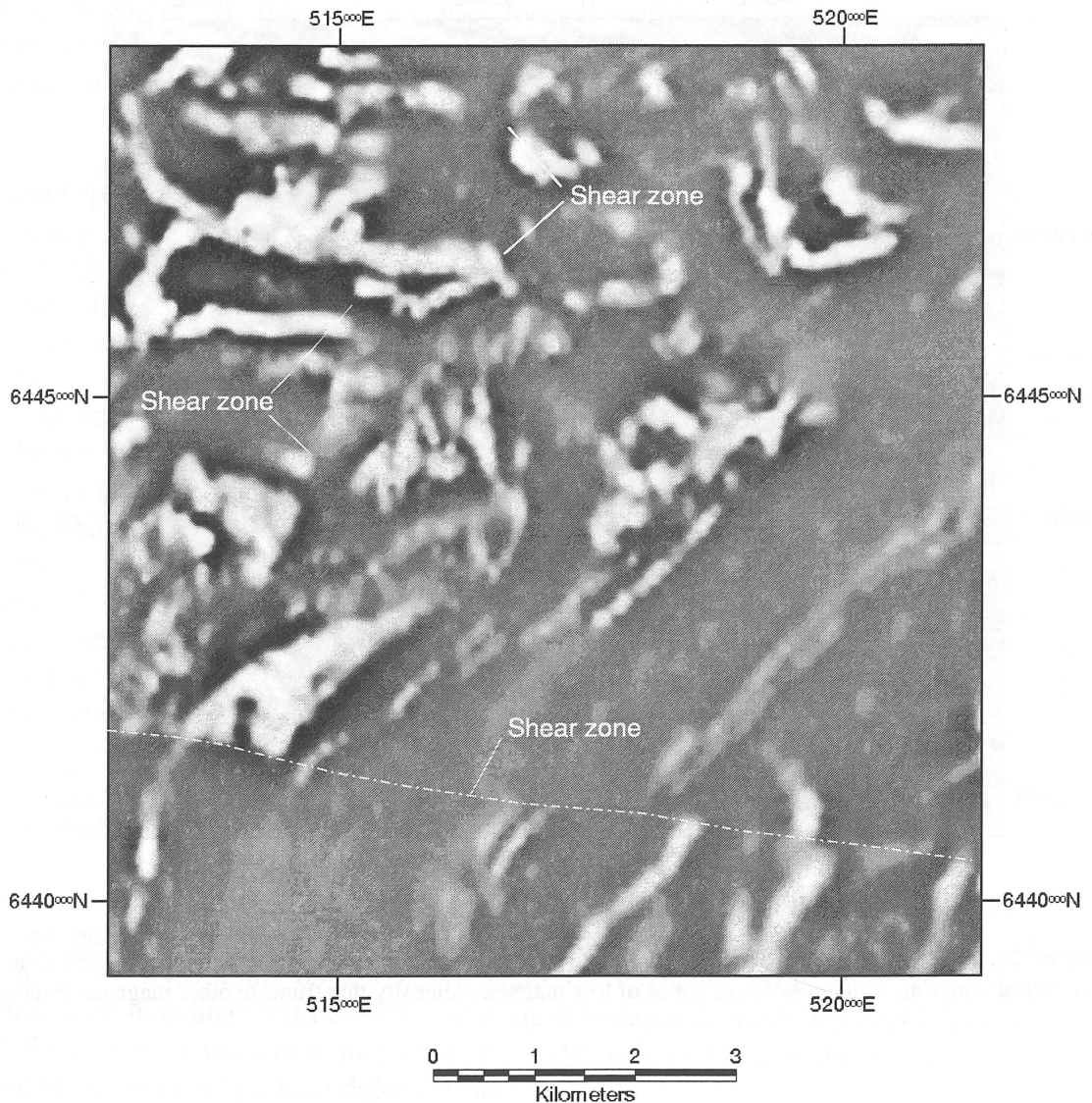


Figure 22. 1<sup>st</sup> vertical derivative of TMI for an area on the Triple Chance 1:25 000 sheet. In this area of generally low background magnetic susceptibility, retrograde shear zones can be delineated where they dislocate and truncate magnetic trends.

## Aeromagnetic signatures of igneous rocks

### Mafic Rocks

#### *Amphibolite*

Amphibolite is widely distributed, occurring in every stratigraphic group older than the Sundown Group. It generally crops out as elongate bodies, often continuous for several kilometres and ranging from 1-200 m in thickness. Most amphibolites in the region are only weakly magnetic ( $\sim 1\ 000 \times 10^{-6}$  SI), with a low oxidation ratio (Fig. 23) and generally do not produce significant aeromagnetic anomalies. Ilmenite is the most common opaque mineral in these rocks and may contribute to the weak susceptibility.

There are notable exceptions to this general rule, however. A small number of amphibolites have very high magnetic susceptibilities and produce some of the most intense anomalies in the region (e.g. the western part of the Stirling Vale synform). The bimodal nature of amphibolite susceptibility could conceivably be due to two separate suites of amphibolite, each with its own initial oxidation state and magnetite concentration. However, U-Pb dating of amphibolite in the region consistently yields ages of around 1690 Ma (e.g. Nutman & Gibson 1998, Donaghy *et al.* 1998), suggesting the amphibolites are related. There is also no apparent link between susceptibility and composition. It therefore seems likely that the highly magnetic amphibolites are a product of localised alteration.

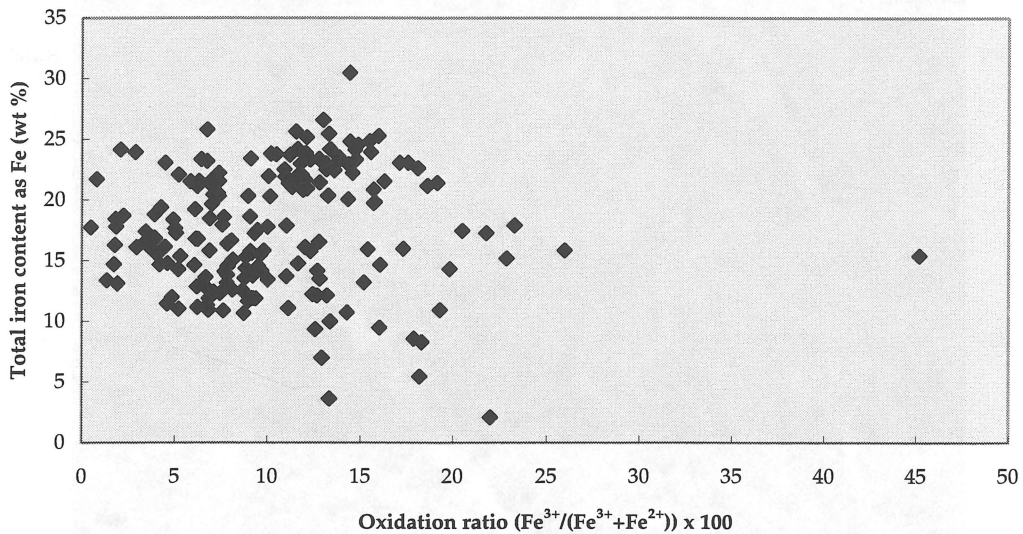


Figure 23. Oxidation ratio of 185 amphibolites from across the region, showing that the oxidation ratio is generally low. Total iron shows no tendency to increase with increasing oxidation ratio, suggesting that iron has not been introduced into the more magnetic amphibolites, but rather oxidised *in situ*. It is unknown how many magnetic amphibolites are included in this dataset; additional analyses of magnetic amphibolites would be required to confirm this pattern.

A relatively intense northeast-trending linear anomaly occurs to the southeast of the Broken Hill orebody (Fig. 24). It is caused by a combination of magnetic amphibolite and banded iron formation. The anomaly runs adjacent to an interpreted stratigraphic break, first noted by Andrews (1922) between the Hanging Wall synform and the Broken Hill synform (interpreted as the Broken Hill antiform by some workers). White *et al.* (1995, 1996) noted that a granite gneiss in this area was ‘a major zone of mylonitisation’ and interpreted the feature as a high-temperature thrust.

The magnetic amphibolite in this area is in contact with the granite gneiss and also in places displays high-temperature mylonitic fabrics (Fig. 42f). Amphibolite with the highest susceptibilities in this area commonly displays abundant layer-parallel partial melting. Amphibolite away from this zone of shearing has no associated anomaly. Magnetite in the amphibolite is recrystallised along with high-temperature hornblende, indicating that it formed pre- or syn-high-temperature metamorphism.

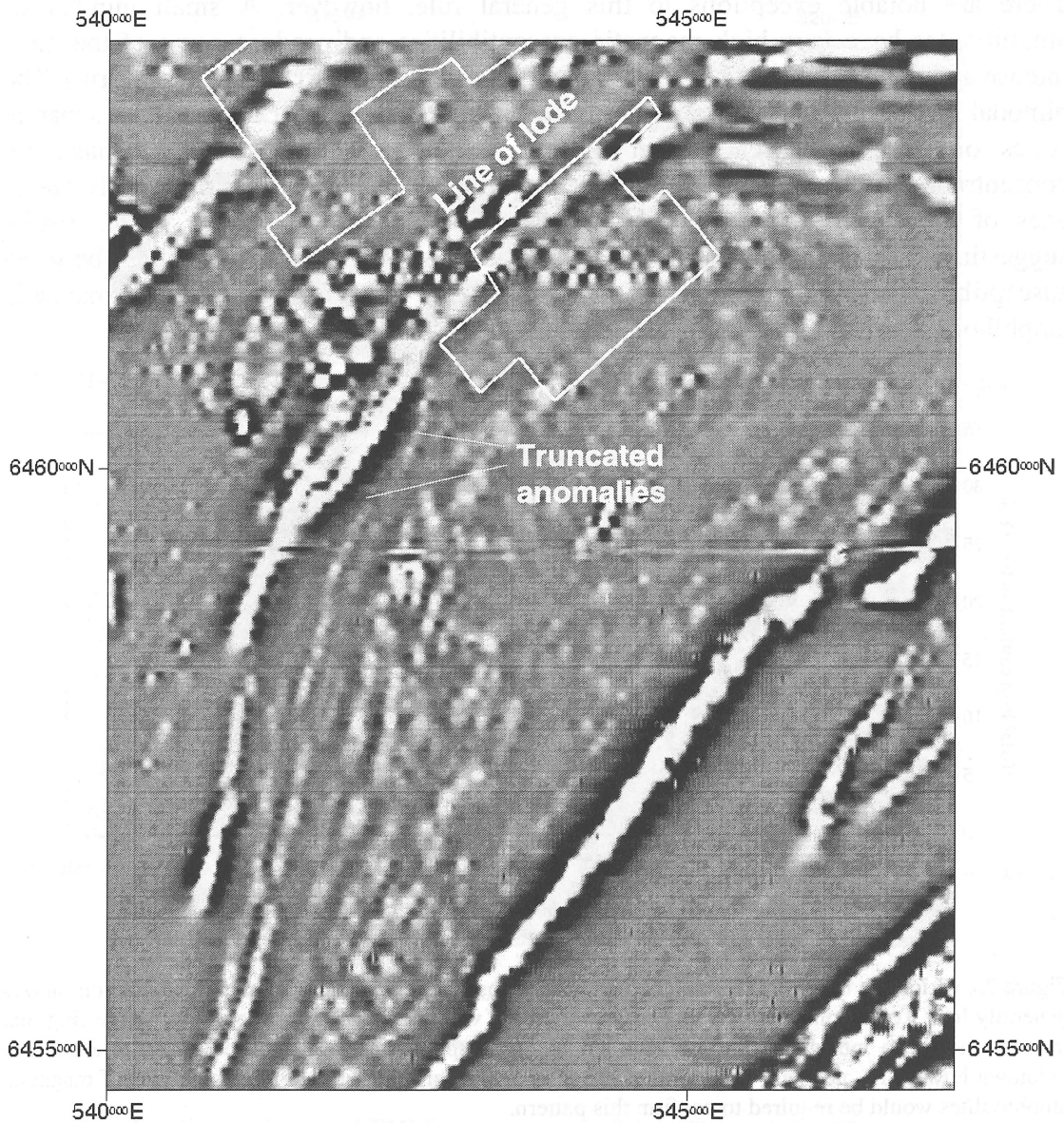


Figure 24. 1<sup>st</sup> vertical derivative of TMI of a magnetic anomaly just to the south of the line of lode. The anomaly is at least in part caused by amphibolite adjacent to a shear zone. Note the truncation of narrow, low amplitude anomalies to the south of Broken Hill.

A similar case exists along the western limb of the Stirling Vale synform (Fig. 25) where one of the most intense anomalies in the region occurs (~1 200 nT). Exposure is very poor along the trace of the anomaly; only a few scattered small outcrops of highly magnetic amphibolite occur. The anomaly is adjacent to an interpreted major shear zone (White *et al.* 1995). In detail, the anomaly consists of two closely-spaced peaks running sub-parallel to each other which do not seem to 'wrap around' the closure of the synform. An anomaly is present on the eastern limb, but this is much weaker (~600 nT) and does not appear to grade smoothly into the western anomaly, as would be expected if it were part of the same feature. Other units of amphibolite are present in the synform that appear similar in outcrop, but host no magnetic anomaly.



In thin section, the amphibolite shows a granoblastic-polygonal texture, with magnetite occurring as discrete grains and as inclusions in hornblende, indicating that the magnetite was stable during high-grade metamorphism. Some magnetite shows redistribution along grain boundaries. No ilmenite is present, in contrast to the bulk of non-magnetic amphibolite in the region.

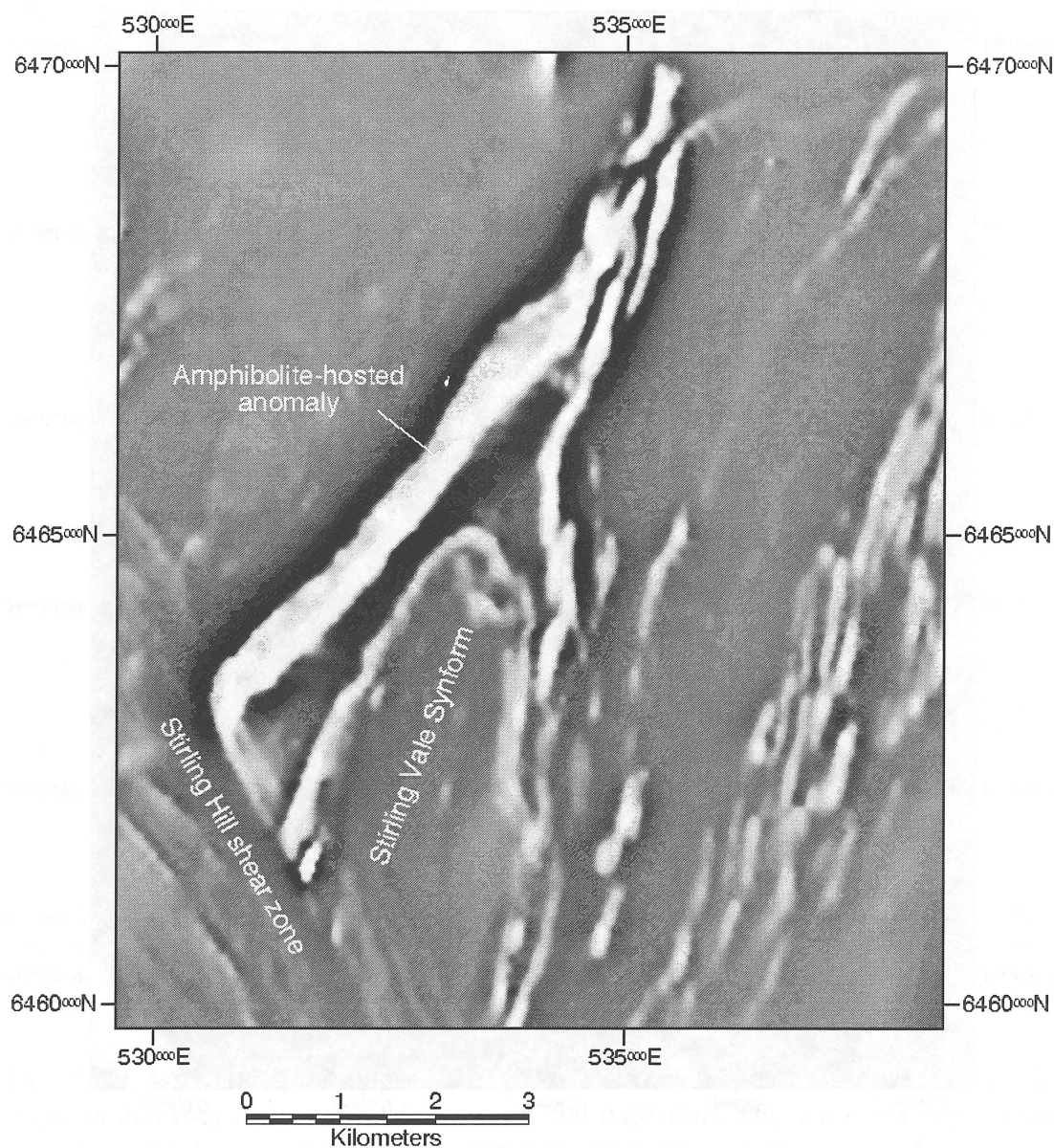


Figure 25. 1<sup>st</sup> vertical derivative of TMI of the Stirling Vale Synform, west of Broken Hill. An intense magnetic anomaly along the western limb is caused by magnetite-rich amphibolite, proximal to an interpreted high-temperature shear zone.

Magnetic amphibolite occurs in association with quartz-albite rocks in the Lakes Creek area (Fig. 26). Amphibolites marginal to thick quartz-albite units generate strong linear anomalies, whereas amphibolites away from and within the quartz-albite rocks tend to have a low susceptibility. In thin section, it is apparent that magnetite formed pre- or syn-high-grade metamorphism, as is the case in other magnetic amphibolites. It seems

plausible that fluid movement has been focussed along the margins of the thick, competent quartz-albite units in much the same manner as Potosi and granite gneiss (see above), oxidising the amphibolite and forming magnetite.

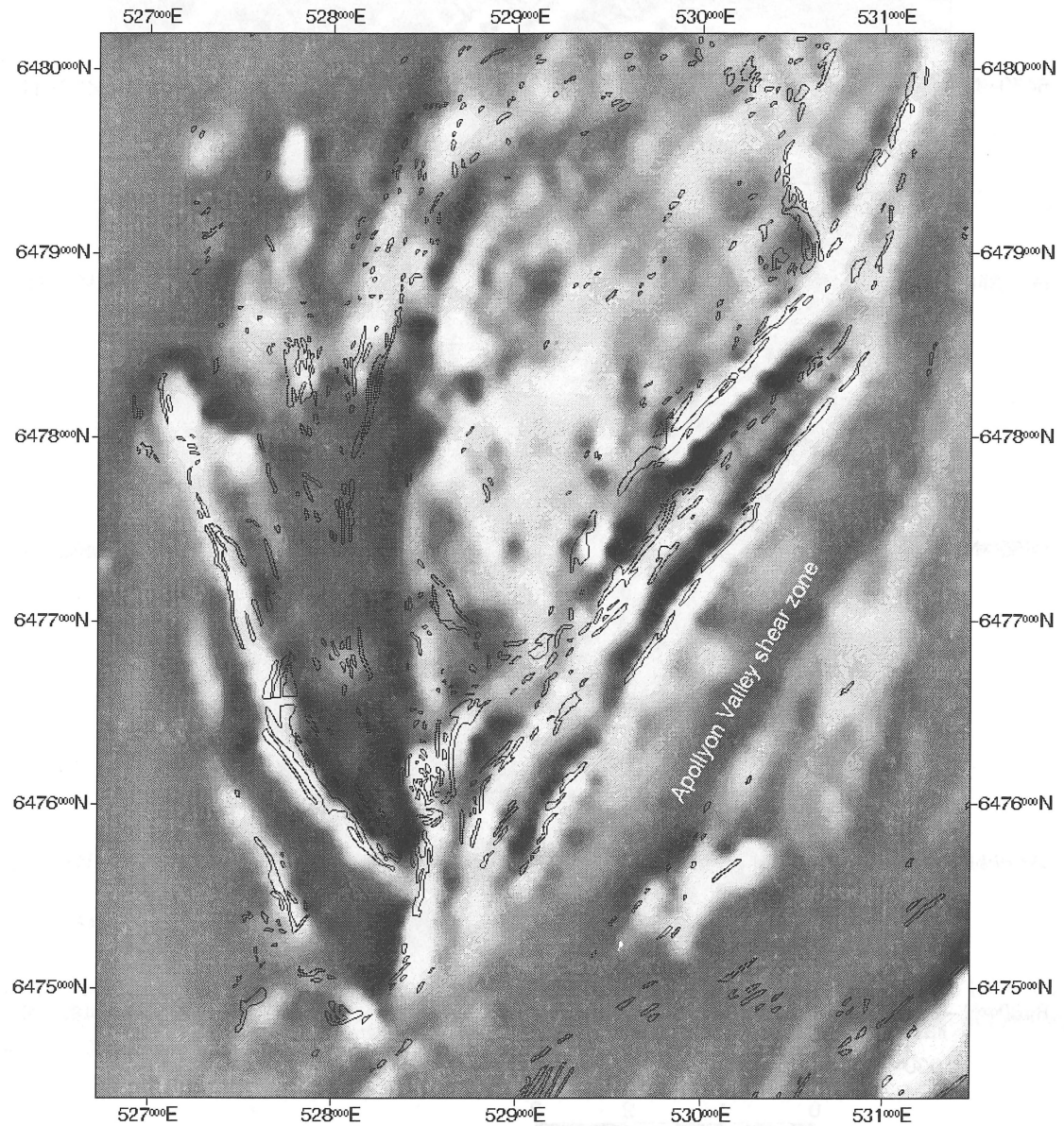


Figure 26. 1<sup>st</sup> vertical derivative of TMI over an area in the Lakes Creek region, northwest of Broken Hill. The outline of outcropping amphibolite bodies are shown in black.

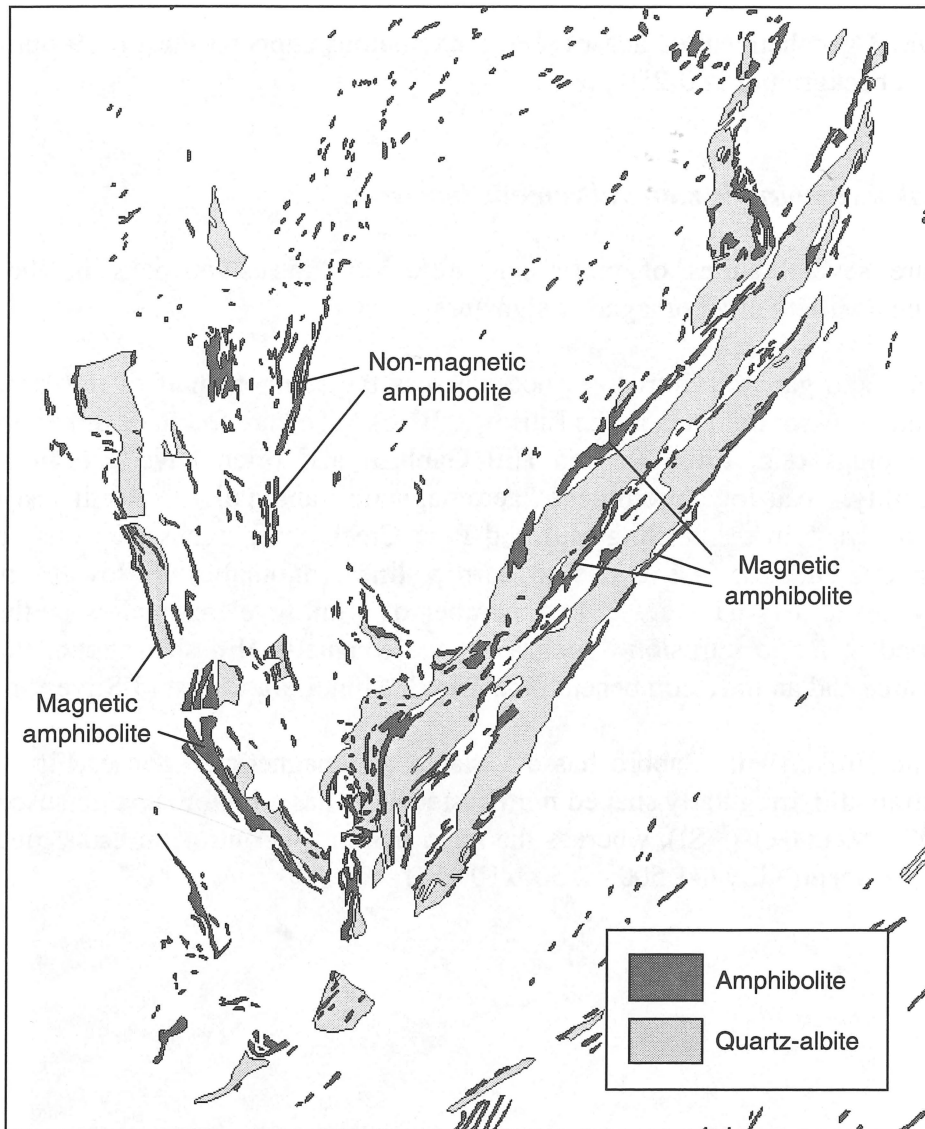


Figure 27. Map of outcropping amphibolite and quartz-albite rock for the same area Figure 25. Note that magnetic amphibolite tends to be associated with the thicker units of quartz-albite, particularly along the margins.

The close association of magnetic amphibolite with zones of inferred fluid flow suggests that they are a result of alteration and oxidation. Magnetite is in equilibrium with hornblende, suggesting the alteration took place pre- or syn-D<sub>3</sub> (the last amphibolite-grade metamorphic event). The recrystallisation has unfortunately obscured any earlier textures that may have been present prior to metamorphism and little textural information can be gained from petrographic examination.

Magnetic amphibolite may have the potential to host Cu-Au mineralisation in the same manner as quartz-magnetite bodies. Mineralising fluids could be introduced by the reactivation of structures that provided the fluid which formed the magnetite. Chalcopyrite occurs as fine grained inclusions in magnetic amphibolite from the Broken Hill Synform, near the high-temperature shear zone described earlier. Geochemical analysis of an amphibolite along strike from the same anomaly

(NSWDMR geochemical database) shows anomalous copper values (639 ppm against a regional background of 0-250 ppm).

### *Post-peak metamorphic mafic/ultramafic intrusives*

There are several suites of mafic and ultramafic intrusive rocks in the region, displaying a variety of aeromagnetic signatures.

Ultramafic and gabbroic intrusives occur across the southern half of the Broken Hill Block and in minor amounts in the Euriowie Block. They are found as dykes and larger intrusive plugs (e.g. Little Broken Hill Gabbro) and often have a high magnetic susceptibility, causing prominent aeromagnetic anomalies. Northwest-trending ultramafic dykes in the Stirling Hill and Pine Creek shear zones are conspicuous in aeromagnetic images, giving rise to narrow linear anomalies of low to moderate intensity, up to 100 nT (Fig. 28). A number of 'bullseye' anomalies in the region correspond to mafic intrusions, such as in the Magnetic Hill shear zone, the Mulga Springs area and an intrusion beneath the Mundi Mundi Plain west of Silverton.

The Little Broken Hill Gabbro has a variable aeromagnetic response (Fig. 29). The more ultramafic, irregularly shaped northeastern part has a high magnetic susceptibility ( $\sim 50\,000 - 60\,000 \times 10^{-6}$  SI), whereas the main mass of the intrusion has a much lower magnetic susceptibility ( $\sim 1\,500 - 2\,500 \times 10^{-6}$  SI).

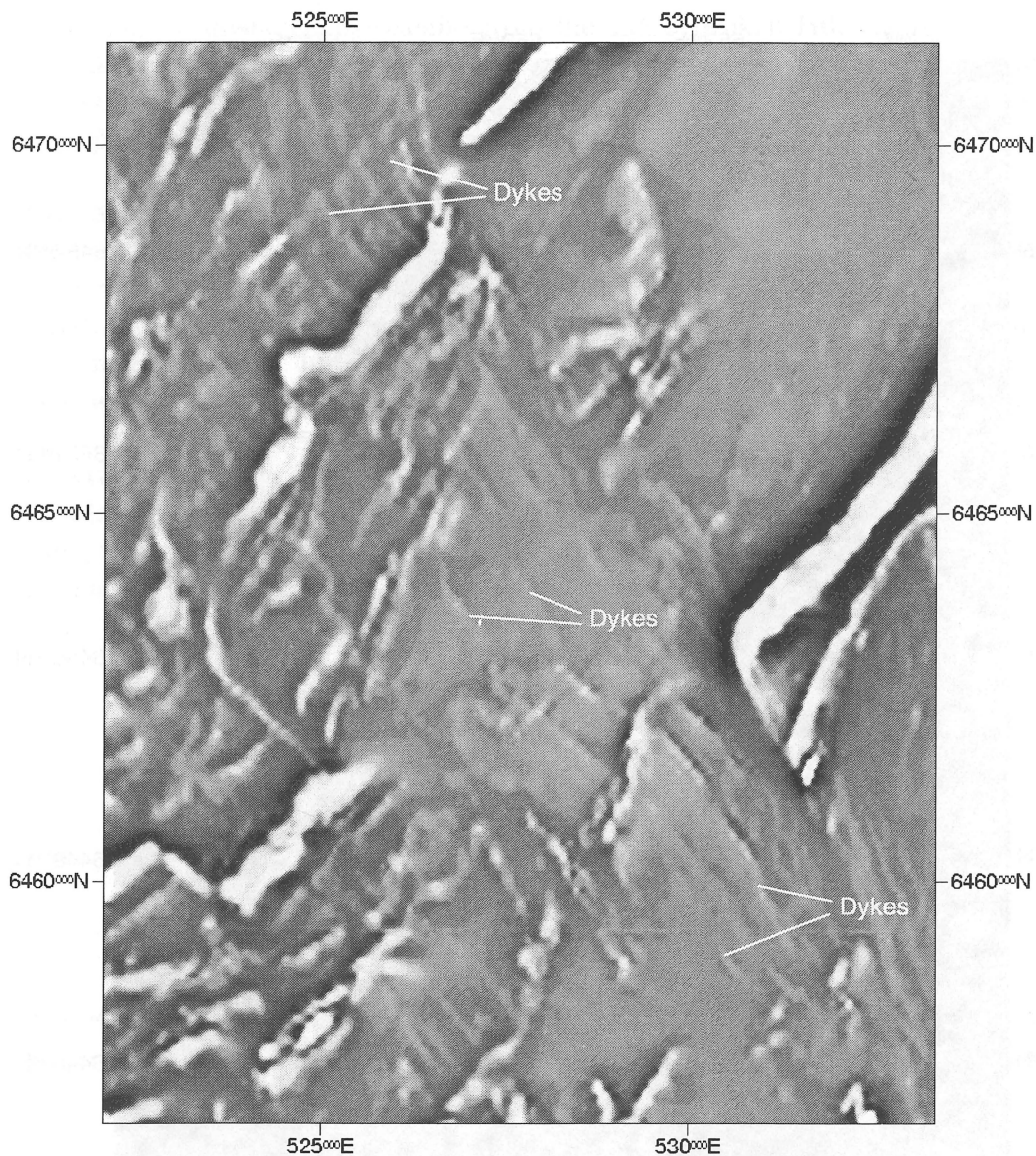


Figure 28. 1<sup>st</sup> vertical derivative of TMI for the Stirling Hill and Pine Creek shear zones. Ultramafic dykes form narrow linear anomalies and are interpreted to have intruded into shears at the time of the breakup of the Rodinian supercontinent. Later metadolerite dykes in the area have no magnetic expression.

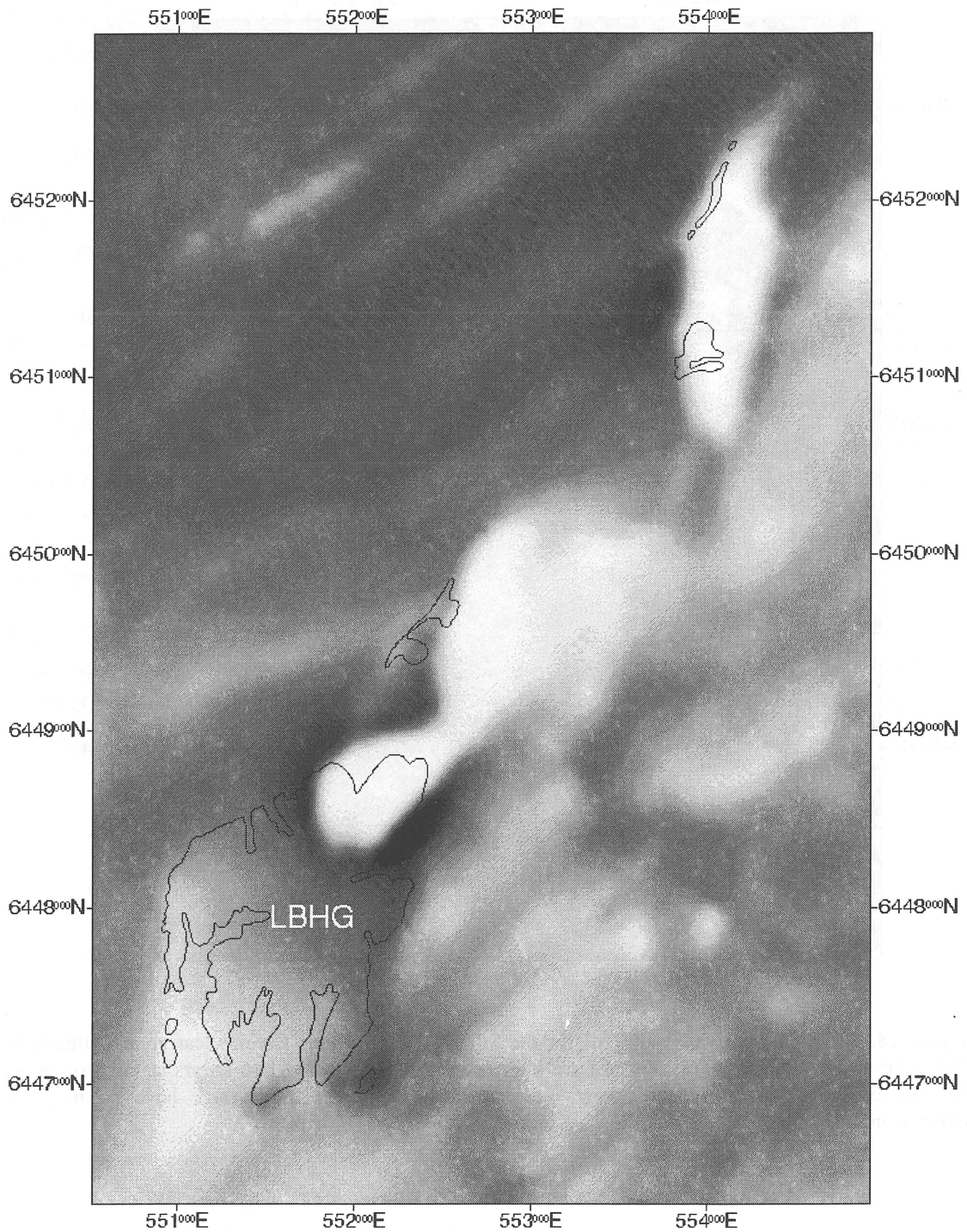


Figure 29. TMI of the Little Broken Hill Gabbro, southeast of Broken Hill. The main mass of the outcropping intrusion is only weakly magnetic, however there is a zone in the northeast part of the intrusion with is highly magnetic and coincides with a more ultramafic and serpentinised phase.

The main cause of this widely varying susceptibility is alteration of iron-bearing minerals such as olivine and pyroxene. Unaltered ultramafic rocks have a low oxidation state and therefore are essentially non-magnetic (Grant 1985). Alteration, in particular serpentinisation, changes olivine and pyroxene into hydrous iron and magnesium silicates plus magnetite (Moody 1976), thereby increasing the magnetic susceptibility, often by orders of magnitude.

A sample of unaltered pyroxenite from the Little Broken Hill Gabbro showed little alteration and has only very minor magnetite. Hydrothermally altered pyroxenite from the same intrusion shows abundant magnetite lying along cleavage planes in altered orthopyroxene crystals.

Metadolerite dykes occur in the same general area as the gabbroic/ultramafic rocks and cross-cut the former (Brown 1980). The bulk of these dykes trend WNW, although there are a significant number in the southern part of the Block that have an east-west trend. These trends are distinct from the ultramafic dykes in the Stirling Hill shear zone that trend northwest. In contrast to the gabbroic rocks, the metadolerites are uniformly very weakly magnetic ( $\sim 300\text{-}900 \times 10^{-6}$  SI) and not visible on aeromagnetic images.

Several other mafic intrusives occur in the region. A set of ENE-trending dykes are visible in aeromagnetic images of the central part of the Broken Hill Block (Fig. 30). The anomalies associated with these dykes are weak and are only apparent when the aeromagnetic data are passed through a high-frequency filter.

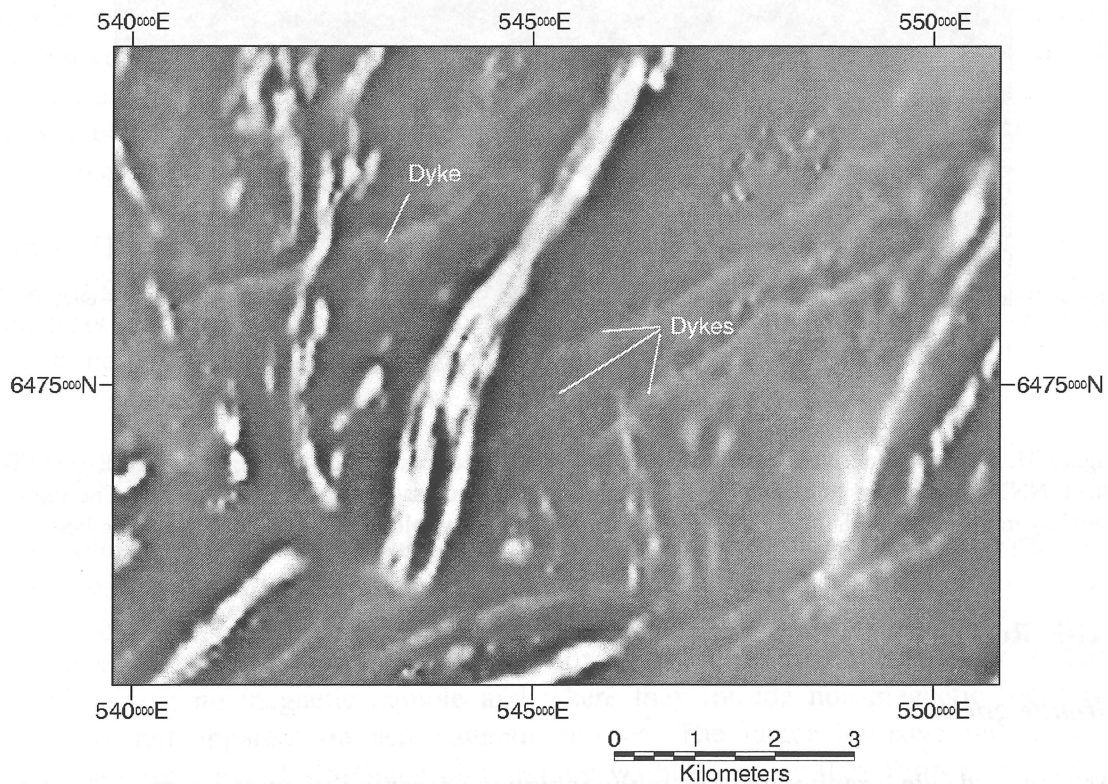


Figure 30. 1<sup>st</sup> vertical derivative of an area north of Broken Hill. Late-stage ENE-trending dykes are visible as narrow, low intensity anomalies cross-cutting other magnetic trends.

A number of prominent linear anomalies cross-cut other anomalies in the eastern part of the Stephens Creek 1:25 000 sheet (Fig. 31). These anomalies have been ground truthed by B. Stevens (pers. comm.) who, in places, found mafic dykes not mapped on the 1:25 000 geological sheet. It is uncertain whether these dykes are part of other mafic dyke swarms in the region or a different magmatic suite.

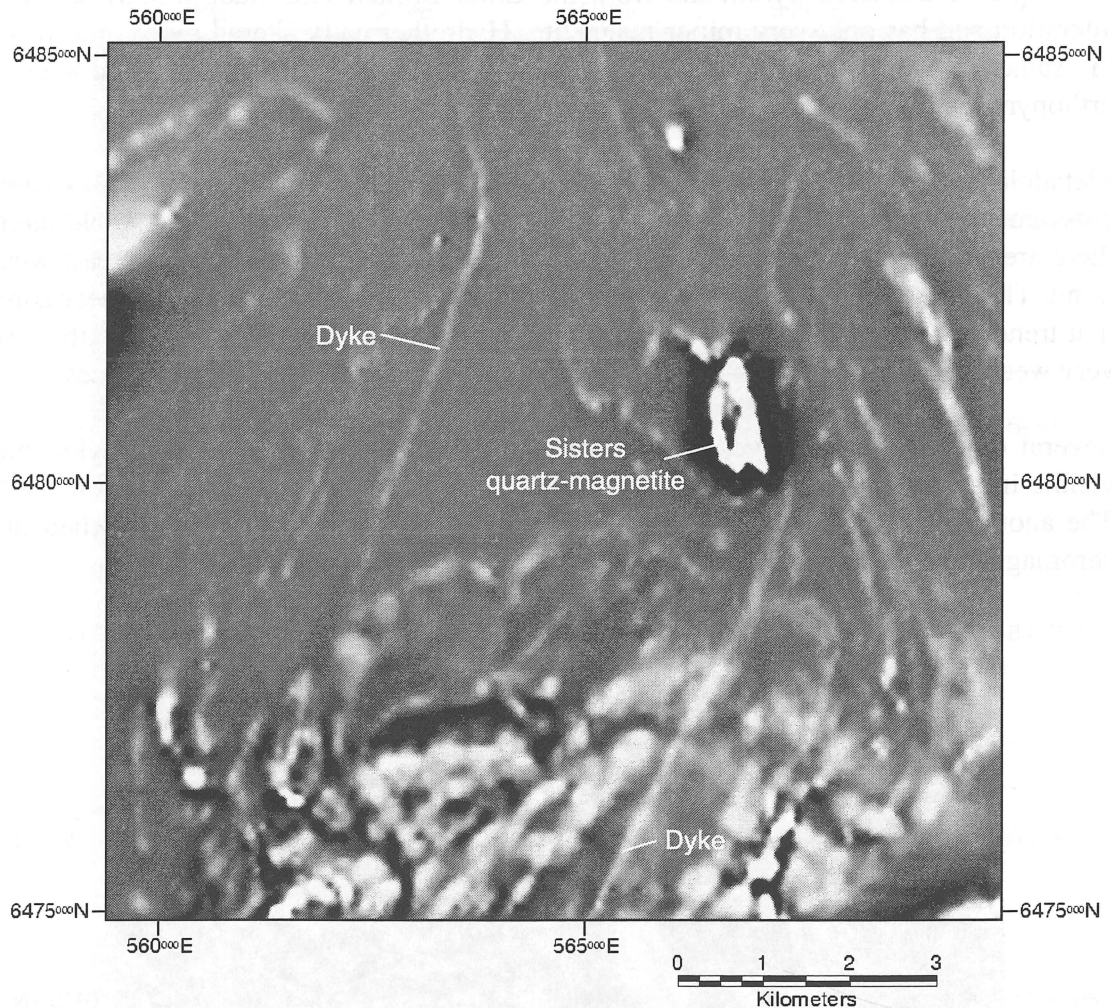


Figure 31. 1<sup>st</sup> vertical derivative of TMI for an area in the eastern part of the Stephens Creek 1:25 000 sheet. NNE-trending dykes extend for kilometres in length, cross-cutting other anomalies. The intense anomaly in the centre-right of the image is caused by the tightly folded Sisters quartz-magnetite body.

## Felsic Rocks

### *Granite gneiss*

As a general rule, granite gneisses in the region are essentially non-magnetic. There are some minor exceptions to this rule, however. Magnetite-rich granite gneiss ('BT' on NSWDMR 1:25 000 geological maps) is fairly common in the Redan Geophysical Zone and present in minor amounts elsewhere in the region (e.g. the Purnamoota area).

Magnetic granite gneiss is also found southeast of the Sentinel quartz-magnetite body in the south of the block. The gneiss is variably magnetic, ranging in susceptibility up to  $25\,000 \times 10^{-6}$  SI and has a pinkish appearance, distinct from the more common grey granite gneisses found elsewhere. It is unclear whether the magnetite is a primary feature of the gneiss or whether it is a result of alteration.



## *Pegmatite*

Pegmatite is ubiquitous in the region. It occurs on a variety of scales, from small partial melts to large masses many square kilometres in size. Lishmund (1982) described four types of pegmatite in the Broken Hill and Euriovie Blocks. Brown *et al.* (1983) reviewed this work and concluded that the zoned pegmatites (type 1 of Lishmund 1982) were intruded during at least three periods, the last possibly less than 600 Ma ago. Both Lishmund (1982) and Brown *et al.* (1983) agree that the other three types of pegmatite are products of local melting during high-grade metamorphism.

These pegmatite types are generally non-magnetic where they occur in non-magnetic rock types. Where pegmatite occurs within or near more magnetic rocks, however, the pegmatite may contain extremely coarse magnetite, often occurring as euhedral octahedra up to 3 cm or more in diameter. These pegmatite bodies are generally small, ranging up to a few tens of metres in length. An exception to this rule are magnetite-bearing pegmatites in the Mount Robe area which cover many square kilometres. The general absence of magnetite-rich pegmatites in non-magnetic regions suggests that the iron in the magnetite has been derived from the local country rock and that the melt has not moved a great distance. Magnetite-bearing pegmatite is commonly associated with structurally controlled linear anomalies (see above). These shears are zones of fluid movement which may have localised pegmatite intrusion and provided a medium for the transport of iron and other elements.

Grant (1995) noted that 'coarsely crystalline magnetite has a higher magnetic susceptibility (and a lower magnetic remanence) than finely crystalline magnetite'. This suggests that the emplacement of pegmatite has the potential to further enhance the magnitude of magnetic anomalies over areas of already high magnetic susceptibility.

## *Granitic intrusives*

Post-folding granitic intrusives occur as dykes and plutons in the north and northwestern part of the Broken Hill Block. Three types have been defined: Mundi Mundi-type; Champion-type and Umberumberka-type (Brown *et al.* 1983). These intrusives are generally non-magnetic (low oxidation state - ilmenite series of Ishahira (1977)), have no magnetic aureole and where they intrude non-magnetic rocks are generally not apparent on aeromagnetic images. The larger intrusive masses (the Brewery Creek and Cusin Creek plutons) are visible because they form magnetically 'quiet' zones in areas of weak anomalies (Fig. 6).

Numerous magnetite-pyrite occurrences associated with Umberumberka-type granitic intrusions occur in the western part of the region, known locally as Iron Duke-type mineralisation. Barnes (1988) lists several forms of mineralisation, including patches of quartz-feldspar-magnetite-pyrite rock in granite and pegmatite, dykes of feldspar ( $\pm$ quartz) magnetite rock, magnetite-pyrite veins and disseminated magnetite and pyrite in altered country rocks. He considers the mineralisation to have formed from iron-rich segregations during emplacement of the granite bodies. Due to their relatively small

size, these occurrences form small, irregular anomalies which may only be apparent on ground magnetometer surveys.

A few small magnetite-rich amphibolites have been mapped on the Uمبرumberka and Purnamoota 1:25 000 sheets. These amphibolites have a close spatial association with granite bodies and may have formed in a similar manner to magnetite-rich country rock associated with Iron Duke-type mineralisation.

## Adelaidean rocks

Rocks of the Adelaidean sequence unconformably overlie the Willyama Supergroup. They predominantly consist of siliciclastic sedimentary rocks, with minor basaltic rocks and ironstones near the base (Cooper *et al.* 1978). The ironstones produce intense magnetic anomalies, which are particularly conspicuous in the Olary Block where the Braemar ironstone delineates fold interference patterns (Fig. 32). An intense 'horseshoe'-shaped anomaly in the area near 'Burta' homestead (Fig. 33) occurs in an area of 100% cover and has been drilled by C.R.A. who intersected iron-rich meta-siltstones and shales (C.R.A. Exploration Pty. Ltd. 1986).

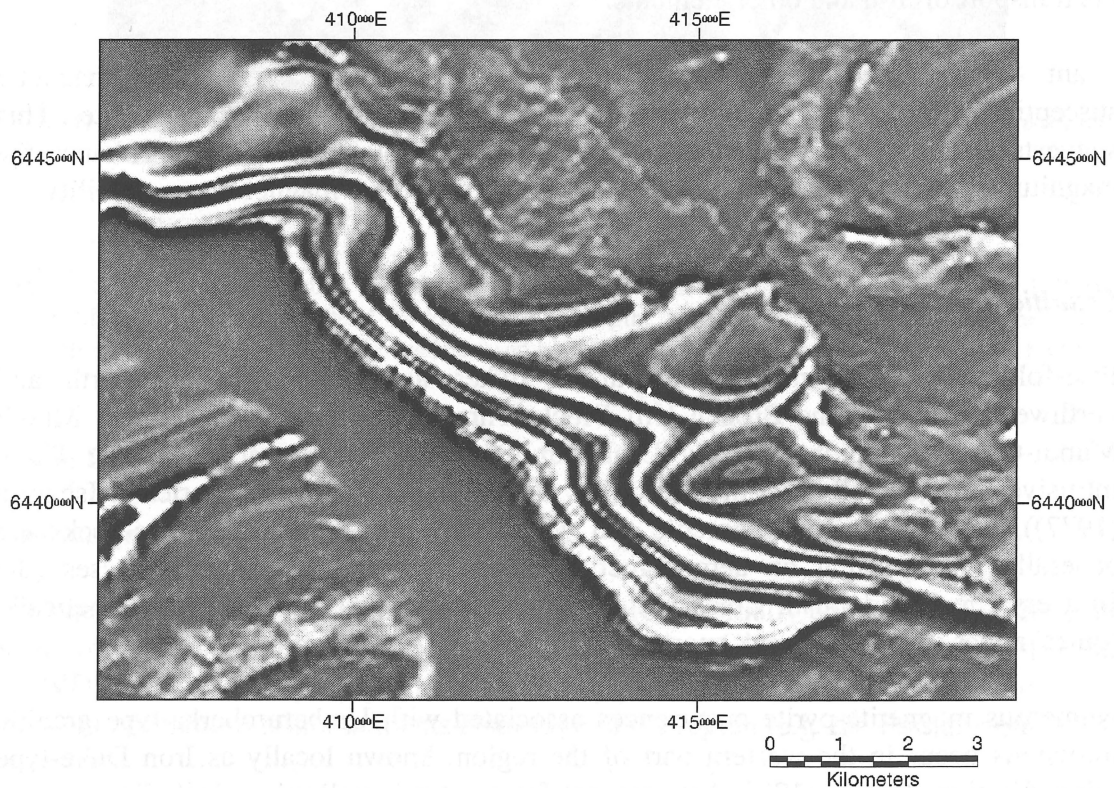


Figure 32. 1<sup>st</sup> vertical derivative of TMI of multiply-deformed Braemar Ironstone in the Olary Block, South Australia. The ironstone defines a striking 'basin and dome'-type interference pattern.

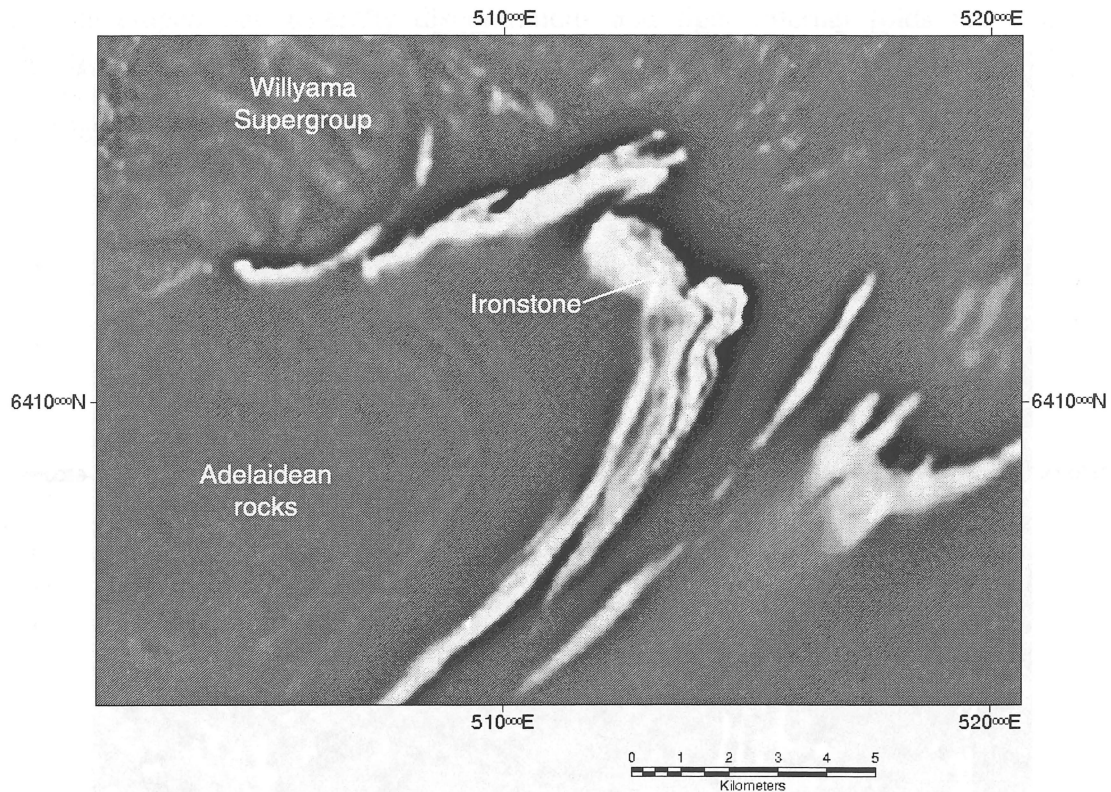


Figure 33. 1<sup>st</sup> vertical derivative of TMI of ironstone in the Burta area in the southern extremity of the Broken Hill Block, showing the typically intense aeromagnetic signature of the lithology.

Mafic volcanics of the Wilangee Basalt, in the lower part of the Adelaidean, crop out in the Campbells Creek area in the north of the block. The basalt is moderately magnetic and forms pronounced anomalies against a generally non-magnetic background.

Neoproterozoic sedimentary rocks in the Torrowangee Synclinal Zone produce thin, continuous linear anomalies that are conspicuously folded on aeromagnetic images (Fig. 34). The anomalies are caused by stratiform magnetite and correspond in detail to individual sedimentary beds, even on a microscale. The magnetic trends are commonly asymmetric, in contrast to many anomalies in the Willyama Supergroup, and define the dip direction of bedding.

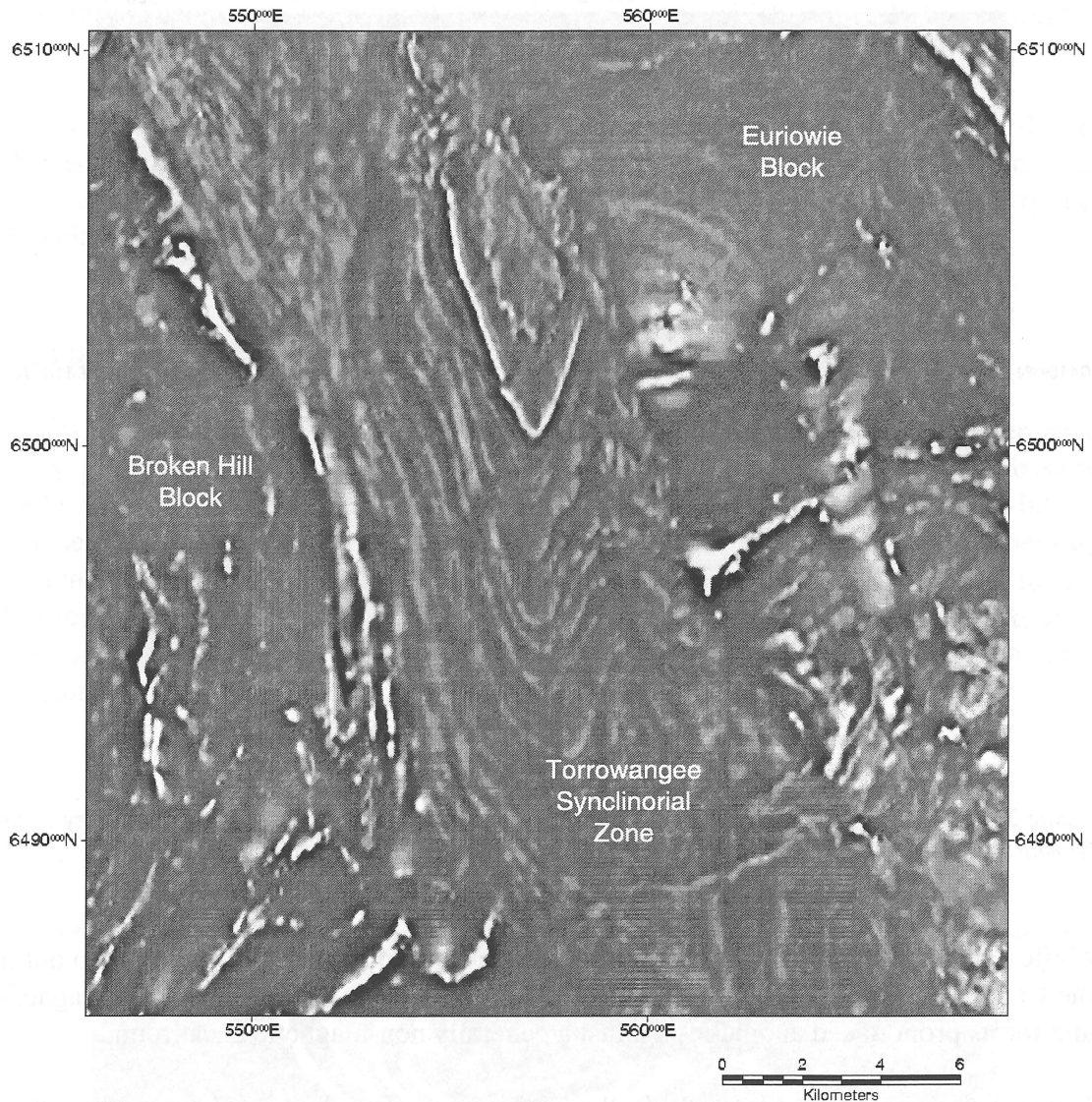


Figure 34. 1<sup>st</sup> vertical derivative of TMI of Adelaidean metasediments in the Torowangee Synclinorium between the Broken Hill and Euriowie Blocks. The anomalies are stratigraphically controlled and caused by magnetite in bedding.

## Other anomaly sources

### Quartz-magnetite rocks

Quartz-magnetite rocks give rise to some of the strongest aeromagnetic anomalies in the region (up to ~5 000 nT). Quartz-magnetite bodies range in size from thin lenses one millimetre thick to bodies up to 5 m thick extending for kilometres in strike length (e.g. Razorback). Quartz-magnetite bodies occur in various places in the Broken Hill and Euriowie Blocks, but are most common in the south and east (Fig. 35), giving rise to prominent landmarks (e.g. the Pinnacles, the Sentinel and Razorback).

The quartz-magnetite rocks differ from banded iron formation in that they contain less apatite, little or no garnet and are coarser-grained. Compositional layering is often

well-developed but generally discontinuous and tight internal folds are common. Quartz-magnetite is often associated with quartz-albite rocks of the Thackaringa Group and is considered to have had a sedimentary protolith (Leyh & Larsen 1983; Barnes *et al.* 1983).

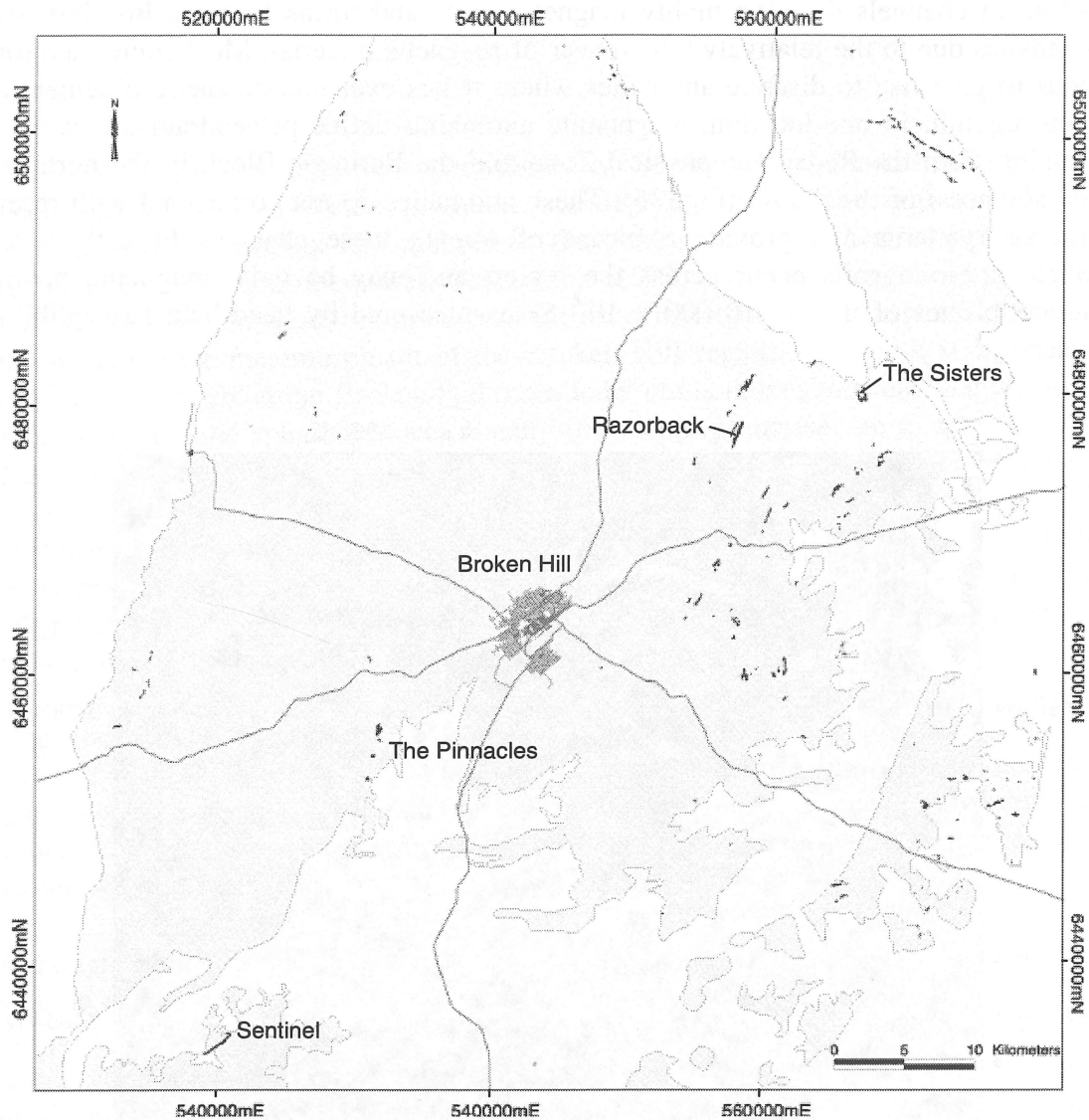


Figure 35. Distribution of outcropping quartz-magnetite rocks in the Broken Hill and Euriowie Blocks.

Shear fabrics are commonly observed in quartz-magnetite rocks. In particular, lenticular quartz layers resemble quartz ‘ribbons’ in a mylonite (Fig. 42a). The shearing is either superimposed on an earlier magnetite-rich sediment which has acted as a focus for strain, or the magnetite has formed during shearing itself.

The close spatial association with quartz-albite rocks is consistent across the region. Quartz-magnetite and quartz-albite are not found above the Thackaringa Group, suggesting that either there is a strong depositional link between the two rock types or that, if the quartz-magnetite is shear-related, that shearing took place before the Broken Hill Group was overlain on the Thackaringa Group.

## Maghemite

Maghemite has a similar magnetic susceptibility to magnetite (1.25-12.5 SI) and is thought to form by the oxidation of magnetite in the presence of water. It typically occurs in channels draining highly magnetic units and forms sinuous, low intensity anomalies due to the relatively thin veneer of magnetic material. Maghemite therefore tends to give rise to discrete anomalies where it lies over non-magnetic basement or deep regolith. In one location, maghemite anomalies define palaeodrainage channels draining from the Redan Geophysical Zone and the Euriowie Block in the northeast and southeast of the region (Fig. 36). These anomalies do not correspond with recent drainage patterns and provide a means of tracing these channels beneath cover. Maghemite-rich soils occur across the region and may be quite magnetic, having susceptibilities of up to  $\sim 10\,000 \times 10^{-6}$  SI as measured by hand-held susceptibility meters.

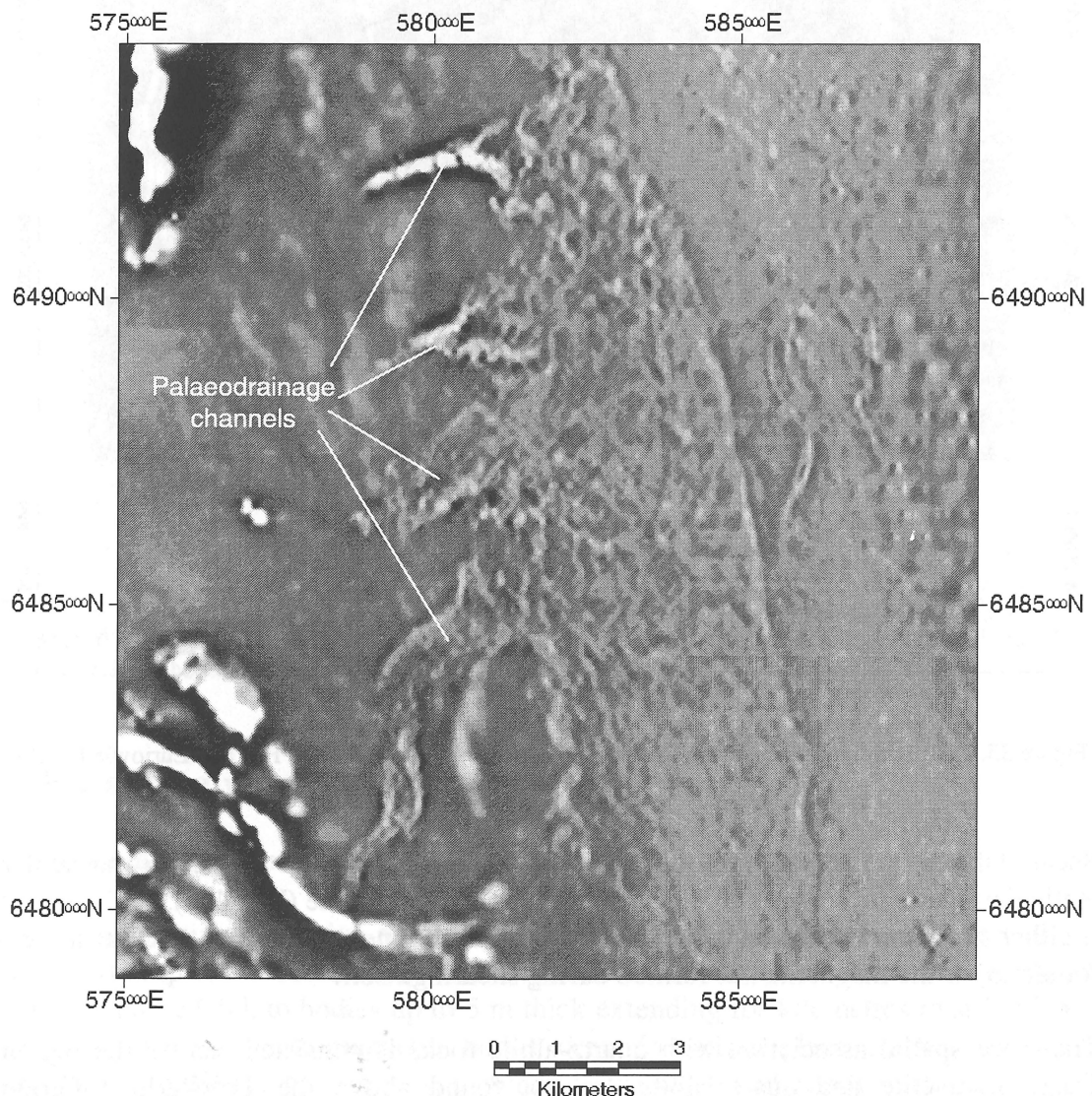


Figure 36. 1<sup>st</sup> vertical derivative of TMI of an area to the east of the Euriowie Block. Sinuous anomalies in the aeromagnetics do not correspond to current drainage and represent palaeodrainage channels rich in maghemite.

The presence of maghemite should be noted during aeromagnetic interpretation, especially if an algorithm such as automatic gain control is applied to the data, which enhances the intensity of weaker anomalies. Maghemite-rich channels may have a similar appearance to weakly magnetic dykes and therefore it is worthwhile overlaying drainage patterns on the aeromagnetic data to check for any correlations.

### **Pyrrhotite**

Pyrrhotite is not an important contributor to aeromagnetic anomalies, but it is mentioned here as it occurs in minor amounts throughout the region and is a component of the Broken Hill main lode. Only the monoclinic form of pyrrhotite is magnetic at ambient temperatures. Scott *et al.* (1977) note that monoclinic pyrrhotite occurs as a common alteration product of primary (metamorphic) hexagonal pyrrhotite during retrograde metamorphism in the Broken Hill region. Pyrrhotite is irregularly distributed throughout the Broken Hill main lode, but is most abundant in areas richer in chalcopyrite and sphalerite, occasionally forming large masses up to 30 cm across (Lawrence 1968). Plimer (1984) notes that monoclinic pyrrhotite is a relatively abundant product of 'waning metamorphism' and retrograde metamorphism. He mentions a pyrrhotite-rich sulphide facies ('pyrrhotite envelope') which partially envelopes the No. 3 lens at the southern end of the main lode. He also notes fracture-filled veinlets of plastically injected monoclinic pyrrhotite, galena and chalcopyrite cross-cutting brecciated ore in retrograde shear zones.

Magnetic pyrrhotite has been intersected in EM basement conductor drill targets in the Little Broken Hill, Nine Mile, Purnamoota and Allendale areas. It is generally associated with pyrite and chalcopyrite and in some instances, galena or sphalerite. The mineralisation occurs as disseminations, cross-cutting veins and cavity fillings, often associated with retrograde shearing.

Although the pyrrhotite veins are quite magnetic (up to  $222\ 500 \times 10^{-6}$  SI), their small volume causes no significant aeromagnetic anomaly. However, this does not rule out the possibility of detecting pyrrhotite-related mineralisation by magnetic methods. A larger volume of pyrrhotite ( $\equiv$  larger orebody?) could be expected to give a more pronounced anomaly. Monoclinic pyrrhotite often has an intense remanent magnetisation, which is easily reset due to its low Curie temperature of  $\sim 250^\circ\text{C}$ . This has the potential to vary the intensity of the anomaly, depending on the orientation of the vector of remanence.

### **Jacobsite**

Jacobsite is an iron-manganese spinel that forms a solid solution series with magnetite. It is highly magnetic and has been recorded from the New Broken Hill Consolidated Mine where it occurred as grains 1-3 mm in diameter in a massive sulphide band 1.5 m wide (Segnit 1977). It is a rare component of the main lode, however, and does not generate an observable aeromagnetic anomaly.

## Remanent magnetisation

Magnetic remanence has not been examined in detail as part of this work and will be the subject of a later study by Giddings *et al.* (in prep.). The direction and strength of the overall vector of remanence will control the effect on the associated anomaly. If the vector varies significantly from the direction of the earth's magnetic field, the anomaly in a reduced to pole image will not lie directly over its source, but will be shifted slightly. If the vector is directed against the Earth's present magnetic field, the intensity of the anomaly may be reduced or even negative.

The effect of remanence on the position of field checked anomalies was negligible. The sources of magnetic anomalies were consistently situated at the position indicated by reduced to pole aeromagnetic images. In detailed work on selected anomalies, Giddings *et al.* (1998) found both upward- and downward-pointing vectors of remanence that tended to cancel each other out. Mean remanent field magnetisations were thus 4-8 times smaller than individual sample magnetisations and remanence could therefore be effectively ignored in modelling.

## Oxidation of magnetite

When exposed to surface conditions, magnetite will oxidise to form minerals such as hematite. Surface exposures of magnetite-rich rocks such as quartz-magnetite may appear relatively fresh, however the magnetic susceptibility of these rocks will be considerably less than the unweathered rock at depth. An appreciation of the effects of weathering on magnetite-bearing rocks is important if modelling of magnetic data is to be attempted.

As part of a rock property study, a drillhole in the Sisters area was examined and samples taken at intervals down the hole. Drillhole BH1 intersected a folded horizon of quartz-magnetite four times along its length, allowing a comparison of magnetic susceptibility at various depths below surface (Fig. 37). Near-surface quartz-magnetite had a susceptibility of around  $30\,000 \times 10^{-6}$  SI, with some magnetite having been oxidised to hematite and goethite. The magnetic susceptibility increased systematically down-hole until at a hole-depth of 175 m (~125 m below surface) a value of  $\sim 2\,220\,000 \times 10^{-6}$  SI was recorded, an increase of two orders of magnitude. Although this is an extreme case, it is apparent that the effects of weathering influence the magnetic susceptibility and that the surface measurement is a minimum value for the overall susceptibility of a unit. Detailed modelling of magnetic anomalies should therefore use susceptibility values determined from the freshest samples available, preferably drillcore.



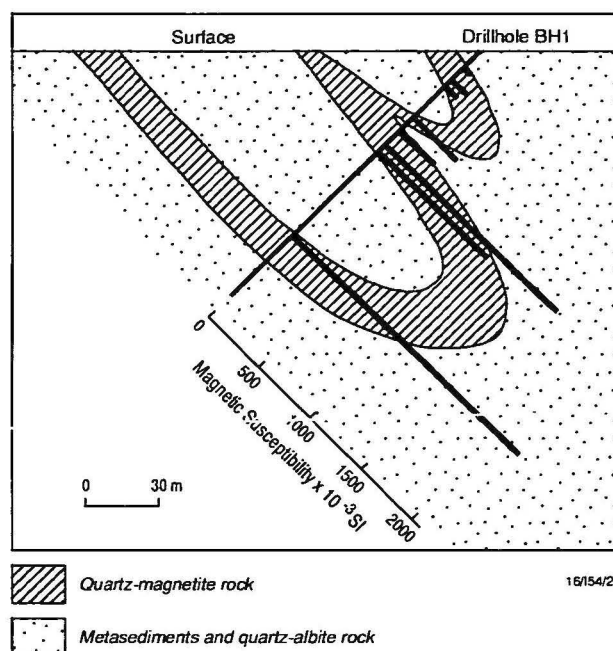


Figure 37. Cross-section of drillhole BH1 in The Sisters area. Oxidised quartz-magnetite rock near the surface has a magnetic susceptibility two orders of magnitude less than fresh quartz-magnetite at a depth of 125 m.

## Magnetic susceptibility patterns

Over 1200 magnetic susceptibility measurements have been acquired by the Broken Hill Exploration Initiative. These include measurements of surface samples and drillcore using hand-held susceptibility meters and laboratory equipment. Field measurements comprise around one third of the dataset and were mainly gathered in areas where magnetic anomalies are present, thereby exaggerating the proportion of rocks with a high susceptibility. The following histograms should therefore not be used to estimate the relative proportions of rocks with high or low susceptibilities. Drillcore samples were collected on a systematic basis, irrespective of magnetic susceptibility.

A plot of all measured rocks shows a peak centred around the low value of  $0.4 \times 10^{-3}$  SI (Fig. 38). This peak is mainly influenced by the large number of metasediments with values in this range (Fig. 39), but is also represented in other rock groupings with the exception of amphibolite (Fig. 40). This peak represents the 'average' susceptibility of many unaltered rock types in the Willyama Supergroup. The population of rocks with susceptibilities up to  $200\text{--}300 \times 10^{-3}$  SI is dominated by structurally controlled magnetite. Rocks with susceptibilities higher than  $\sim 300 \times 10^{-3}$  SI consist mostly of banded iron formation, quartz-magnetite rocks and magnetite-rich pegmatites.

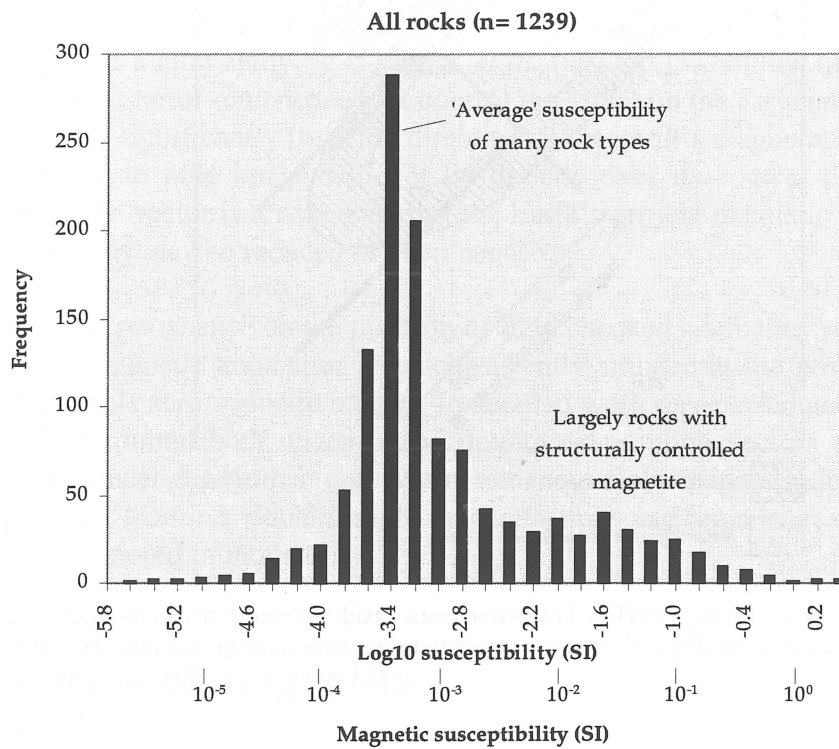


Figure 38. Histogram of magnetic susceptibility of rocks of the Willyama Supergroup. The main peak around  $0.4 \times 10^{-3}$  SI represents the 'average' susceptibility of many unaltered rock types. A large proportion of rocks with susceptibilities higher than these contain structurally controlled magnetite.

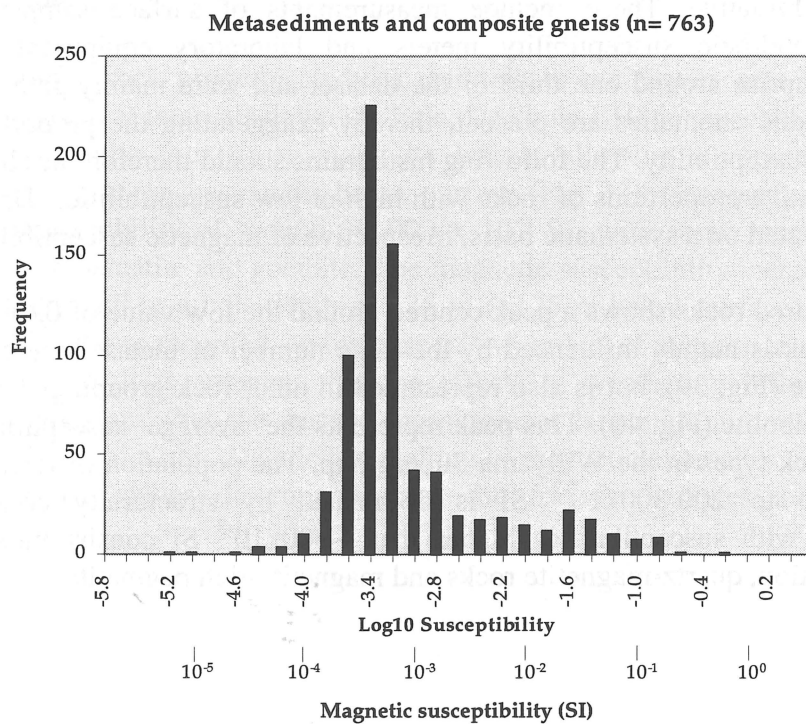


Figure 39. Histogram of magnetic susceptibility of metasediments and composite gneiss. The rocks with high susceptibilities are generally associated with structurally controlled anomalies.

The susceptibility of amphibolite commonly falls within the range of  $0.8-2 \times 10^{-3}$  SI (Fig. 40). Although this value is higher than the most common susceptibility of metasediments ( $0.3-0.4 \times 10^{-3}$  SI), the difference is small and unaltered amphibolite is generally not visible on aeromagnetic images. Higher susceptibilities are interpreted to be a result of alteration.

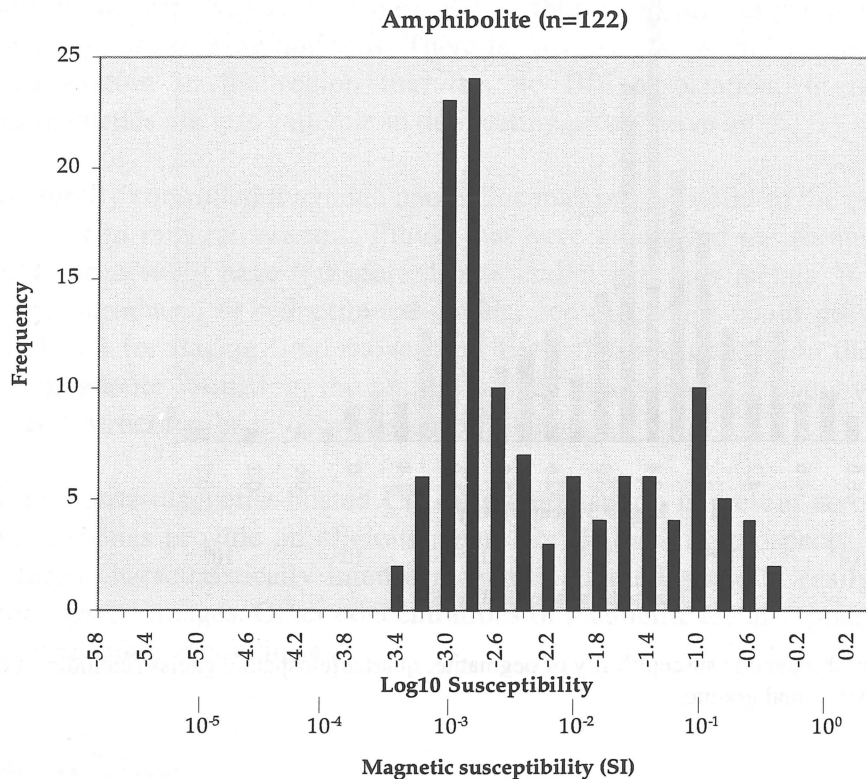


Figure 40. Histogram of magnetic susceptibility of amphibolite. Unaltered amphibolite has a susceptibility in the range of  $\sim 0.8-2 \times 10^{-3}$  SI.

The susceptibilities of pegmatite, quartzofeldspathic gneisses and granite are plotted in Fig. 41. The lowest susceptibilities are largely comprised of quartz  $\pm$  feldspar pegmatite. The main peak consists of Potosi gneiss, granitic gneiss and minor granite and is centred around  $0.3-0.4 \times 10^{-3}$  SI. The highest susceptibilities were measured from Potosi gneiss and granite gneiss in zones where lithological contrast has localised the formation of magnetite.

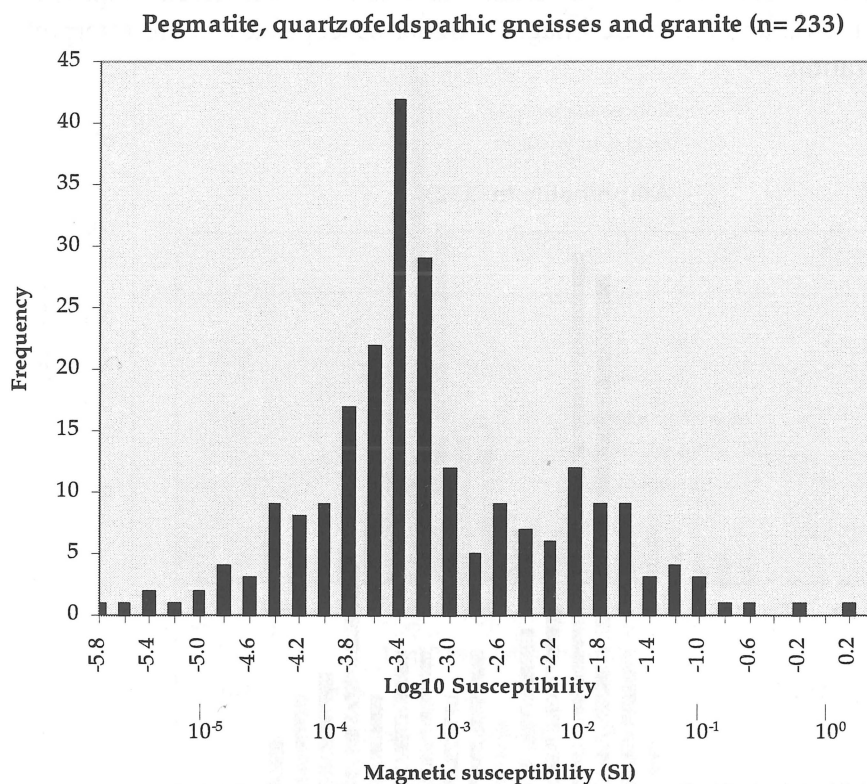


Figure 41. Histogram of magnetic susceptibility of pegmatite, quartzofeldspathic gneiss (including Potosi gneiss and granite gneiss) and granite.

## Mineralisation and aeromagnetics

The Broken Hill main lode currently has no aeromagnetic anomaly. The original aeromagnetic characteristics of the orebody are, of course, difficult to determine as most of the ore has been removed. Magnetite was recorded by Plimer (1984) as a minor product of high grade metamorphism of the main lode. It is widespread in small amounts and, in places, occurs as rich patches which interfere with ore recovery (Birch *et al.* 1982). Monoclinic pyrrhotite is also present in the main lode, as noted above, and where present in areas of higher concentration, such as the 'pyrrhotite envelope' of No.3 lens, could be expected to generate a noticeable magnetic anomaly. The general scarcity of magnetic minerals, however, means that the orebody as a whole is essentially non-magnetic and is unlikely to have formed an aeromagnetic 'bullseye' drilling target.

The Cannington deposit in the Cloncurry district of northwestern Queensland is considered to be Broken Hill-type (e.g. Williams 1996) and has an associated magnetic anomaly which was a significant factor in its discovery (Bailey 1998). One school of thought considers that the magnetite responsible for the anomaly is a peak-metamorphic product, while another proposes that the magnetite is a product of retrograde oxidation of Fe-rich silicates (see Bailey 1998). Ririe (1982) studied Precambrian Pb-Zn-Cu deposits in Colorado, USA and found that magnetite and

gahnite formed from a reaction between sulphides and silicates during amphibolite-grade metamorphism. Secondary magnetite does not appear to be present in the Broken Hill main lode, but the potential for secondary magnetic anomalies associated with Broken Hill-type mineralisation should not be overlooked, given suitable conditions.

The close spatial association of Broken Hill-type mineralisation to banded iron formation has long been recognised. The high susceptibility of the BIF makes it readily apparent on aeromagnetic images and is thus a useful marker horizon proximal to potentially ore-bearing horizons. There is, however, an abundance of Broken Hill-type mineralisation in the region that has no BIF association. In these occurrences, aeromagnetics are less valuable in delineating prospective units.

Structurally controlled magnetic anomalies may prove useful in the delineation of fluid pathways in mineral systems. Fluids that have controlled the formation of magnetite could conceivably have transported base and/or precious metals. If these fluids have indeed introduced or redistributed metals, aeromagnetics could provide an extremely useful tool for tracing fluid movement. Even if metal deposition did not occur along with magnetite formation, the ability to map fluid migration paths would be valuable for reconstructing the mineral system as a whole.

Minor quartz-magnetite-hosted Cu-Au mineralisation is present across the region and aeromagnetics provide an obvious means for delineating prospects. Quartz-magnetite produces characteristically intense magnetic anomalies and is easily recognisable on aeromagnetic images. Other concentrations of magnetite are also potential traps for Cu-Au given suitable conditions.

## Discussion

Structurally controlled magnetite is not well documented in the published literature. In one of the few examples, Urquhart (1966) examined magnetite deposits in Proterozoic rocks of the Savage River-Rocky River region of northwestern Tasmania. He found a strong structural control on magnetite distribution, noting that magnetite was concentrated in zones of intensely developed, steeply-dipping schistosity (greenschist facies) within amphibolite and at the contact between amphibolites and metasediments. He considered that the magnetite was of magmatic hydrothermal origin, and formed by deposition in permeable greenschist channels and replacement outward from these zones. It is unclear whether iron has been introduced in the Broken Hill region, but it is apparent that fluid flow plays an important role in both areas.

There is considerable evidence of fluid flow along shear zones in the Broken Hill region. Tourmaline is present in association with some zones of high strain (e.g. adjacent to Potosi gneiss in the Southern Cross mine area). Extremely coarse-grained sillimanite is also associated with some shear zones, forming rock that may be comprised of almost 100% sillimanite (e.g. magnetite-sillimanite rocks in the Broken Hill Synform and sillimanite-tourmaline-magnetite rocks in the Southern Cross area). This sillimanite may be the refractory component of a rock which has had most of its other minerals removed or replaced by permeating fluids. Coarse-grained muscovite is

widespread and indicates fluid movement during or post D<sub>3</sub>. Retrograde assemblages in the latest-formed and reactivated shear zones are also evidence of considerable fluid flow.

An acidic chloride brine is capable of carrying significant quantities of iron in solution (Holser & Schneer 1953, 1961; McPhail 1993). Holser & Schneer (1953) argue that iron oxides may be deposited when a halide-rich brine enters a region of higher water content and that composition is more important a factor than temperature or pressure changes in magnetite deposition. McPhail (1993) studied high temperature fluids and found that large volumes of magnetite may be deposited as the temperature drops from 500°C to 350°C. His calculations show that 150 g of magnetite may be deposited from only 1 kg of a 15 wt.% chlorine fluid, as a result of a change in iron chloride complexing. He therefore argued that precipitation of iron oxides would not require fluid mixing, wall-rock interaction or boiling and that temperature change alone would result in magnetite precipitation.

It is unclear to what extent iron has been introduced or oxidised *in situ* in the Willyama Supergroup. It is possible that both processes have operated to some degree to influence magnetite distribution. In some cases, carbonate-rich lithologies have localised the formation of magnetite. Higher susceptibilities have been measured in some calc-silicate ellipsoids in pelitic schist in the Sculptures area. This process is not widespread, however, and does not seem to be an important contributor to the formation of magnetic anomalies.

Structurally controlled magnetite has also been reported in rocks of the Olary Block which lie to the west of the Broken Hill Block (Fig. 1) and are broadly correlated with the Willyama Supergroup of the Broken Hill Block (Clarke *et al.* 1986). Four regional alteration events have been recognised in the Olary Block, the first three of which are associated with the mobilisation of iron oxides: pre- or early-tectonic sodic metasomatism; more localised syn-tectonic Na-Ca-Fe alteration; garnet ± epidote replacements and potassic-Fe oxide-carbonate alteration (Ashley *et al.* 1997; Ashley & Plimer 1998).

Skirrow & Ashley (1998) describe these alteration events and the fluids responsible for the alteration. The pre- or early-tectonic sodic metasomatism was largely stratabound and associated with disseminated (partly metasomatic) magnetite. This event appears to correlate with the sodic alteration of sediments in the Broken Hill Block to form quartz-albite rocks ± magnetite. Syntectonic Na-Ca-Fe alteration, not recognised at Broken Hill, formed magnetite-rich veins, replacements and breccias within the Calcsilicate Suite. Potassic and haematitic alteration is present in the north of the Olary Block and is commonly associated with mineralisation. It consists of K-feldspar and/or biotite with carbonate±magnetite±amphibole±quartz and formed relatively late in the tectonic history (possibly late D<sub>3</sub>). This type of alteration was also recognised at Copper Blow in the south of the Broken Hill Block.

The Eastern Fold Belt of the Mount Isa Block in northwestern Queensland has undergone similar regional-scale metasomatism to the Olary Block (e.g. Jaques *et al.*, 1982; Oliver & Wall, 1987; Williams & Phillips, 1992) and has been linked with the Willyama Supergroup (e.g. Laing 1996). Williams & Blake (1993) recognise a high-

temperature sodic alteration event followed by four later-stage alteration events which took place during brittle deformation.

The high-temperature sodic metasomatism resulted in extensive redistribution and concentration of magnetite, controlled to a large degree by shear zones. Later-stage sodic alteration and, to a lesser extent, potassic alteration also resulted in iron mobilisation and magnetite formation. The latest, lowest temperature alteration events were more oxidising and resulted in the formation of haematite rather than magnetite. The fluids involved in metasomatism are high salinity (NaCl equivalent salinity 20-40 wt.% - Williams & Blake (1993)).

Pre- or early-tectonic sodic metasomatism is a common feature of the Broken Hill, Olary and Eastern Fold Belt regions. In the Broken Hill and Euriovie Blocks this metasomatism has affected the lower parts of the sequence (Thackaringa Group and lower). Many of these units are magnetite-bearing and distinct from the upper parts of the Willyama Supergroup which have not seen sodic alteration and are magnetite-poor. In contrast, late-stage sodic metasomatism has not taken place on a large scale in the Broken Hill region as in the Olary Block and the Eastern Fold Belt. Later-stage magnetite formation in the Broken Hill region is caused by fluids of different composition.

### **Significance of structurally controlled anomalies**

The presence of structurally controlled magnetite in the Broken Hill region has important implications for aeromagnetic interpretation in the region. Many of the anomalies in aeromagnetic images do not reflect primary sedimentary units and can not be used to extrapolate lithology beneath cover. In the cases presented above, bedding and magnetic trends are not necessarily parallel and in some places the two are nearly perpendicular. Many areas are much more structurally complex than aeromagnetic images suggest because the rocks have been deformed prior to the formation of magnetite.

The structurally controlled anomalies formed at different times. The earliest observed magnetite formed during high temperature (sillimanite grade) conditions. Magnetite formation also occurred later during the amphibolite grade D<sub>3</sub> deformation and commonly lies within the S<sub>3</sub> fabric. Magnetite associated with chlorite in the Gairdners Tank area is lower temperature yet again and is possibly D<sub>4</sub> in age.

Reduced to pole aeromagnetic images show that most of the magnetic anomalies are symmetrical and that therefore their sources dip steeply to vertically. S<sub>3</sub> fabrics across the region are also consistently steeply-dipping and where the attitudes of both the anomaly sources and S<sub>3</sub> fabric are known, they are parallel and both dip eastward. In contrast, bedding in these areas varies from shallow to vertical. These observations imply a genetic relationship between magnetite formation and the S<sub>3</sub> fabric.

One of the few anomalies with obvious asymmetry is the folded high-temperature shear zone in the core of the Broken Hill synform, where the northwest limb of this anomaly

apparently dips moderately towards the south. This anomaly is not, however, associated with  $S_3$ , but is rather an earlier structure that has been folded around an  $F_3$  fold and reorientated.

Magnetite that has formed in zones of strain partitioning between competent units such as Potosi gneiss and metasediments gives a means of tracing lithological boundaries beneath cover using anomalies generated by structural controls. It should be borne in mind, however, that these anomalies are not constrained to follow these boundaries along strike and may diverge from the contact if other structural controls are more important in directing fluid flow. An example of this is in the Nine Mile area where a linear anomaly tracks the contact between Potosi gneiss and pelitic schist. The anomaly coincides with the contact for 3 km before diverging to have a trend oblique to the Potosi gneiss unit.

The 'magnetic lithostratigraphy' proposed by Tucker (1983) was based on the assumption that the magnetic anomalies reflected original bedding. The paucity of true stratigraphic anomalies within metasediments means that most stratigraphic formations are unable to be characterised by their magnetic signature and are difficult, if not impossible to trace beneath cover.

## Conclusions

The most important result of this study is the recognition that magnetic anomalies are generated by a number of different sources of differing ages and that structurally controlled anomalies are widespread.

These various magnetic sources include:

- Magnetic stratigraphic units, including banded iron formation and some composite gneisses.
- Magnetite formed in structural sites including shear zones, tectonic foliations and lithological contacts.
- Various magnetic intrusive rocks.

Very few stratigraphic sources of anomalies are present in the Willyama Supergroup which would allow detailed interpretation of lithology beneath cover. Some of few that are present include banded iron formation, garnet-poor composite gneiss and weakly magnetic beds in Paragon Group. Instead, structurally controlled anomalies predominate in the bulk of the Willyama sequence. Many of these anomalies are associated with the steeply-dipping  $S_3$  schistosity, while others formed under peak metamorphic conditions. Strain has been partitioned in some areas along the contacts between competent lithologies such as quartzofeldspathic gneisses and less competent metasediments. Fluids have been focussed into these zones as a result of dynamically induced permeability and resulted in the formation of magnetite, either by *in situ* oxidation or by introduction of iron. Alteration by oxidising fluids also seems to be the cause of greatly increased susceptibility in some amphibolites.



Quartz-magnetite rocks were unable to be confidently classified as having either stratigraphic or structural origin. Shear fabrics within these rocks may have overprinted an earlier chemical sediment or, alternatively, may reflect high-temperature shearing which has resulted in syn-deformational magnetite formation.

There are various suites of post-peak metamorphic mafic intrusives which display varying magnetic signatures. Ultramafics are commonly highly magnetic as a result of alteration. Dolerite dykes on the other hand are consistently non-magnetic. Other mafic dykes are moderately magnetic and prominent on aeromagnetic images. Felsic intrusives are generally non-magnetic. Exceptions include pegmatites related to structurally-controlled anomalies and some granite gneisses.

Fluid flow along structural conduits appears to be an important factor in the formation of many of the linear anomalies in the Willyama Supergroup. Without good geological control, magnetic anomalies beneath cover are difficult to interpret and should not be assumed to be conformable to bedding.

## **Acknowledgments**

Our thanks to Barney Stevens, John Giddings, Roger Skirrow and Kevin Capnerhurst for their time spent discussing our interpretation of magnetic anomalies. Phil Schmidt made many of the laboratory rock properties measurements. Richard Haren and Lynton Jaques were involved in management and the initial planning of interpretive work. Peter Wellman and Morrie Duggan kindly reviewed the manuscript.

## References

- Andrews E.C. 1922. The geology of the Broken Hill district. *Memoirs of the Geological Survey of New South Wales* 8, 1-432.
- Archibald N.J. 1978. Stratigraphic controls of Pb-Zn sulphide mineralisation in the Proterozoic Willyama Supergroup. Report to the Broken Hill Mine Managers Association.
- Ashley P.M., Lawie D.C., Connor C.H.H. & Plimer I.R. 1997. Geology of the Olary Domain, Curnamona Province, South Australia, and field guide to 1997 Excursion stops. *Mines & Energy, South Australia, Report Book 97/17*.
- Ashley P.M. & Plimer I.R. 1998. Proterozoic Olary Domain, South Australia: regional and local scale alteration and mineralisation. *Geological Society of Australia Abstracts* 49, 14.
- Bailey A. 1998. Cannington silver-lead deposit. In: Berkman D.A. & Mackenzie D.H. eds. *Geology of Australian and Papua New Guinean Mineral Deposits*, pp. 783-792. The Australian Institute of Mining and Metallurgy, Melbourne.
- Barnes R.G. 1988. Metallogenic studies of the Broken Hill and Euriowie Blocks, New South Wales. 1. Styles of mineralisation in the Broken Hill Block. 2. Mineral deposits of the southwestern Broken Hill Block. *New South Wales Geological Survey, Bulletin* 32, 250pp.
- Barnes R.G., Stevens B.P.J., Stroud W.J., Brown R.E., Willis I.L. & Bradley G.M. 1983. Zinc, manganese and iron-rich rocks and various minor rock types. In: *Rocks of the Broken Hill Block: their classification, nature, stratigraphic distribution and origin*. NSW Geological Survey, *Records* 21, 289-323.
- Birch B., Chapman A. & Pecover S. 1982. The Minerals. In: *Minerals of Broken Hill*. Australian Mining & Smelting Limited, Melbourne.
- Brown R.E. 1980. The geology of the Broken Hill 1:25 000 sheet area, Broken Hill, New South Wales. *Geological Survey of New South Wales, Report GS 1980/143* (unpubl.).
- Brown R.E. 1985. Gairdners Tank 1:25,000 Geological Sheet, 7234-IV-N. *New South Wales Geological Survey, Sydney*.
- Brown R.E., Stevens B.P.J., Willis I.L. Stroud W.J., Bradley G.M. & Barnes R.G. 1983. 3. Quartzofeldspathic rocks. In: *Rocks of the Broken Hill Block: their classification, nature, stratigraphic distribution and origin*. NSW Geological Survey, *Records* 21, 127-226.
- Burton G.R. 1990. Pre-mining tonnages of the individual ore lenses of the Broken Hill Main Lode. *Geological Survey of New South Wales, Report GS 1990/322* (unpubl.).

Chinner G.A. 1960. Pelitic gneisses with varying ferrous/ferric ratios from Glen Clova, Angus, Scotland. *Journal of Petrology* 1, 178-217.

Clark D.A. 1981. Relationship between magnetic fabric and geological structure in the Northern Leases area, Broken Hill. CSIRO Restricted Investigation Report 1237R (unpubl.).

Clark D.A. 1988. Magnetic properties, magnetic stratigraphy and magnetic fabric of rocks from the Northern Leases, the Redan/Farmcote Area, the Rise and Shine Area and the Rupee trend, Broken Hill Block. CSIRO Restricted Investigation Report 1743R, (unpubl.).

Clarke G.L., Burg J.P. & Wilson C.J.L. 1986. Stratigraphic and structural constraints on the Proterozoic tectonic history of the Olary Block, South Australia. *Precambrian Research* 34, 107-137.

Cooper P.F., Tuckwell K.D., Gilligan L.B. & Meares R.M.D. 1978. Geology of the Torrawangee and Fowlers Gap 1:100 000 sheets 7135, 7235. Geological Survey of New South Wales, Sydney.

Corbett G.J. 1981. Geology of the Redan 1:25 000 sheet area, Broken Hill, New South Wales. New South Wales Geological Survey, Report 1981/371, (unpubl.).

C.R.A. Exploration Pty. Ltd. 1986. Exploration report EL2602, Hawsons Knob, Broken Hill area. Geological Survey of New South Wales File GS 1986/240, (unpubl.).

Donaghy T., Hall M. & Gibson G. 1998. The Palaeoproterozoic Thackaringa Group: deposition, deformation and stratigraphy. Abstracts from the 1998 Broken Hill Exploration Initiative meeting. Australian Geological Survey Organisation Record 1998/25, 17-20.

Gibson G.M., Maidment D.W. & Haren R. 1996. Re-evaluating the structure of Broken Hill. *AGSO Research Newsletter* 25, 1-3.

Gibson G.M., Maidment D.W. & Haren R. 1997. Willyama Supergroup, Broken Hill, Australia: a 1600 Ma granulite terrane situated along the Neoproterozoic margin of Gondwana following continental rifting and breakup of Rodinia. In: Bradshaw J.D., Weaver S.D. eds., *Terrane Dynamics 97*, Abstracts of the International conference on Terrane Geology, Christchurch, N.Z., 71-74.

Gibson G.M., Drummond B., Fomin T., Owen A., Maidment D.W., Gibson D., Peljo M. & Wake-Dyster K. 1998. Re-evaluation of crustal structure in the Broken Hill Inlier through structural mapping and seismic profiling. Australian Geological Survey Organisation Record 1998/11.

Gibson G.M., Fomin, T., Drummond B., Owen A., Maidment D. & Wake-Dyster K. 1998. Structure and tectonic evolution of Broken Hill Inlier revisited in the light of new

structural mapping and seismic reflection data. Geological Society of Australia, Abstracts 49, 165.

Giddings J., Ruszkowski P., Gibson G., Maidment D. & Rokovic U. 1998. Petrophysical studies in the Broken Hill Block: implications for magnetic modelling and the control mechanism of linear magnetic anomalies. Abstracts from the 1998 Broken Hill Exploration Initiative meeting. Australian Geological Survey Organisation Record 1998/25, 41-45.

Grant F.S. 1985. Aeromagnetics, geology and ore environments, I. Magnetite in igneous sedimentary and metamorphic rocks: an overview. *Geoexploration* 23, 303-333.

Gustafson J.K., Burrell H.C. & Garretty M.D. 1950. Geology of the Broken Hill ore deposit, Broken Hill, New South Wales. *Geological Society of America Bulletin* 61, 1369-1414.

Holser W.T. & Schneer C.J. 1953. Deposition of high temperature, non-magmatic magnetite. *Economic Geology* 48, 620.

Holser W.T. & Schneer C.J. 1961. Hydrothermal magnetite. *Geological Society of America Bulletin* 72, 369-386.

Ishahira S. 1977. The magnetite-series and ilmenite-series granitic rocks. *Mining Geology* 27, 293-305.

Isles D.J. 1983. A regional geophysical study of the Broken Hill Block, N.S.W., Australia. PhD thesis (unpubl.), University of Adelaide.

Jaques A.L., Blake D.H. & Donchak P.J.T. 1982. Regional metamorphism in the Selwyn Range area, northwest Queensland. *BMR Journal of Australian Geology & Geophysics* 7, 181-196.

Laing W.P. 1996. The Diamantina orogen linking the Willyama and Cloncurry Terranes, eastern Australia. In: *New developments in Broken Hill-type deposits*, CODES Special Publication 1, 67-72.

Laing W.P., Marjoribanks R.W. & Rutland R.W.R. 1978. Structure of the Broken Hill Mine area and its significance for the genesis of the orebodies. *Economic Geology* 73, 1112-1136.

Lauren L. 1969. On magnetite bearing pegmatites in Se Sottunga, Aland Islands. *Bulletin of the Geological Society of Finland* 41, 107-115.

Lawrence L.J. 1968. The minerals of the Broken Hill district. *Proceedings of the Australasian Institute of Mining and Metallurgy* 226, 103-136.

Leyh W.R. & Larsen D.F. 1983. Iron formation related base metal prospects, Broken Hill, New South Wales. AUSIMM Conference, Broken Hill. NSW July 1983, 133-156.

Lishmund S.R. 1982. Non-metallic and tin deposits of the Broken Hill district. NSW Geological Survey Bulletin 28, 1-176.

McIntyre J.I. & Wyatt B.W. 1978. Contributions to the regional geology of the Broken Hill area from geophysical data. BMR Journal of Geology and Geophysics 3, 265-280.

McIntyre J.I. 1979. Aeromagnetism - an effective geological mapping aid for the Willyama Complex? Bulletin of the Australian Society of Exploration Geophysics 10, 42-53.

McIntyre J.I. 1980a. Magnetic marker horizons in the Willyama Complex - second derivative maps from the BMR 1975 detailed Broken Hill aeromagnetic survey. Geological Survey of New South Wales Report GS 1980/008 (unpubl.).

McIntyre J.I. 1980b. Geological significance of magnetic patterns related to magnetite in sediments and metasediments - a review. Bulletin of the Australian Society of Exploration Geophysics 11, 19-33.

McPhail D.C. 1993. The behaviour of iron in high-temperature chloride brines. Geological Society of Australia Abstracts 34, 50-51.

Maidment D.W., Gibson G.M. & Stevens B.P.J. 1997. Lithological interpretation of the Mount Gipsy 1:25 000 sheet. Australian Geological Survey Organisation, Canberra.

Marjoribanks R.W., Rutland R.W.R, Glen R.A. & Laing W.P. 1980. The structure and tectonic evolution of the Broken Hill region, Australia. Precambrian Research 13, 209-240.

Moody J.B. 1976. Serpentinisation: a review. Lithos 9, 125-138.

Nutman A.P. & Ehlers K. 1998. Evidence for multiple Palaeoproterozoic thermal events and magmatism adjacent to the Broken Hill Pb-Zn-Ag orebody, Australia. Precambrian Research 90, 203-238.

Nutman A.P. & Gibson G.M. 1998 Zircon ages from metasediments, granites and mafic intrusions: reappraisal of the Willyama Supergroup. Abstracts from the 1998 Broken Hill Exploration Initiative meeting. Australian Geological Survey Organisation Record 1998/25, 86-88.

Oliver N.H. & Wall V.J. 1987. Metamorphic plumbing system in Proterozoic calc-silicates, Queensland, Australia. Geology 15, 793-796.

Plimer I.R.. 1984. The mineralogical history of the Broken Hill Lode, NSW. Australian Journal of Earth Sciences 31, 379-402.

Richards S.M. 1966. The banded iron formations at Broken Hill, Australia and their relationship to the lead-zinc orebodies Part I. Economic Geology 61, 72-96.

Richards S.M. 1966. The banded iron formations at Broken Hill, Australia and their relationship to the lead-zinc orebodies Part II. *Economic Geology* 61, 257-274.

Ririe G.T. 1982. A model for gahnite and magnetite formation during metamorphism of sulfide-rich rocks. *Geological Society of America Abstracts with Programs* 14, 227-228.

Scott S.D., Both R.A. & Kissin S.A. 1977. Sulfide petrology of the Broken Hill region, New South Wales. *Economic Geology* 72, 1410-1425.

Segnit E.R. 1977. Jacobsite and magnetite from Broken Hill, NSW. *Australian Mineralogist* 9, 37-39.

Skirrow R.G. & Ashley P.M. 1998. Copper-gold mineral systems and regional alteration, Curnamona Craton. Abstracts of the Broken Hill Exploration Initiative Conference, Broken Hill 1998. Australian Geological Survey Organisation Record 1998/25, 104-108.

Stanton R.L. 1976a. Petrochemical studies of the ore environment at Broken Hill, New South Wales: 1 - constitution of 'banded iron formation'. Institution of Mining and Metallurgy (London) - Transactions/Section B, *Applied Earth Science* 85, B33-B46.

Stanton R.L. 1976b. Petrochemical studies of the ore environment at Broken Hill, New South Wales: 2 - regional metamorphism of banded iron formations and their immediate associates. Institution of Mining and Metallurgy (London) - Transactions/Section B, *Applied Earth Science* 85, B118-B131.

Stanton R.L. 1976c. Petrochemical studies of the ore environment at Broken Hill, New South Wales: 3 - banded iron formations and sulphide orebodies: constitutional and genetic ties. Institution of Mining and Metallurgy (London) - Transactions/Section B, *Applied Earth Science* 85, B132-B141.

Stanton R.L. 1976d. Petrochemical studies of the ore environment at Broken Hill, New South Wales: 4 - environmental synthesis. Institution of Mining and Metallurgy (London) - Transactions/Section B, *Applied Earth Science* 85, B221-B233.

Stevens B.P.J. 1986. Post-depositional history of the Willyama Supergroup in the Broken Hill Block, NSW. *Australian Journal of Earth Sciences* 33, 73-98.

Stevens B.P.J. 1997. Geological controls on magnetite in metasediments, Broken Hill. Broken Hill Exploration Initiative: Abstracts from 1997 Annual Meeting. Australian Geological Survey Organisation Record 1997/49, 38-39.

Stevens B.P.J. 1998. Investigations of aeromagnetic anomalies at Broken Hill. NSW Department of Mineral Resources Minfo 58, 18-22.

Stevens B.P.J. & Corbett G.J. 1993. The Redan Geophysical Zone, part of the Willyama Supergroup? Broken Hill, Australia. *Australian Journal of Earth Sciences* 40, 319-338.

Stevens B.P.J. & Stroud W.J. (eds) 1983. *Rocks of the Broken Hill Block: their classification, nature, stratigraphic distribution and origin*. NSW Geological Survey, Records 21, 323pp.

Stevens B.P.J., Willis I.L., Brown R.E. & Stroud W.J. 1983. The Early Proterozoic Willyama Supergroup: definitions of stratigraphic units from the Broken Hill Block, New South Wales. Geological Survey of New South Wales, Records 21, 407-442.

Stroud W.J., Willis I.L., Bradley G.M., Brown R.E., Stevens B.P.J. & Barnes R.G. 1983. Amphibole and/or pyroxene-bearing rocks. In: *Rocks of the Broken Hill Block: their classification, nature, stratigraphic distribution and origin*. NSW Geological Survey, Records 21, 227-287.

Tucker D.H. 1983. The characteristics and interpretation of regional magnetic and gravity fields in the Broken Hill district. AUSIMM Conference, Broken Hill. NSW July 1983, 81-114.

Urquhart G. 1966. Magnetite deposits of the Savage River-Rocky River region. *Bulletin of the Geological Survey of Tasmania* 48, 145 pp.

Vernon R.H. & Williams P.F. 1988. Distinction between intrusive and extrusive or sedimentary parentage of felsic gneisses: Examples from the Broken Hill Block, NSW. *Australian Journal of Earth Sciences* 35, 379-388.

Vernon R.H. 1996. Structural evidence of parent rocks in high-grade metamorphic areas - especially Broken Hill. In: *New developments in Broken Hill-type deposits*, Centre for Ore Deposit and Exploration Studies, University of Tasmania Special Publication 1, 17-20.

White S.H., Rothery E., Lips A.L.W. & Barclay T.J.R. 1995. Broken Hill area, Australia, as a Proterozoic fold and thrust belt: implications for the Broken Hill base-metal deposit. *Institution of Mining and Metallurgy, Transactions* 104, B1-B17.

White S.H., Rothery E., Lips A.L.W. & Barclay T.J.R. 1996. Author's reply to discussion by Stevens, of White et al. 1995. *Institution of Mining and Metallurgy, Transactions* 104. B90-98.

Williams P.J. & Blake K.L. 1993. Alteration in the Cloncurry district. *EGRU Contribution* 49, James Cook University.

Williams P.J., Chapman L.H., Richmond J., Baker T., Heinemann M. & Pendergast W.J. 1996. Significance of late orogenic metasomatism in the Broken Hill-type deposits of the Cloncurry district, NW Queensland. In: *New developments in Broken*

Hill-type deposits, Centre for Ore Deposit and Exploration Studies, University of Tasmania Special Publication 1, 119-132.

Williams P.J. & Phillips G.N. 1992. Cloncurry Mapping Project 1990. James Cook University Economic Geology Research Unit Contribution 40.

Willis I.L. 1989. Broken Hill stratigraphic map. New South Wales Geological Survey, Sydney.

Willis I.L., Brown R.E., Stroud W.J. & Stevens B.P.J. 1983. The Early Proterozoic Willyama Supergroup: stratigraphic subdivision and interpretation of the high to low-grade metamorphic rocks in the Broken Hill Block, New South Wales. *Journal of the Geological Society of Australia* 30, 195-224.

Willis I.L., Stevens B.P.J., Stroud W.J., Brown R.E., Bradley G.M. & Barnes R.G. 1983. Metasediments, composite gneisses and migmatites. In *Rocks of the Broken Hill Block: their classification, nature, stratigraphic distribution and origin*. NSW Geological Survey, Records 21, 57-125.

Wingate M.T.D., Campbell I.H., Compston W. & Gibson G.M. 1998. Ion microprobe U-Pb ages for Neoproterozoic basaltic magmatism in south-central Australia and implications for the breakup of Rodinia. *Precambrian Research* 87, 135-159.



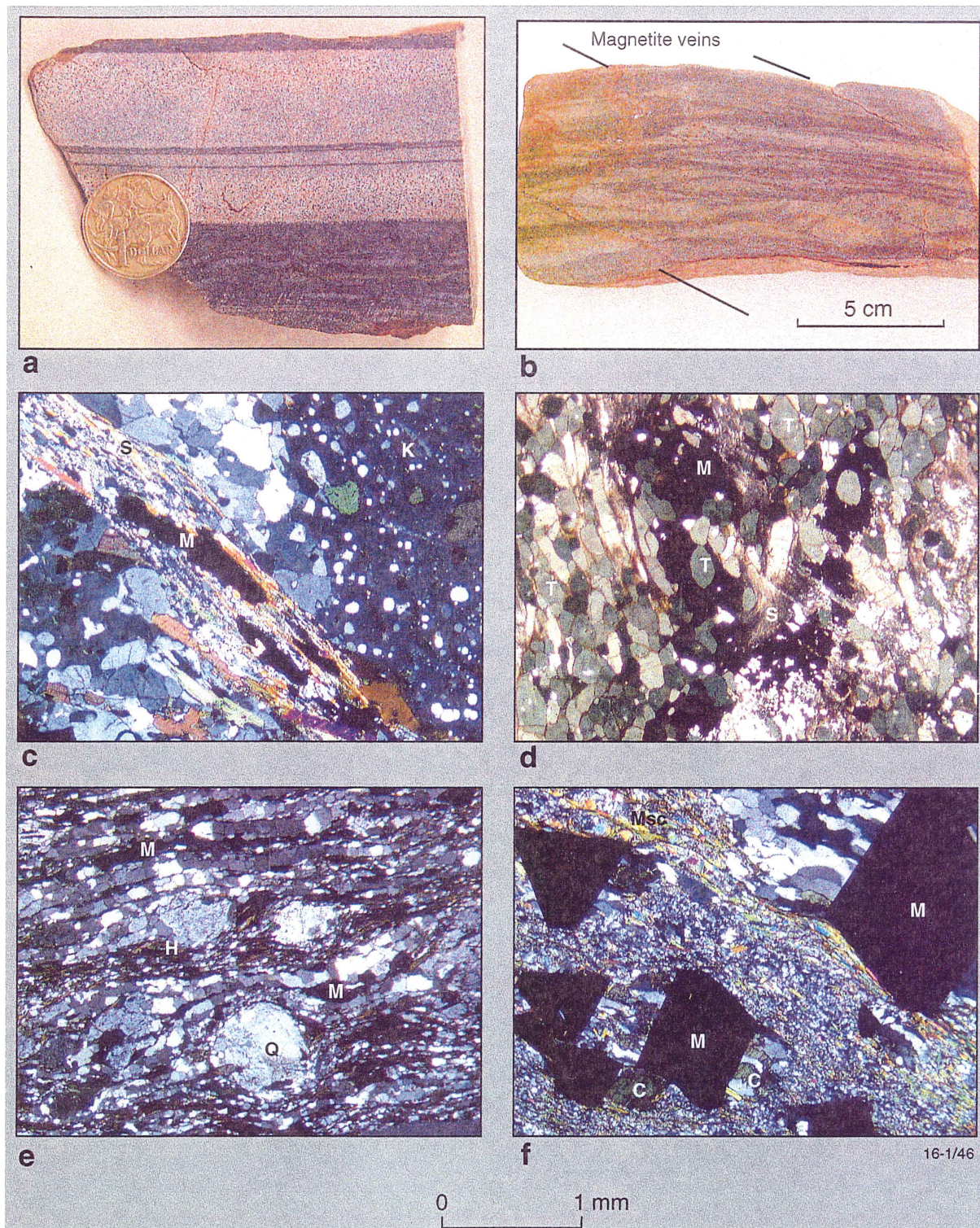


Figure 42. a - Quartz-magnetite rock in quartz-albite rock with layering defined by magnetite concentration; b - Quartz-albite rock with possible sedimentary structures defined by magnetite-rich layers; c - Magnetite-sillimanite rock from the Broken Hill Synform showing magnetite lying within a sillimanite fabric (?D2); d - Tourmaline-magnetite rock from the contact between Potosi Gneiss and metasediments in the Southern Cross Mine area, showing an equilibrium assemblage of magnetite, tourmaline and sillimanite; e - Mylonitic magnetite-rich amphibolite from water tower area at Broken Hill; f - Euhedral magnetite in chlorite schist from the Gairdners Tank area.

**Key**

M: magnetite; S: sillimanite; T: tourmaline; K: K-feldspar; Q: quartz; H: hornblende; C: chlorite.